



DESIGN AND SYNTHESIS OF SMALL MOLECULES FOR ORGANIC AND GRÄTZEL SOLAR CELLS.

Lydia Cabau Parra

Dipòsit Legal: T 1617-2015

ADVERTIMENT. L'accés als continguts d'aquesta tesi doctoral i la seva utilització ha de respectar els drets de la persona autora. Pot ser utilitzada per a consulta o estudi personal, així com en activitats o materials d'investigació i docència en els termes establerts a l'art. 32 del Text Refós de la Llei de Propietat Intel·lectual (RDL 1/1996). Per altres utilitzacions es requereix l'autorització prèvia i expressa de la persona autora. En qualsevol cas, en la utilització dels seus continguts caldrà indicar de forma clara el nom i cognoms de la persona autora i el títol de la tesi doctoral. No s'autoritza la seva reproducció o altres formes d'explotació efectuades amb finalitats de lucre ni la seva comunicació pública des d'un lloc aliè al servei TDX. Tampoc s'autoritza la presentació del seu contingut en una finestra o marc aliè a TDX (framing). Aquesta reserva de drets afecta tant als continguts de la tesi com als seus resums i índexs.

ADVERTENCIA. El acceso a los contenidos de esta tesis doctoral y su utilización debe respetar los derechos de la persona autora. Puede ser utilizada para consulta o estudio personal, así como en actividades o materiales de investigación y docencia en los términos establecidos en el art. 32 del Texto Refundido de la Ley de Propiedad Intelectual (RDL 1/1996). Para otros usos se requiere la autorización previa y expresa de la persona autora. En cualquier caso, en la utilización de sus contenidos se deberá indicar de forma clara el nombre y apellidos de la persona autora y el título de la tesis doctoral. No se autoriza su reproducción u otras formas de explotación efectuadas con fines lucrativos ni su comunicación pública desde un sitio ajeno al servicio TDR. Tampoco se autoriza la presentación de su contenido en una ventana o marco ajeno a TDR (framing). Esta reserva de derechos afecta tanto al contenido de la tesis como a sus resúmenes e índices.

WARNING. Access to the contents of this doctoral thesis and its use must respect the rights of the author. It can be used for reference or private study, as well as research and learning activities or materials in the terms established by the 32nd article of the Spanish Consolidated Copyright Act (RDL 1/1996). Express and previous authorization of the author is required for any other uses. In any case, when using its content, full name of the author and title of the thesis must be clearly indicated. Reproduction or other forms of for profit use or public communication from outside TDX service is not allowed. Presentation of its content in a window or frame external to TDX (framing) is not authorized either. These rights affect both the content of the thesis and its abstracts and indexes.

Lydia Cabau Parra

Design and Synthesis of Small
Molecules for Organic and
Grätzel Solar Cells

Doctoral Thesis

Supervised by Prof. Emilio Palomares
ICIQ-URV



UNIVERSITAT ROVIRA I VIRGILI

Tarragona-June 2014

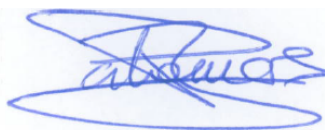
Emilio Palomares Gil, Group Leader of the Institute of Chemical Research of Catalonia (ICIQ) in Tarragona, and Research Professor of the Catalan Institution for research and Advanced Studies (ICREA) in Barcelona.

CERTIFIES:

That the present thesis, entitled “Design and Synthesis of Small Molecules for Organic and Grätzel Solar Cells” presented by **Lydia Cabau Parra** for the award of the degree of Doctor, has been carried out under my supervision at ICIQ.

Tarragona, June 2014

Prof. Dr. Emilio Palomares Gil



UNIVERSITAT ROVIRA I VIRGILI

A tots els meus

Acknowledgements

First of all, I would like to say thank you to my supervisor Emilio Palomares for his support and for giving me the chance to do a PhD, as well as trusting on me and in my capability to do the thesis.

I also want to say thank you to John Noel Clifford, and Vijay Kumar Challuri for their help during all the time teaching me not only on synthesis, but also on the photophysics measurements. I am also thankful for all the discussion about the work, and of course the happy moments spent with Vijay in the fumehood in the last two years.

Another person that I want to say thank you is Toni Moncho because without his patient probably I wouldn't have the results that I have in my thesis. Thank you for preparing the DSSC devices for me, and for the serenity that you have shown when I came to change all the conditions.

Núria, thank you not only for teaching me a lot of things on OPVs, but also for the very funny moments that we have spent in the lab, in the office or any place. You will achieve whatever you want.

Also I want to say thank you to one of the best persons I've ever meet in my life. Thank you Georgiana. You always are available to help everybody and give some advises, please, don't change never.

I also want to say thank you to all the people that are in the group or not: Alba, Beloqui, Werther, Bea, Eva, Anna, Toni, Miquel, Amparo, Eugenia, Josep, Margherita, James, Ivan, Ma, Mustafa, Taye, Laia and Aurelien.

Thank you to my Mother (Maika) because without her I wouldn't be here. She teached me all I know and she is a referent for me.

I am also grateful to my small family, Victor and Truska. Thank you Victor for everything. I love you, and also thank you Truska for relaxing me every day and for making possible taking rid all the accumulate stress.

At the end, I want to say thank you to my close friends Sara, Karla and my "micus" (Anna, Mar, Nieves, Teiraks, Cere, Sumoi, Susana, Mariona, Sandra and Meritxell) to be always there.

Table of contents

CHAPTER 1: Introduction	3
CHAPTER 2: Materials and Methods	39
CHAPTER 3: Organic dyes sensitizers for DSSC	53
CHAPTER 4: Porphyrins as sensitizers for DSSC	79
CHAPTER 5: Porphyrins as donor for OPV	107
CHAPTER 6: Final Conclusions	129
ANNEX: Scientific Contribution	133

Chapter 1

Introduction

Table of contents

1.1 Introduction	7
1.2 Dye Sensitized solar cells	9
1.2.1 Principles of DSSC	9
1.2.2 Basic Solar Cells parameters	11
1.2.3 Initial requisites for efficient sensitizers in DSSC	12
1.2.4 Ruthenium Complexes	13
1.2.5 Metal free Organic dyes. The Donor- π -Acceptor dyes	16
1.2.6 Porphyrins	21
1.3 Organic Solar Cells	28
1.3.1 Donor and Acceptor Materials	30
1.3.1.1 Electron Acceptor Materials	30
1.3.1.2 Electron Donor Materials	30
1.4 Aim of this Thesis	32
1.5 References	33

1.1 INTRODUCTION

The human population is growing up every year with the concomitant consumption of energy, In recent years, only 9% of the energy was provided by so-called renewable energies, 4% from nuclear source and the 87% from fossil fuels such as coal, oil or gas worldwide¹. The last ones, oil and gas, being dominating the energy market. An observation of major concern is the difficulties to find novel oil reserves that can be exploited with the actual technology. As the new oil reserves are every day more difficult to access, the price increases and, thus, there is a real risk that most human population will not have access to energy².

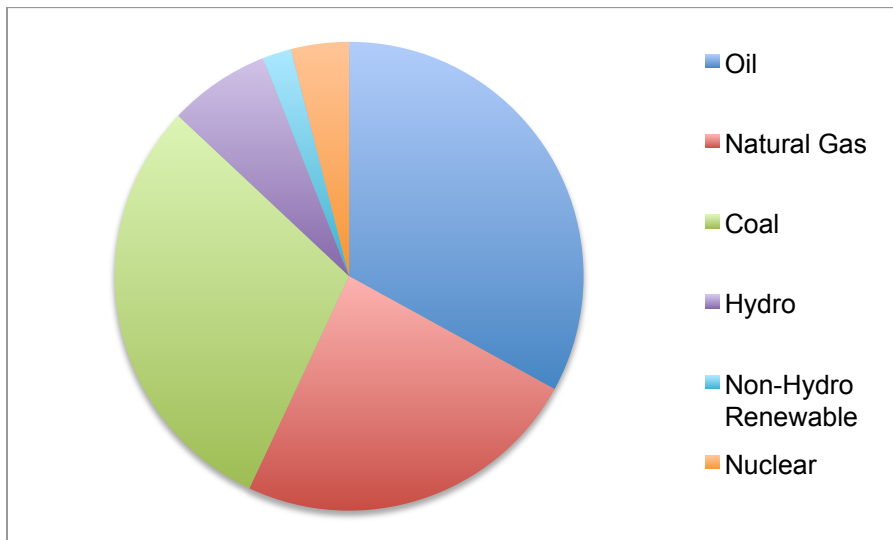


Figure 1.1: The world energy consumption by source in 2014

Solar energy is available for everyone and, for this reason, is a long-standing focus of research to make efficient and cheap light-to-energy (either electrical or chemical energy) conversion devices. The current solar PV (photovoltaic) market is mainly devoted to silicon solar cells (average efficiency 16%) and the best solar panels (triple junction solar cells made using Indium and Gallium) are just made available for space technology (average efficiency 40%) (ei:

Chapter 1

communication satellites). The cost/energy conversion associated to this type of light-to-electrical conversion devices makes nowadays a dream to expand worldwide the use of solar energy and the reality is that only those countries that subsidise the use of solar panels have a flourished solar energy market. Thus the scientific and industrial community have developed efforts towards the research of new type of materials and devices to decrease the cost/efficiency value. In the next Figure NREL (National Renewable Energy Labs, USA) have illustrate all actual solar cell technologies³.

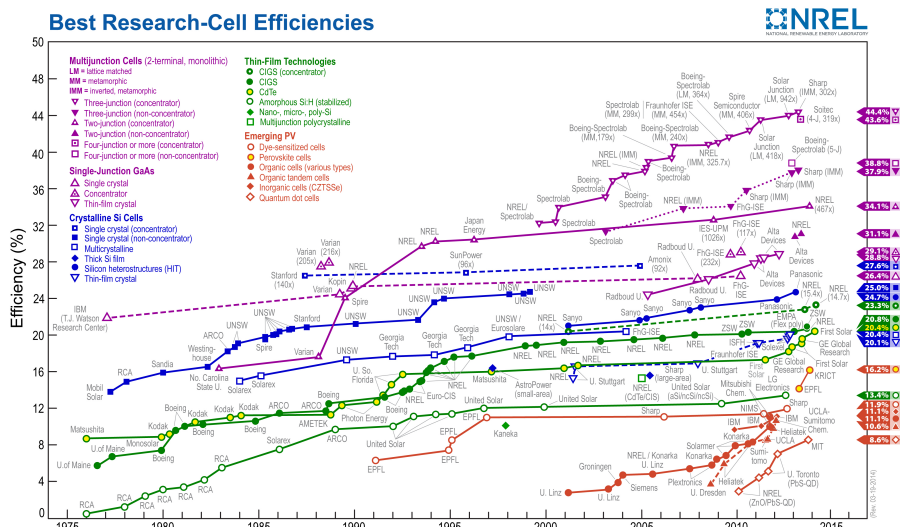


Figure 1.2: Progress on solar cells technologies. Copyright NREL

Two of these types of promising technologies are Dye Sensitized Solar Cells (DSSC) also known as Grätzel solar cells and Organic solar Cells (OPV).

1.2 DYE SENSITIZED SOLAR CELLS

The Dye Sensitized solar Cells (DSSC) are photoelectrochemical cells based on the use of a dye to sensitize a wide band-gap semiconductor metal oxide (generally TiO_2) supported in a transparent conducting glass (Fluorine-doped tin oxide, FTO) that works as a working electrode. The counter electrode consists of a layer of platinum coated on the FTO conducting glass. These two electrodes are sealed with a polymer and a redox electrolyte that serves to regenerate the dye ground state completes the solar cell.

1.2.1 Principles of DSSC

A typical DSSC basically contains 6 components: semiconductor photoanode or working electrode, the sensitizer, the electrolyte (redox pair), the spacer (usually Surilyn©) and the counter electrode.

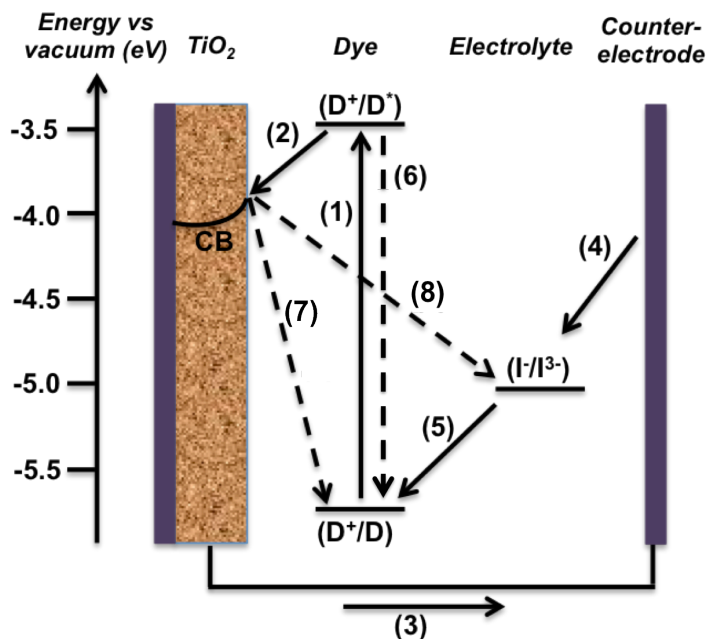
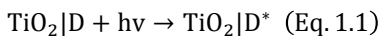


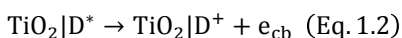
Figure 1.3 Scheme of a DSSC and the most relevant charge transfer events taking place upon illumination.

Chapter 1

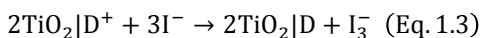
First of all the incoming light is absorbed by the sensitizer promoting an electron from the ground state to the excited state **(1)**.



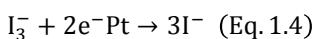
Thereafter, the electron is transferred to the semiconductor conduction band **(2)**, and in an ideal case the electron will flow through an external circuit to the counter electrode **(3)**.



From the counter electrode, the electron is transferred to the electrolyte (redox couple) **(4)** and the electron donating species at the electrolyte regenerates the oxidized dye **(5)**.



The red/ox electrolyte (often iodine/iodide) is then regenerated at the counter electrode by reduction of triiodide.



However, these devices have also undesirable charge recombination reactions, (Figure 1.3), which are responsible for the losses in the device efficiency. One of these reactions is the deactivation of the dye excited state **(6)**. Nonetheless, this process occurs is nanosecond time scale (10^{-9} s) while the electron injection from the excited state into the semiconductor conduction band occurs at least one order of magnitude faster, making the electron injection more favourable than the deactivation of the dye excited state. Another undesired reaction is the recombination of the photoinjected electrons at the semiconductor with the oxidised sensitizer **(7)**. This process as in the same case that for the first one loss mechanism is slower (10^{-6} - 10^{-3} s) than the regeneration of the sensitizer **(5)**

(10^{-9} - 10^{-6} s). In order to have a slow recombination we have to make sure that the regeneration of the dye is produced efficiently. To be sure of this, the HOMO (Highest Occupied Molecular Orbital) of the molecule has to be far from the surface of the semiconductor, and, moreover, its energy has to be lower in energy respect to the redox electrolyte potential to favour the regeneration driving force. The last recombination reaction is produced after the regeneration of the sensitizer, because the oxidized electrolyte is close to the surface of the semiconductor therefore, recombination of photoinjected electrons in the semiconductor with the oxidized electrolyte can occur and the lifetimes are in a range from 10^{-3} - 10^{-1} s, making this mechanism one of the principal loss reactions⁴.

1.2.2 Basic Solar Cell Parameters

When a solar cell is illuminated, a photocurrent and a voltage are generated which can be depicted as in figure 1.4

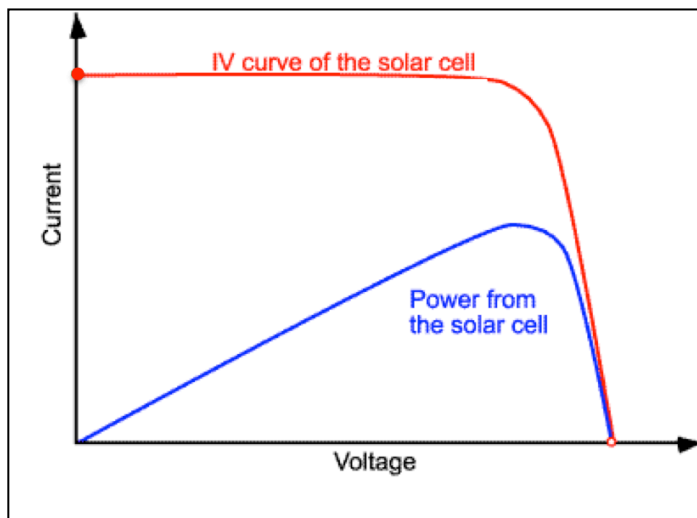


Figure 1.4: Typical IV-Curve of a solar cell

The overall energy conversion of a solar cell is defined as the ratio of the output power of the cell per incident irradiance (equation 1.7)

$$\eta = \frac{P_{\max}}{P_{\text{light}}} = \frac{J_{\text{sc}} \cdot V_{\text{oc}} \cdot \text{FF}}{P_{\text{light}}} \quad (\text{Eq. 1.7})$$

Where J_{sc} (mA/cm^2) is the photocurrent density at short circuit, V_{oc} (V) the Voltage at open circuit, FF is the Fill Factor that measures the how squarer is the I-V curve (the higher Fill Factor the higher efficiency at a given J_{sc} and V_{oc}), and the P_{light} the power of the incident light.

As one could imagine, the device efficiency and, thus, the IV curve is affected by the charge transfer reactions detailed above. Yet, in this Thesis we have focused on the sensitizers used mainly in DSSC and in an example of OPV.

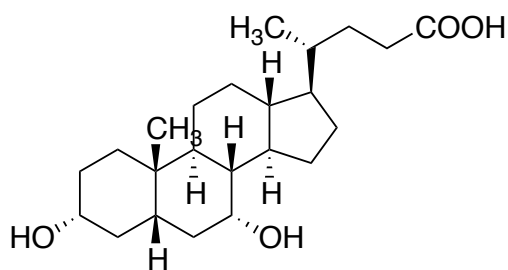
1.2.3 Initial requisites for efficient sensitizers in DSSC

The sensitizer in a DSSC plays a very important role in order to achieve the maximum efficiency in devices. First of all, the sensitizer has to have the capability to capture the light, absorbing the incident photons from a wide range of wavelengths from the solar spectrum. Moreover, the sensitizer must have an anchoring group in order to bind strongly (covalently) to the semiconductor surface. Although several anchoring groups have described in the bibliography as, for example, phosphonates, catechols etc...^{5,6}. The most common chemical group used is the carboxylic acid⁷. The hydroxyl group react with the TiO_2 surface forming a covalent bond in the best cases.

The HOMO and LUMO (Lowest Unoccupied Molecular Orbital) energy of the sensitizers is key in order to achieve good efficiency by decreasing unfavoured electron transfer reactions. As already mentioned above, the dye HOMO level has to be away from the semiconductor surface and with lower energy than the oxidation potential of the redox active electrolyte. On the other hand the LUMO

of the sensitizer has to be close to the surface of the semiconductor in order to achieve an efficient electron injection. So called unidirectional electron transfer. Furthermore, it is paramount that the LUMO level is placed higher than the conduction band energy level of the TiO_2 to favour the electron injection from the dye excited state.

Secondly, the dye solubility in organic solvents preferably non-halogenated solvents is also of importance, as well as, the minimization of the presence of dye aggregates in the solution and in the semiconductor surface after sensitization. This last requisite can be partially solved with the addition of a co-sensitizer such as Chenodeoxycholic Acid⁸ (CDCA) which decreases the formation of aggregates at the semiconductor surface (Figure).



CDCA

Figure 1.5: Molecular structure of CDCA

As an example of efficient dyes used in DSSC we will now detail the use of Ruthenium complexes.

1.2.4 Ruthenium Complexes

The first efficient dyes used for DSSC were Ru complexes (trinuclear Ruthenium dye), giving a light-to-photoelectrical conversion efficiency between 7.1 and 7.9%⁹. The trinuclear $\text{RuL}_2(\mu\text{-(CN)Ru(CN)L}'_2)_2$, where L is 2,2'-bipyridine-4,4'-dicarboxylic acid and L' is 2,2'-bipyridine. One of the first reasons to use the Ruthenium complexes is due to broad absorbance from the

visible region to the near-infrared¹⁰. The general structure of a Ruthenium dye for DSSC consist usually on a Ru(II) atom coordinated by polypyridyl ligands and thiocyanate moieties in an octahedral geometry. The carboxylic acids are used as anchoring groups and are attached to the bipyridyl moiety leading to easy injection of electrons in the semiconductor from the excited state. This complexes show an absorption band in the visible region of the sun spectra that can be tuned, which is due to the MLCT (metal to ligand charge transfer band) transition¹¹.

Since the seminal paper by Gratzel and O'Regan using ruthenium complexes many studies modifying these complexes have been published. Only in 2 years Professor Grätzel an co-workers increased the efficiency up to 10% ($J_{sc}=18.2\text{mA/cm}^2$, $V_{oc}=720\text{mV}$, $FF= 0.73$) with cis-di(thiocyanato)bis(2,2'-bipyridyl-4,4'-dicarboxylate)ruthenium (II) most commonly known as **N3** (Figure 1.6) dye^{12,13}. The following years many ruthenium complexes were reported as the trithiocyanato-4,4',4''-tricarboxy-2,2':6,2''-terpyridine ruthenium(II) also called **Black dye** (Figure 1.6) with and efficiency of 10.4%¹⁴ that was in 2012 updated to 11.4%¹⁵. Moreover, other Ru-complexes have been published with efficiencies close to the paradigm dye **N719** (Figure 1.6)¹⁶ as , for example, the **Z907** (Figure 1.6) that presents long alkyl chains to increase the solubility and slows the recombination reaction between the photo-injected electrons and the oxidised electrolyte. Yet, a milestone was set in 2008 with the design of Ruthenium complexes bearing π -conjugated moieties as thiophene and other derivates at the bipyridyl ligands. The aim was to increase the absorption in the near-infrared region as well as to increase the molecular extinction coefficient of the dye. Needless to say that most of these novel dyes lead to higher efficiencies as in the case of the dye **C101**¹⁷ that presents a 2-hexylthiophene in the bipyridyl ligand reaching an 11.0% ($J_{sc}=17.9\text{mA/cm}^2$, $V_{oc}=778\text{mV}$, $FF= 0.78$) (Figure 1.6) similar to the efficiency obtained with the dye **CYC-B1**¹⁸ (Figure 1.6), the dye **CYC-B11**¹⁹ (Figure 1.6) and the maximum performance achieved with Ruthenium dyes, with the moetiyl 2-(hexylthio)-5-methylthiophene, the dye

C106²⁰ with an 11.7% ($J_{sc}=19.8\text{mA/cm}^2$, $V_{oc}=758\text{mV}$, $FF= 0.78$) of efficiency (Figure 1.6).

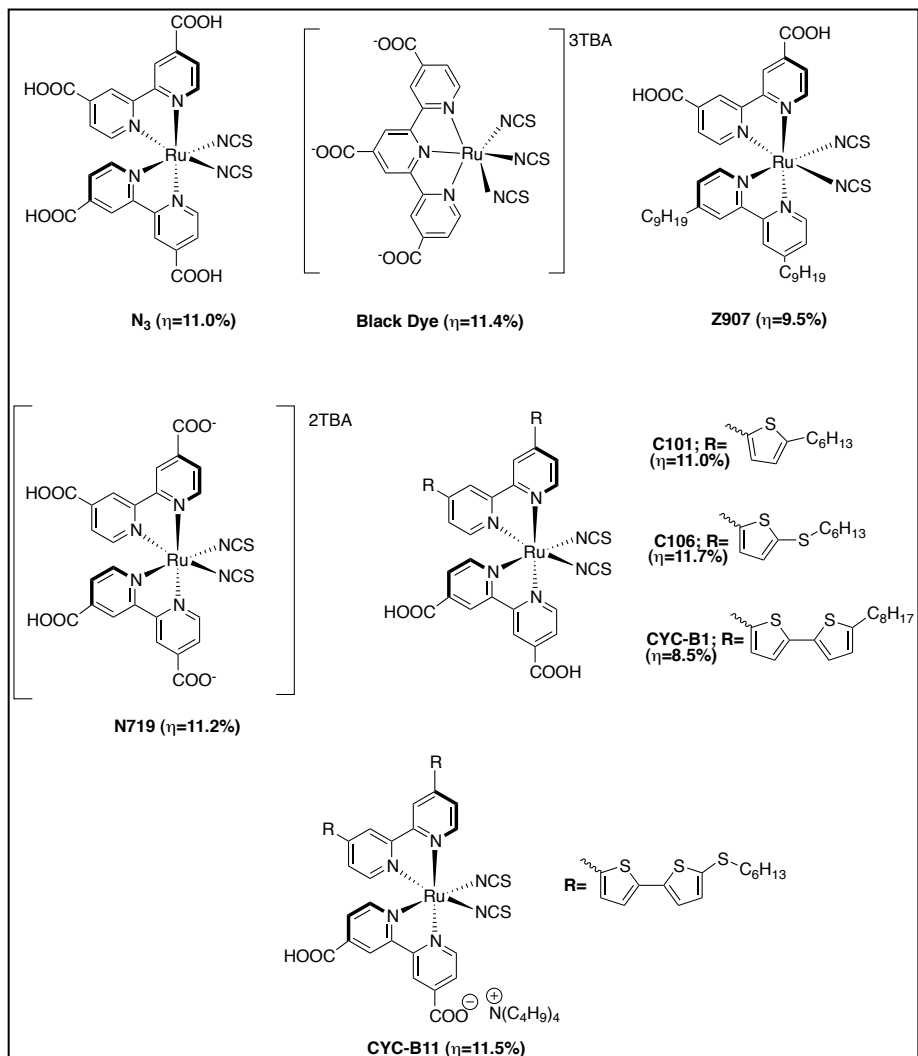


Figure 1.6: Efficient Ruthenium complexes used as sensitizers in DSSC

The Ruthenium complexes present high efficiency and also broad absorption; however, many drawbacks are associated to them. For example the cost; Ruthenium is considered a non-abundant earth metal and, moreover, there are increasing concerns on the environmental assessment of Ruthenium

complexes. Last but not least, is also the moderate absorption coefficient. All these drawbacks make that many scientist make efforts in alternative sensitizers based on metal free organic dyes.

1.2.5 Metal free organic dyes. The Donor- π -Acceptor dyes

The donor- π -Acceptor dyes also known as push pull dyes consist in an electron donor and electron acceptor molecular unit linked covalently with a π conjugated spacer (Figure 1.7) The photophysical properties associated to these dyes are directly related to the intramolecular charge transfer (ICT) from the donor to the acceptor moiety. This ICT makes that the dyes present high molar extinction coefficients.

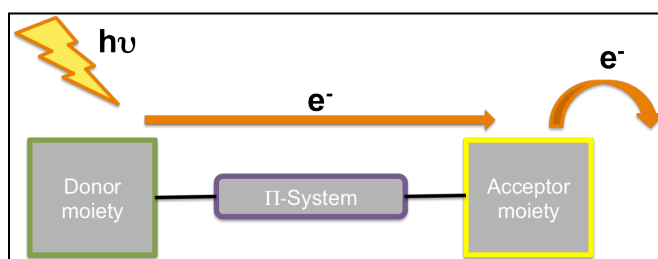


Figure 1.7: Structure of D- π -A dyes

These dyes with easy-to-tune absorption and high molecular extinction coefficients are a good alternative for Ruthenium complexes.

The design of these push-pull dyes is very important in order to achieve good results; otherwise organic dyes lie below the efficiency values obtained with Ruthenium complexes. For example, it is paramount to have a very good donor moiety, which remains stable when oxidised upon light irradiation. For example the use of oligoenes by Hara and co-workers, displayed efficiencies about 6% but the use of coumarin as donor moieties increased the efficiency up to 8.2²¹⁻

23

In 2008 Professor Grätzel and co-workers published the **D205** dye (Figure 1.8) achieving an efficiency of 9.52% ($J_{sc}=18.7\text{mA/cm}^2$, $V_{oc}=710\text{mV}$, $FF= 0.71$). The structure of this dye shows an indoline group with an n-octyl moiety onto the rhodanine structure. The key issue, to include this long alkyl chain, was/is to decrease the dye aggregation and to make more soluble the molecule in organic solvents. The control over the formation of aggregates is an important issue for organic sensitizers in order to obtain excellent performances. In this particular work, they observed that the combination of a long alkyl chain and the use of CDCA lead to outstanding increase in efficiency²⁴.

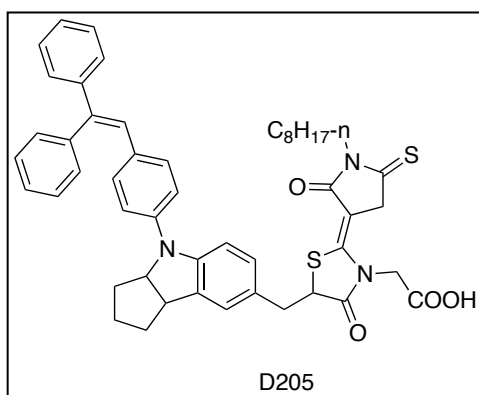


Figure 1.8: D205 molecular structure

Much recently, in 2010, Prof. Peng Wang and co-workers reported the **C219** dye (Figure 1.9) reaching, for the first time, efficiencies close or above 10%. The **C219** was reported to deliver an efficiency of 10.1% ($J_{sc}=17.9\text{mA/cm}^2$, $V_{oc}=770\text{mV}$, $FF= 0.73$). This novel dye consists in a binary π spacer: a 3,4-ethylenedioxythiophene unit (EDOT) connected to the donor moiety (alkoxy-substituted triphenylamine) to lift the HOMO and dihexyl-substituted dithienosilole (DTS) attached to the acceptor to achieve an appropriate LUMO²⁵.

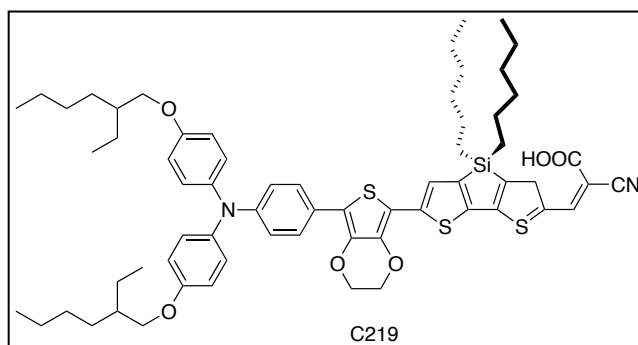


Figure 1.9: Molecular structures of C219

It is important to notice that until this year this moment all the best devices were fabricated using iodide/triiodide electrolyte. Yet, in 2010 a Cobalt²⁺/Cobalt³⁺ electrolyte was used for DSSC with a remarkable efficiency of 6.2% as reported by Hagfeldt, Sun and co-workers for the **D35** dye (Figure 1.10). In their work they synthesized two new sensitizers the **D35** and the **D29** with the same π -bridge and identical acceptor moiety but with a different donor group. For the **D29** dye the electron donating group was the group p-N,N-dimethylaminelnyl at the TPA moiety (triphenylamine) and for the **D35** it was the o,p-dibutoxypheny grup at the TPA. These two dyes were investigated to compare the effect of bulky alkoxy substituents in devices employing Cobalt electrolyte. For this, a series of cobalt electrolytes were synthesized to optimize the best one for use in the device and the election was done tacking into account the different oxidential potentials of the different cobalt complexes to achieve efficient dye regeneration and higher V_{oc} .²⁶

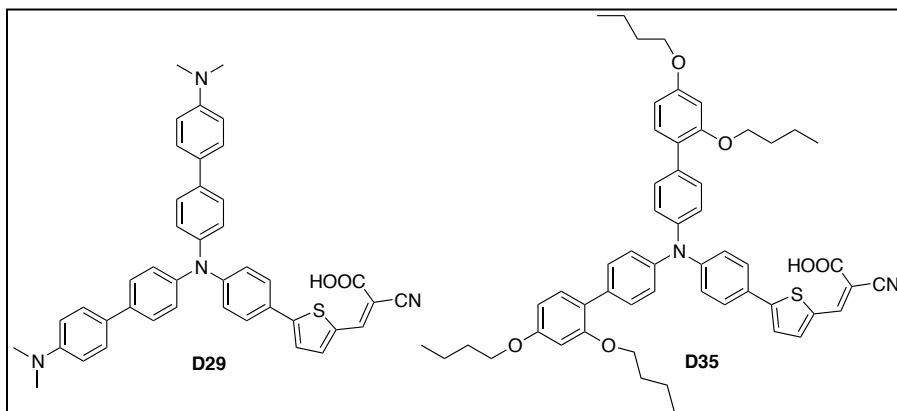


Figure 1.10: Molecular structures of C219

Professor Peng Wang and co-workers reported the sensitizer **C218** (Figure 1.11) which introduced the 4,4-dihexyl-4H-cyclopenta[2,1-b:3,4-b']dithiophene (CPDT) group, as a conjugated spacer to achieve a high molar absorption coefficient with an outstanding record efficiency of 8.95% ($J_{sc}=15.8\text{mA}/\text{cm}^2$, $V_{oc}=768\text{mV}$, $FF=0.74$) using iodine electrolyte²⁷. Thereafter, Professor Peng wang reported the same dye comparing their device performance in the same conditions with iodine/iodide and Cobalt electrolytes achieving 7.1% ($J_{sc}=13.6\text{mA}/\text{cm}^2$, $V_{oc}=720\text{mV}$, $FF=0.71$) and 8.3% respectively ($J_{sc}=14.1\text{mA}/\text{cm}^2$, $V_{oc}=820\text{mV}$, $FF=0.73$)²⁸. Showing that using cobalt electrolyte make to increase to V_{oc} in 100mV. The dye efficiency was improved to 9.4% ($J_{sc}=13.0\text{mA}/\text{cm}^2$, $V_{oc}=950\text{mV}$, $FF=0.76$)²⁹ just one year later, in 2012.

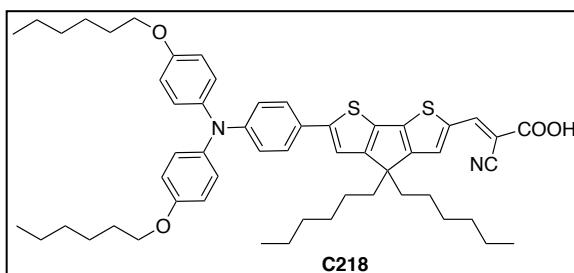


Figure 1.11: The C218 dye molecular structure.

Professor Peng Wang and his group focussed on the synthesis of organic dyes for DSSC in order to achieve record efficiencies by using Cobalt electrolytes and, in 2011, reported a new dye called the **C229** (Figure 1.12) with a similar structure as the C218 dye, however, in that work they decided to enlarge the π spacer introducing two thiophenes units and, thus, increasing the molar absorption coefficient owing a better delocalizability of π spacer. Meanwhile, the efficiency achieved using iodine/iodide electrolyte was just about 6.7% ($J_{sc}=15.20\text{mA/cm}^2$, $V_{oc}=680\text{mV}$, $FF= 0.65$). Nevertheless, in the same conditions with the cobalt electrolyte they reached 9.4% ($J_{sc}=15.3\text{mA/cm}^2$, $V_{oc}=850\text{mV}$, $FF= 0.73$)³⁰.

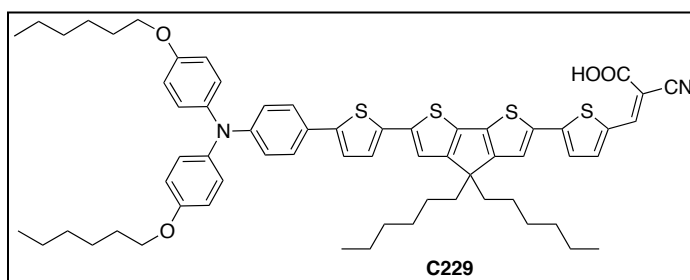


Figure 1.12: The dye C229 molecular structure.

Professor Michael Grätzel and co-workers reported also in 2011 the Y123 dye with the highest device performance using cobalt electrolyte reaching 9.6% in their champion cell³¹ (Figure 1.13). Later in 2012 other study with this dye was reported for high open circuit Voltage with an impressive V_{oc} of 1V just by using a Cobalt electrolyte³².

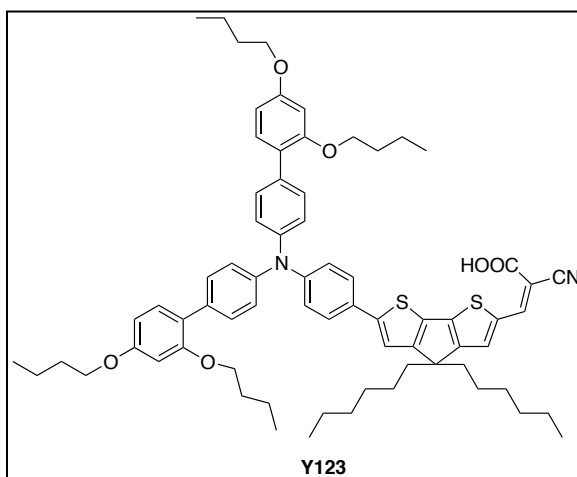


Figure 1.13: The dye Y123 molecular structure.

1.2.6 Porphyrins.

Porphyrins consist on a tetra pyrrole macrocycle composed of four modified pyrrole connected at carbon α by methine (Figure 1.14). Porphyrins follow Huckel's rule of aromaticity (possessing $4n+2$ π electrons). This feature makes porphyrins outstanding dyes with a high molecular extinction coefficient and also is responsible for the nice colours that often porphyrin solutions have³³. Porphyrins are present in nature in many biological systems as chlorophyll, hemoglobine, cytochromes, and many enzymes too. Due to their excellent optical properties porphyrins are used in medicine³⁴⁻³⁶, in electronic³⁷⁻³⁹ devices and due to their role in photosynthesis these molecules have been a long-standing promise for efficient organic photovoltaic devices^{40,41}.

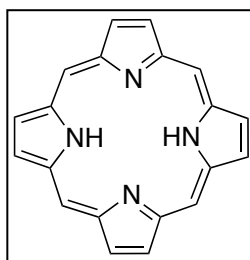


Figure 1.14: Basic core at the porphyrin molecules.

The typical absorption profile in porphyrins consists of an intense absorption band close to 400nm called Soret band and moderate absorption bands between 500 and 700nm³³. In order to use these molecules for DSSC applications one point to take in account is that the molecule requires an anchoring group to attach in the semiconductor as in the case of the previous discussed organic dyes. The structure of porphyrins presents different positions to functionalize them. Four meso-positions and eight β -positions (figure 1.15) to attach the anchoring group, that in case of porphyrins the carboxylic acid is also considered the best^{42,43}.

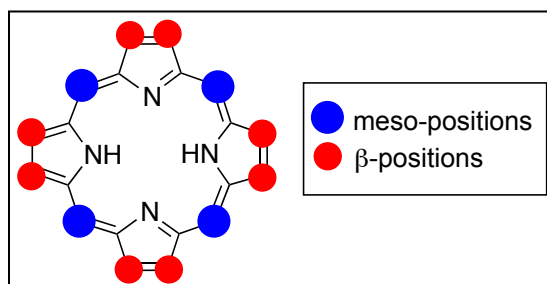


Figure 1.15: Available positions to functionalize porphyrins.

During the last decades many porphyrins have been synthesized for DSSC applications, with functionalization in the β and in meso-positions. The first remarkable example was the work by Professor Michael Grätzel and Professor Kay in 1993 with a modest efficiency of 2.6%⁴⁴. Analogously, the first example for meso-position substituted porphyrin was published by Professor Cherian and Professor Wamser in 2000 with an efficiency of 3.5%⁴⁵.

During the last years several works with different porphyrins have been published in order to increase the efficiency, minimizing dye aggregation, and achieve good charge separation^{46,47}. Nonetheless, it was not until the research groups of Professor Yeh and Professor Diau added a donor group in a porphyrin structure, as in the case of **YD1** and **YD2** (figure 1.16) when the efficiency increased by a factor of 5 or 6, adding a donor group at the porphyrin core did extend the absorption and improved the charge separation efficiency⁴⁸.

These groups tried to solve some aggregation problems too by adding different concentrations of chenodeoxycholic acid (CDCA) ⁴⁹.

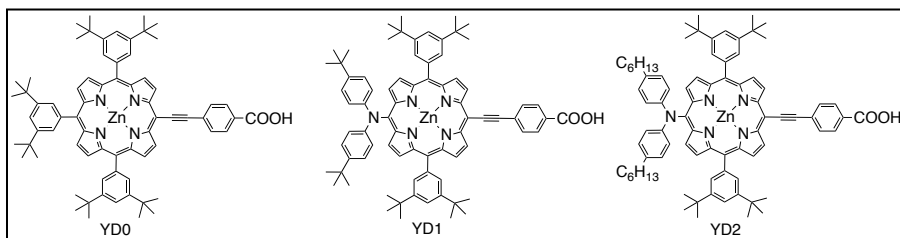


Figure 1.16: Dye molecular structures for YD1 and YD2.

In their work, it was synthesized the dye **YD0** (used as a reference) and the dyes **YD1** and **YD2**. The devices were made using different concentrations of CDCA. The dye **YD2** exhibited a cell performance close to 6.8% ($J_{sc}=13.7\text{mA/cm}^2$, $V_{oc}=711\text{mV}$, $FF= 0.69$). This efficiency is slightly smaller comparing the Ruthenium paradigm, **N719** 7.3% ($J_{sc}=13.8\text{mA/cm}^2$, $V_{oc}=760\text{mV}$, $FF= 0.70$). The high efficiencies were obtained with **YD2** and **YD1** compared with the **YD0** due to the slower recombination of the electrons with the oxidised electrolyte. In 2010 the device performance for **YD2** was improved by Professor Grätzel and co-workers exhibiting an overall efficiency of 10.9% ($J_{sc}=18.6\text{mA/cm}^2$, $V_{oc}=770\text{mV}$, $FF= 0.76$)⁵⁰.

During 2011, some porphyrins had been synthesised trying to achieve greater efficiencies than the dye **YD2**⁵¹⁻⁵⁷. However, it was not possible until the end of 2011 when Dr. Aswani Yella and co-workers⁵⁸ published the new record porphyrin: The dye **YD2-0-C8** (figure 1.17).

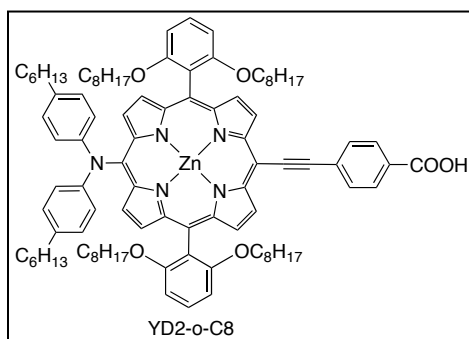


Figure 1.17: Molecular structure of YD2-o-C8

The structure of this porphyrin was similar to the **YD2** with the difference that new one incorporates two octyloxy groups in the ortho positions of each meso-phenyl ring increasing the electronic density on the porphyrin π -system compared to the **YD2** dye. This increase in electronic density is directly related to the LUMO level that now lies at higher energy. With this new dye, very promising results have been achieved using Cobalt electrolyte in D- π -A porphyrins making devices that achieved a record in efficiency of 11.9% (J_{sc} =17.3mA/cm², V_{oc} =965mV, FF= 0.71). This new value is higher than the previous record achieved with organic dyes³¹. In the same work, trying to increase the efficiency, the group added a co-sensitizer. The dye used for the “cocktail” was the **Y123**. They achieved a remarkable efficiency of 12.3% (J_{sc} =17.7mA/cm², V_{oc} =935mV, FF= 0.74).

The same group carried out further efforts to increase the efficiency achieved by using the dye **YD2-o-C8** and in 2014 they published two new porphyrins the **GY21** and **GY50** (Figure 1.18). In this work their strategy was the introduction of the benzothiadazole (BDT) unit as π -conjugated linker between the anchoring group and the porphyrin core to broaden the absorption spectra. Moreover, in this structure it was also introduced a phenyl group as a spacer between the BDT moiety and the carboxylic group.

The photovoltaic devices were made using Cobalt electrolyte due the high performance achieved for the **YD2-o-C8** dye. The results for **GY21** and **GY50** were 2.5% ($J_{sc}=5.03\text{mA/cm}^2$, $V_{oc}=615\text{mV}$, $FF= 0.80$) and 12.75% ($J_{sc}=18.53\text{mA/cm}^2$, $V_{oc}=885\text{mV}$, $FF= 0.77$) respectively.

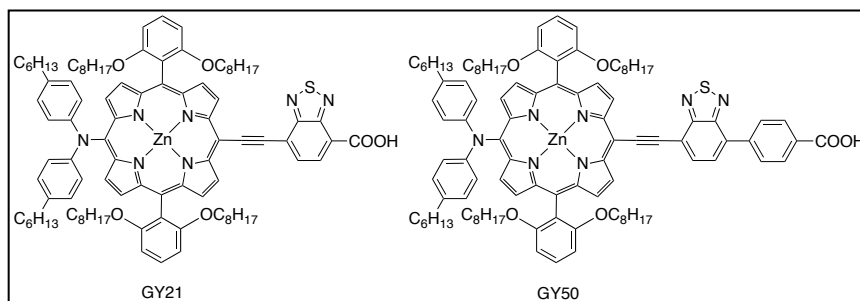


Figure 1.18: Molecular structure of GY21 and GY50

In one hand, the higher efficiency achieved with the **GY50** is due to the panchromatic absorption, which avoids the use of a secondary dye.

On the other hand, the lower conversion efficiency for **GY21** compared to **GY50** is due to the lack of directionality of the excited state and, thus, the observation of much less photocurrent⁵⁹.

During the same year different studies on porphyrins have been published too. For example the work presented by Professor Chin-Li Wang and co-workers where they synthesized a new porphyrin the, **LD31** and the **LD14**⁶⁰, inserting between the donor unit and the core porphyrin an ethynyl-anthracenyl moiety to extend the π -conjugation in order to improve light-harvesting efficiency⁵¹ (figure 1.19).

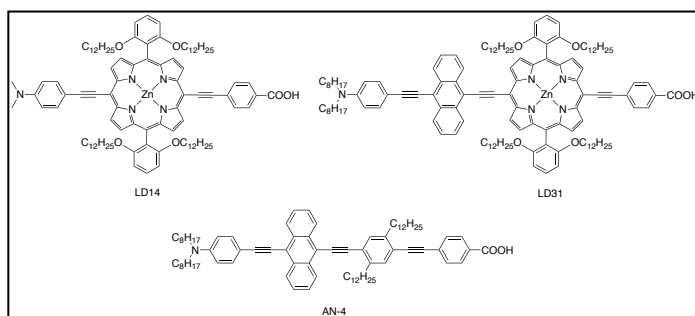


Figure 1.19: Molecular structures of LD14, LD31 and AN-4

The new porphyrins with and without the use of co-sensitization with the dye **AN-4** achieved 9.95% ($J_{sc}=20.02\text{mA}/\text{cm}^2$, $V_{oc}=699\text{mV}$, $FF=0.71$) and 10.3% ($J_{sc}=20.3\text{mA}/\text{cm}^2$, $V_{oc}=704\text{mV}$, $FF=0.72$) respectively.

Finally, this year, 2014, it was reported the champion molecule for DSSC achieving a power conversion of 13% by the group of Professor Michael Grätzel and co-workers. In that work they synthesized two new porphyrins called **SM371** and **SM315** (Figure 1.20)

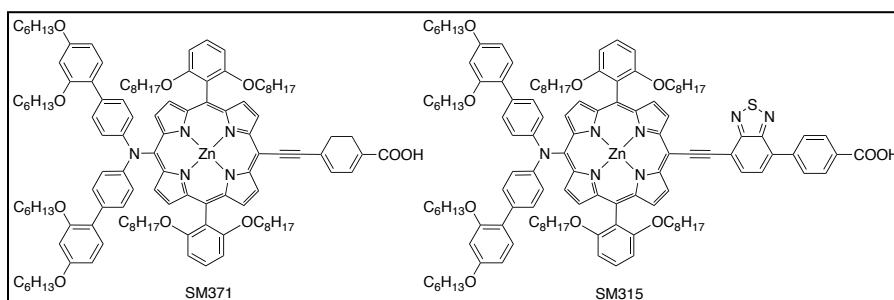


Figure 1.20: Molecular structures of SM371 and SM315

The structure of these porphyrins is similar to the previously reported Professor Grätzel and co-workers (**GY21** and **GY50**). However in that case, they use as donor moiety the bis (2',4'-bis(hexyloxy)-[1,1'-biphenyl]-4-yl)amine. This donor group has been used before in several organic dyes reporting good efficiencies in DSSC based on cobalt electrolyte^{26,31}. The efficiencies achieved for **SM371**

and **SM315** are 12% ($J_{sc}=15.9\text{mA/cm}^2$, $V_{oc}=960\text{mV}$, $FF= 0.79$) and 13.0% ($J_{sc}=18.1\text{mA/cm}^2$, $V_{oc}=910\text{mV}$, $FF= 0.78$) respectively using cobalt electrolyte. The higher J_{sc} obtained by SM315 is due to the dramatically improved absorption properties that lead to a high IPCE with an 80% across all visible wavelength (450nm-750nm). A small difference of just 50mV at the V_{oc} under standard irradiation conditions is observed between these two porphyrins presenting **SM371** higher voltage compared to the **SM315**. In their studies they observed that the electron lifetime is 6 times slower for the **SM371** dye. The slower recombination kinetics is likely to be produced by the BDT unit which improves the excited state directionality and prevents also back electron transfer to the oxidised electrolyte⁶¹.

In the following figure (figure 1.21) we can observe how has been the evolution of photovoltaic performances of DSSC from 1991 to 2014 showing the most important family of dyes explained above.

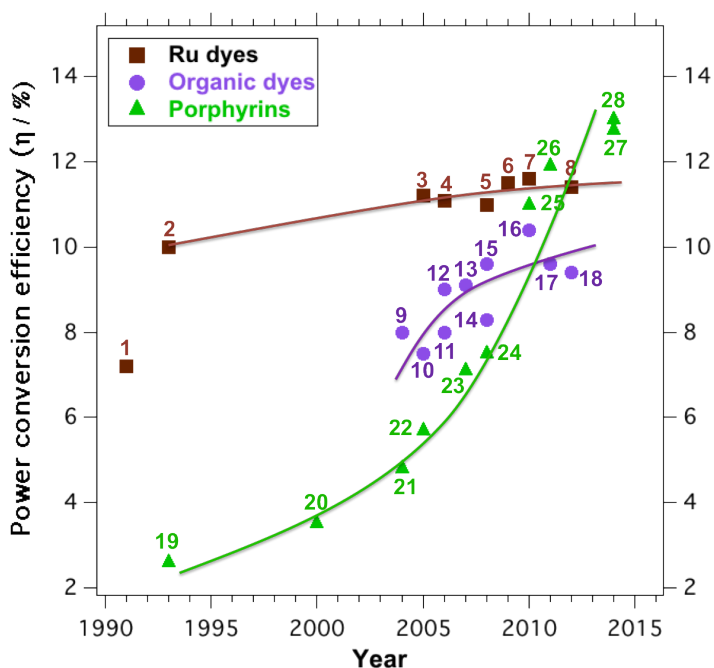


Figure 1.21: Progress on DSSC efficiency of the most relevant dyes involving Ruthenium complexes (1-8); organic dyes (9-18) and porphyrins (19-28). 1.-trinuclear

trinuclear $\text{RuL}_2(\mu\text{-(CN)Ru(CN)L}_2)_2$ ⁹; **2.**-N3¹³; **3.**-N3¹²; **4.**-N719¹⁶; **5.**-C101¹⁷; **6.**-CYC-B11¹⁹; **7.**-C106²⁰; **8.**-Black dye¹⁵; **9.**-Indoline dye⁶²; **10.**-NKX-2677⁶³; **11.**-JK2⁶⁴; **12.**-D149⁶⁵; **13.**-TA-St-CA⁶⁶; **14.**-MK-2⁶⁷; **15.**-D205²⁴; **16.**-C219²⁵; **17.**-Y123³¹; **18.**-C218²⁹; **19.**-Cu-a-oxymesoisichlorin⁴⁴; **20.**- TCPP⁴⁵; **21.**-Zn-1a⁶⁸; **22.**-Zn-3⁶⁹; **23.**-GD2⁷⁰; **24.**-tda-2b-bd-Zn⁷¹; **25.**-YD2⁵⁰; **26.**-YD2oC8⁵⁸; **27.**-GY50⁵⁹; **28.**-SM371⁶¹

Another promising molecular solar cells studied in our group are the OSC (organic solar cells). In this Thesis the Chapter 5 shows my input to this field under Professor Palomares supervision.

Below is shown a short but detailed explanation about the fundamentals of OSC.

1.3 ORGANIC SOLAR CELLS (OSC)

OSC combine the use of two organic materials an electron donor or hole transport material (HTM) and an electron acceptor material or electron transport material (ETM), which are “sandwiched” between to metal electrodes with different work function (Figure 1.22). The photo-induced charges are separated at the interface between both type of organic materials and the free carriers are collected selectively at each electrode.

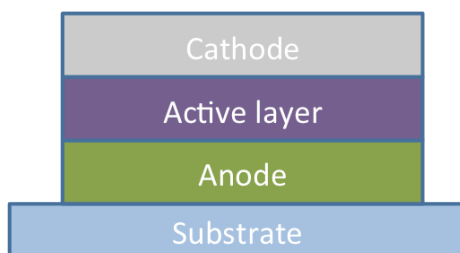


Figure 1.22: Schematic representation of the most simple OSC.

The electron-hole pairs (so called excitons) are generated upon irradiation of the solar cells and their lifetime is short being able to being transported a few nanometers (10-12nm) depending on the nature of the organic material. When the exciton arrives at the interface of both organic materials it separates in free

carriers of different charge (so called polarons). The polarons must be transported before they can recombine to the contact electrodes (Figure 1.23).

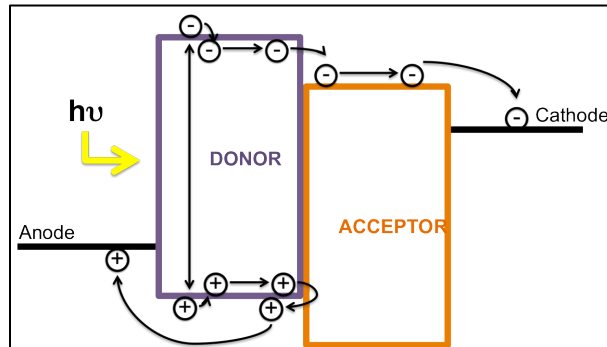


Figure 1.23: Schematic principle operation of OPV

Thus, the efficient formation of excitons as well as the optimization of the exciton separation and polaron collection is key to achieve excellent device performance. A first approach is to select the adequate donor and acceptor materials with sufficient energy onset to be able to separate efficiently the charges at the interface. For this reason, the study of new materials and the morphology at the nanoscale have attracted much attention in recent years. From the original device in the eighties by Professor Tang (Figure 1.24), with efficiencies as low as 1%⁷² by using a bi-layer type device to the actual bulk-heterojunction solar cells, that mixes both type of organic materials, a great quantum leap in efficiency has been achieved to almost 10% for single junction solar cells.

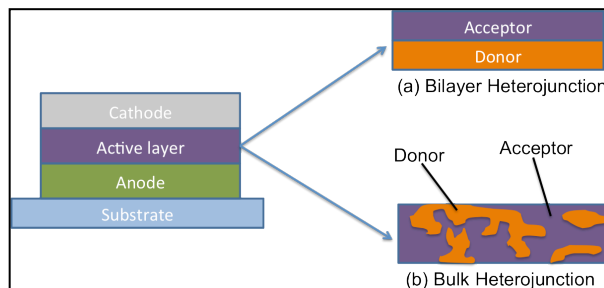


Figure 1.24: Architecture structure of a bilayer heterojunction (a) and a bulk heterojunction (b)

Chapter 1

1.3.1 Donor and Acceptor Materials

Here, in this section, we describe briefly the most relevant materials used in OSC.

1.3.1.1 Electron Acceptor Materials:

The fullerenes and their derivatives are the dominating molecules used as electron acceptor materials in OSC. The use of these type of molecules is justified due to their strong capability to accept electrons from donor materials and also their electron mobility⁷³. The derivatives of C₆₀ and C₇₀ as PC₆₁BM and PC₇₁BM are the most used in solution processed OPVs (Figure 1.25).

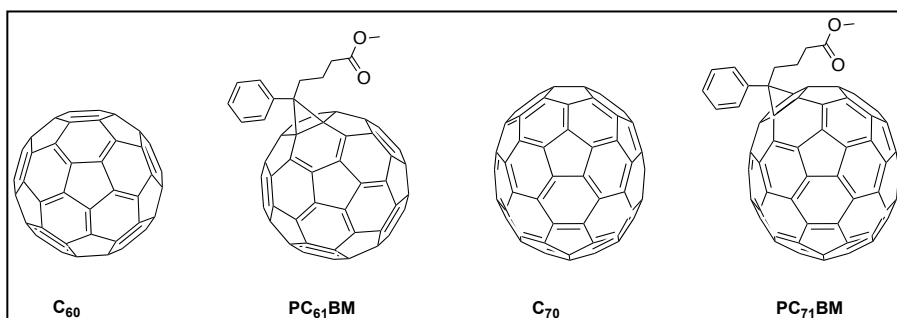


Figure 1.25: Principals fullerenes used as acceptor moieties

1.3.1.2 Electron Donor Materials:

The electron donor materials have been much more explored as they are used as the main light-harvesting moiety in the OSC. Several type of molecules have been designed and synthesized for their applications in solution processed OSC as squaraines (SQ)⁷⁴⁻⁷⁸, diketo-pyrrolopyrroles (DPP)⁷⁹⁻⁸¹, BODIPY⁸² and also D- π -A dyes bearing triphenylamine units as secondary electron donor⁸³⁻⁸⁵ all of them with efficiencies ranging between 4% to 6% under standard illumination conditions of 1 sun (100mW/cm² of sun simulated light 1.5AM G spectrum)

Nowadays, the best reported OSC using small molecules for single junction devices is the work by C. Bazan and Alan J. Heeger at University of California (USA) that has achieved an impressive 8.9%(figure 1.26)⁸⁶.

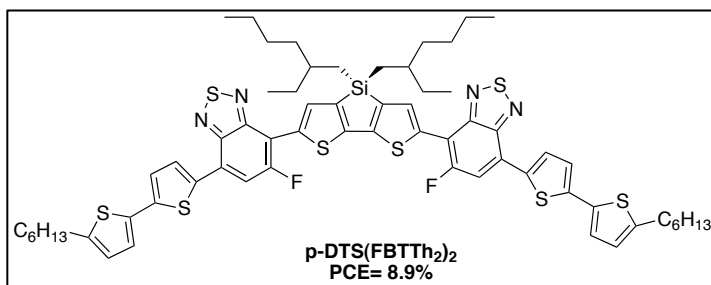


Figure 1.26: Molecular structure of p-DTS(FBTTh₂)₂

Alternatively, porphyrins (POR) have been also widely studied and used in many BHJ-OSC⁸⁷⁻⁹¹. Professor Xiaobin Peng and co-workers have published in 2014 the best porphyrin for solution-processed BHJ OSC based in small molecule with an efficiency up to 7.23% (J_{sc} =16.0mA/cm², V_{oc} =710mV, FF= 0.63)⁹².

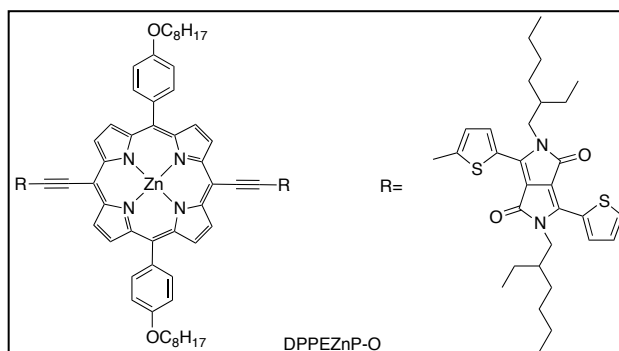


Figure1.27: Molecular structure of DPPEZnP-O

1.4 AIM OF THIS THESIS

Dye Sensitized Solar Cells and Organic Solar Cells have great much attention during the last decades as molecular photovoltaic devices that hold the long-standing promise for inexpensive light-to-energy conversion devices. In both technologies the organic dyes play a very important role. The molecules structure and their physical properties determine the overall device efficiency.

In this Thesis a series of new sensitizers have been design and synthesized in order to study their applications in DSSC and OSC photovoltaics. Furthermore, the study about the relationship between the molecules structure, the film morphology in the case of OSC of these novel sensitizers and the device performance has been also studied.

1.5 REFERENCES

- (1) <http://www.instituteforenergyresearch.org/2013/06/27/statistical-review-of-world-energy-2013-viva-la-shale-revolucion/>.
- (2) <http://www.eia.gov/forecasts/AEO/>.
- (3) <http://www.treehugger.com/slideshows/energy-efficiency/all-solar-efficiency-breakthroughs-single-chart/>.
- (4) Martinson, A. B. F.; Hamann, T. W.; Pellin, M. J.; Hupp, J. T. *Chemistry – A European Journal* **2008**, 14, 4458.
- (5) Fung, A. K. M.; Chiu, B. K. W.; Lam, M. H. W. *Water Research* **2003**, 37, 1939.
- (6) Zaban, A.; Ferrere, S.; Gregg, B. A. *The Journal of Physical Chemistry B* **1998**, 102, 452.
- (7) Hagberg, D. P.; Yum, J.-H.; Lee, H.; De Angelis, F.; Marinado, T.; Karlsson, K. M.; Humphry-Baker, R.; Sun, L.; Hagfeldt, A.; Grätzel, M.; Nazeeruddin, M. K. *Journal of the American Chemical Society* **2008**, 130, 6259.
- (8) Neale, N. R.; Kopidakis, N.; van de Lagemaat, J.; Grätzel, M.; Frank, A. J. *The Journal of Physical Chemistry B* **2005**, 109, 23183.
- (9) O'Regan, B.; Gratzel, M. *Nature* **1991**, 353, 737.
- (10) Polson, M. I. J.; Medlycott, E. A.; Hanan, G. S.; Mikelsons, L.; Taylor, N. J.; Watanabe, M.; Tanaka, Y.; Loiseau, F.; Passalacqua, R.; Campagna, S. *Chemistry – A European Journal* **2004**, 10, 3640.
- (11) Hagfeldt, A.; Graetzel, M. *Chemical Reviews* **1995**, 95, 49.
- (12) Nazeeruddin, M. K.; De Angelis, F.; Fantacci, S.; Selloni, A.; Viscardi, G.; Liska, P.; Ito, S.; Takeru, B.; Grätzel, M. *Journal of the American Chemical Society* **2005**, 127, 16835.
- (13) Nazeeruddin, M. K.; Kay, A.; Rodicio, I.; Humphry-Baker, R.; Mueller, E.; Liska, P.; Vlachopoulos, N.; Graetzel, M. *Journal of the American Chemical Society* **1993**, 115, 6382.
- (14) Péchy, P.; Renouard, T.; Zakeeruddin, S. M.; Humphry-Baker, R.; Comte, P.; Liska, P.; Cevey, L.; Costa, E.; Shklover, V.; Spiccia, L.; Deacon, G. B.; Bignozzi, C. A.; Grätzel, M. *Journal of the American Chemical Society* **2001**, 123, 1613.
- (15) Han, L.; Islam, A.; Chen, H.; Malapaka, C.; Chiranjeevi, B.; Zhang, S.; Yang, X.; Yanagida, M. *Energy & Environmental Science* **2012**, 5, 6057.
- (16) Wang, Q.; Ito, S.; Grätzel, M.; Fabregat-Santiago, F.; Mora-Seró, I.; Bisquert, J.; Bessho, T.; Imai, H. *The Journal of Physical Chemistry B* **2006**, 110, 25210.
- (17) Gao, F.; Wang, Y.; Shi, D.; Zhang, J.; Wang, M.; Jing, X.; Humphry-Baker, R.; Wang, P.; Zakeeruddin, S. M.; Grätzel, M. *Journal of the American Chemical Society* **2008**, 130, 10720.

- (18) Chen, C.-Y.; Wu, S.-J.; Wu, C.-G.; Chen, J.-G.; Ho, K.-C. *Angewandte Chemie International Edition* **2006**, 45, 5822.
- (19) Chen, C.-Y.; Wang, M.; Li, J.-Y.; Pootrakulchote, N.; Alibabaei, L.; Ngoc-le, C.-h.; Decoppet, J.-D.; Tsai, J.-H.; Grätzel, C.; Wu, C.-G.; Zakeeruddin, S. M.; Grätzel, M. *ACS Nano* **2009**, 3, 3103.
- (20) Yu, Q.; Wang, Y.; Yi, Z.; Zu, N.; Zhang, J.; Zhang, M.; Wang, P. *ACS Nano* **2010**, 4, 6032.
- (21) Clifford, J. N.; Yahioğlu, G.; Milgrom, L. R.; Durrant, J. R. *Chemical Communications* **2002**, 1260.
- (22) Hara, K.; Sato, T.; Katoh, R.; Furube, A.; Yoshihara, T.; Murai, M.; Kurashige, M.; Ito, S.; Shinpo, A.; Suga, S.; Arakawa, H. *Advanced Functional Materials* **2005**, 15, 246.
- (23) Wang, Z.-S.; Cui, Y.; Dan-oh, Y.; Kasada, C.; Shinpo, A.; Hara, K. *The Journal of Physical Chemistry C* **2007**, 111, 7224.
- (24) Ito, S.; Miura, H.; Uchida, S.; Takata, M.; Sumioka, K.; Liska, P.; Comte, P.; Péchy, P.; Grätzel, M. *Chemical Communications* **2008**, 5194.
- (25) Zeng, W.; Cao, Y.; Bai, Y.; Wang, Y.; Shi, Y.; Zhang, M.; Wang, F.; Pan, C.; Wang, P. *Chemistry of Materials* **2010**, 22, 1915.
- (26) Feldt, S. M.; Gibson, E. A.; Gabrielsson, E.; Sun, L.; Boschloo, G.; Hagfeldt, A. *Journal of the American Chemical Society* **2010**, 132, 16714.
- (27) Li, R.; Liu, J.; Cai, N.; Zhang, M.; Wang, P. *The Journal of Physical Chemistry B* **2010**, 114, 4461.
- (28) Zhou, D.; Yu, Q.; Cai, N.; Bai, Y.; Wang, Y.; Wang, P. *Energy & Environmental Science* **2011**, 4, 2030.
- (29) Xu, M.; Zhang, M.; Pastore, M.; Li, R.; De Angelis, F.; Wang, P. *Chemical Science* **2012**, 3, 976.
- (30) Bai, Y.; Zhang, J.; Zhou, D.; Wang, Y.; Zhang, M.; Wang, P. *Journal of the American Chemical Society* **2011**, 133, 11442.
- (31) Tsao, H. N.; Yi, C.; Moehl, T.; Yum, J.-H.; Zakeeruddin, S. M.; Nazeeruddin, M. K.; Grätzel, M. *ChemSusChem* **2011**, 4, 591.
- (32) Yum, J.-H.; Baranoff, E.; Kessler, F.; Moehl, T.; Ahmad, S.; Bessho, T.; Marchioro, A.; Ghadiri, E.; Moser, J.-E.; Yi, C.; Nazeeruddin, M. K.; Grätzel, M. *Nat Commun* **2012**, 3, 631.
- (33) Kadish, K. M. S., K.M.; Guillard, R., *The Porphyrin Handbook* **1999**.
- (34) Bonnett, R. *Chemical Society Reviews* **1995**, 24, 19.
- (35) Hamblin, M. R.; Hasan, T. *Photochemical & Photobiological Sciences* **2004**, 3, 436.
- (36) Henderson, B. W.; Dougherty, T. J. *Photochemistry and Photobiology* **1992**, 55, 145.
- (37) Di Natale, C.; Paolesse, R.; Macagnano, A.; Mantini, A.; Goletti, C.; D'Amico, A. *Sensors and Actuators B: Chemical* **1998**, 52, 162.

- (38) Di Natale, C.; Salimbeni, D.; Paolesse, R.; Macagnano, A.; D'Amico, A. *Sensors and Actuators B: Chemical* **2000**, 65, 220.
- (39) Xu, Y.; Zhao, L.; Bai, H.; Hong, W.; Li, C.; Shi, G. *Journal of the American Chemical Society* **2009**, 131, 13490.
- (40) Choi, M.-S.; Yamazaki, T.; Yamazaki, I.; Aida, T. *Angewandte Chemie International Edition* **2004**, 43, 150.
- (41) Gust, D.; Moore, T. A.; Moore, A. L. *Accounts of Chemical Research* **2009**, 42, 1890.
- (42) Campbell, W. M.; Burrell, A. K.; Officer, D. L.; Jolley, K. W. *Coordination Chemistry Reviews* **2004**, 248, 1363.
- (43) He, H.; Gurung, A.; Si, L. *Chemical Communications* **2012**, 48, 5910.
- (44) Kay, A.; Grätzel, M. *The Journal of Physical Chemistry* **1993**, 97, 6272.
- (45) Cherian, S.; Wamser, C. C. *The Journal of Physical Chemistry B* **2000**, 104, 3624.
- (46) Imahori, H.; Umeyama, T.; Ito, S. *Accounts of Chemical Research* **2009**, 42, 1809.
- (47) Radivojevic, I.; Varotto, A.; Farley, C.; Drain, C. M. *Energy & Environmental Science* **2010**, 3, 1897.
- (48) Hsieh, C.-P.; Lu, H.-P.; Chiu, C.-L.; Lee, C.-W.; Chuang, S.-H.; Mai, C.-L.; Yen, W.-N.; Hsu, S.-J.; Diau, E. W.-G.; Yeh, C.-Y. *Journal of Materials Chemistry* **2010**, 20, 1127.
- (49) Lin, C.-Y.; Lo, C.-F.; Luo, L.; Lu, H.-P.; Hung, C.-S.; Diau, E. W.-G. *The Journal of Physical Chemistry C* **2008**, 113, 755.
- (50) Bessho, T.; Zakeeruddin, S. M.; Yeh, C.-Y.; Diau, E. W.-G.; Grätzel, M. *Angewandte Chemie International Edition* **2010**, 49, 6646.
- (51) Chang, Y.-C.; Wang, C.-L.; Pan, T.-Y.; Hong, S.-H.; Lan, C.-M.; Kuo, H.-H.; Lo, C.-F.; Hsu, H.-Y.; Lin, C.-Y.; Diau, E. W.-G. *Chemical Communications* **2011**, 47, 8910.
- (52) Lee, M. J.; Seo, K. D.; Song, H. M.; Kang, M. S.; Eom, Y. K.; Kang, H. S.; Kim, H. K. *Tetrahedron Letters* **2011**, 52, 3879.
- (53) Orbelli Biroli, A.; Tessore, F.; Pizzotti, M.; Biaggi, C.; Ugo, R.; Caramori, S.; Aliprandi, A.; Bignozzi, C. A.; De Angelis, F.; Giorgi, G.; Licandro, E.; Longhi, E. *The Journal of Physical Chemistry C* **2011**, 115, 23170.
- (54) Pasunooti, K. K.; Song, J.-L.; Chai, H.; Amaladass, P.; Deng, W.-Q.; Liu, X.-W. *Journal of Photochemistry and Photobiology A: Chemistry* **2011**, 218, 219.
- (55) Warnan, J.; Buchet, F.; Pellegrin, Y.; Blart, E.; Odobel, F. *Organic Letters* **2011**, 13, 3944.
- (56) Xiang, N.; Zhou, W.; Jiang, S.; Deng, L.; Liu, Y.; Tan, Z.; Zhao, B.; Shen, P.; Tan, S. *Solar Energy Materials and Solar Cells* **2011**, 95, 1174.

(57) Zhou, W.; Zhao, B.; Shen, P.; Jiang, S.; Huang, H.; Deng, L.; Tan, S. *Dyes and Pigments* **2011**, 91, 404.

(58) Yella, A.; Lee, H.-W.; Tsao, H. N.; Yi, C.; Chandiran, A. K.; Nazeeruddin, M. K.; Diau, E. W.-G.; Yeh, C.-Y.; Zakeeruddin, S. M.; Grätzel, M. *Science* **2011**, 334, 629.

(59) Yella, A.; Mai, C.-L.; Zakeeruddin, S. M.; Chang, S.-N.; Hsieh, C.-H.; Yeh, C.-Y.; Grätzel, M. *Angewandte Chemie International Edition* **2014**, 53, 2973.

(60) Wang, C.-L.; Hu, J.-Y.; Wu, C.-H.; Kuo, H.-H.; Chang, Y.-C.; Lan, Z.-J.; Wu, H.-P.; Wei-Guang Diau, E.; Lin, C.-Y. *Energy & Environmental Science* **2014**, 7, 1392.

(61) Mathew, S.; Yella, A.; Gao, P.; Humphry-Baker, R.; Curchod/Basile, F. E.; Ashari-Astani, N.; Tavernelli, I.; Rothlisberger, U.; Nazeeruddin/Md, K.; Grätzel, M. *Nat Chem* **2014**, 6, 242.

(62) Horiuchi, T.; Miura, H.; Sumioka, K.; Uchida, S. *Journal of the American Chemical Society* **2004**, 126, 12218.

(63) Hara, K.; Wang, Z.-S.; Sato, T.; Furube, A.; Katoh, R.; Sugihara, H.; Dan-oh, Y.; Kasada, C.; Shinpo, A.; Suga, S. *The Journal of Physical Chemistry B* **2005**, 109, 15476.

(64) Kim, S.; Lee, J. K.; Kang, S. O.; Ko, J.; Yum, J. H.; Fantacci, S.; De Angelis, F.; Di Censo, D.; Nazeeruddin, M. K.; Grätzel, M. *Journal of the American Chemical Society* **2006**, 128, 16701.

(65) Ito, S.; Zakeeruddin, S. M.; Humphry-Baker, R.; Liska, P.; Charvet, R.; Comte, P.; Nazeeruddin, M. K.; Péchy, P.; Takata, M.; Miura, H.; Uchida, S.; Grätzel, M. *Advanced Materials* **2006**, 18, 1202.

(66) Hwang, S.; Lee, J. H.; Park, C.; Lee, H.; Kim, C.; Park, C.; Lee, M.-H.; Lee, W.; Park, J.; Kim, K.; Park, N.-G.; Kim, C. *Chemical Communications* **2007**, 4887.

(67) Wang, Z.-S.; Koumura, N.; Cui, Y.; Takahashi, M.; Sekiguchi, H.; Mori, A.; Kubo, T.; Furube, A.; Hara, K. *Chemistry of Materials* **2008**, 20, 3993.

(68) Nazeeruddin, M. K.; Humphry-Baker, R.; Officer, D. L.; Campbell, W. M.; Burrell, A. K.; Grätzel, M. *Langmuir* **2004**, 20, 6514.

(69) Wang, Q.; Campbell, W. M.; Bonfantani, E. E.; Jolley, K. W.; Officer, D. L.; Walsh, P. J.; Gordon, K.; Humphry-Baker, R.; Nazeeruddin, M. K.; Grätzel, M. *The Journal of Physical Chemistry B* **2005**, 109, 15397.

(70) Campbell, W. M.; Jolley, K. W.; Wagner, P.; Wagner, K.; Walsh, P. J.; Gordon, K. C.; Schmidt-Mende, L.; Nazeeruddin, M. K.; Wang, Q.; Grätzel, M.; Officer, D. L. *The Journal of Physical Chemistry C* **2007**, 111, 11760.

(71) Park, J. K.; Lee, H. R.; Chen, J.; Shinokubo, H.; Osuka, A.; Kim, D. *The Journal of Physical Chemistry C* **2008**, 112, 16691.

- (72) Tang, C. W. *Applied Physics Letters* **1986**, 48, 183.
- (73) He, Y.; Li, Y. *Physical Chemistry Chemical Physics* **2011**, 13, 1970.
- (74) Bagnis, D.; Beverina, L.; Huang, H.; Silvestri, F.; Yao, Y.; Yan, H.; Pagani, G. A.; Marks, T. J.; Facchetti, A. *Journal of the American Chemical Society* **2010**, 132, 4074.
- (75) Silvestri, F.; Irwin, M. D.; Beverina, L.; Facchetti, A.; Pagani, G. A.; Marks, T. J. *Journal of the American Chemical Society* **2008**, 130, 17640.
- (76) Viterisi, A.; Montcada, N. F.; Kumar, C. V.; Gispert-Guirado, F.; Martin, E.; Escudero, E.; Palomares, E. *Journal of Materials Chemistry A* **2014**, 2, 3536.
- (77) Wei, G.; Wang, S.; Sun, K.; Thompson, M. E.; Forrest, S. R. *Advanced Energy Materials* **2011**, 1, 184.
- (78) Wei, G.; Xiao, X.; Wang, S.; Zimmerman, J. D.; Sun, K.; Diev, V. V.; Thompson, M. E.; Forrest, S. R. *Nano Letters* **2011**, 11, 4261.
- (79) Lee, O. P.; Yiu, A. T.; Beaujuge, P. M.; Woo, C. H.; Holcombe, T. W.; Millstone, J. E.; Douglas, J. D.; Chen, M. S.; Fréchet, J. M. J. *Advanced Materials* **2011**, 23, 5359.
- (80) Tamayo, A. B.; Dang, X.-D.; Walker, B.; Seo, J.; Kent, T.; Nguyen, T.-Q. *Applied Physics Letters* **2009**, 94.
- (81) Walker, B.; Tamayo, A. B.; Dang, X.-D.; Zalar, P.; Seo, J. H.; Garcia, A.; Tantiwivat, M.; Nguyen, T.-Q. *Advanced Functional Materials* **2009**, 19, 3063.
- (82) Rousseau, T.; Cravino, A.; Bura, T.; Ulrich, G.; Ziessel, R.; Roncali, J. *Journal of Materials Chemistry* **2009**, 19, 2298.
- (83) Chiu, S.-W.; Lin, L.-Y.; Lin, H.-W.; Chen, Y.-H.; Huang, Z.-Y.; Lin, Y.-T.; Lin, F.; Liu, Y.-H.; Wong, K.-T. *Chemical Communications* **2012**, 48, 1857.
- (84) Lin, H.-W.; Lin, L.-Y.; Chen, Y.-H.; Chen, C.-W.; Lin, Y.-T.; Chiu, S.-W.; Wong, K.-T. *Chemical Communications* **2011**, 47, 7872.
- (85) Lin, L.-Y.; Chen, Y.-H.; Huang, Z.-Y.; Lin, H.-W.; Chou, S.-H.; Lin, F.; Chen, C.-W.; Liu, Y.-H.; Wong, K.-T. *Journal of the American Chemical Society* **2011**, 133, 15822.
- (86) Kyaw, A. K. K.; Wang, D. H.; Wynands, D.; Zhang, J.; Nguyen, T.-Q.; Bazan, G. C.; Heeger, A. J. *Nano Letters* **2013**, 13, 3796.
- (87) Hatano, J.; Obata, N.; Yamaguchi, S.; Yasuda, T.; Matsuo, Y. J. *Mater. Chem.* **2012**, 22, 19258.
- (88) Huang, Y.; Li, L.; Peng, X.; Peng, J.; Cao, Y. *Journal of Materials Chemistry* **2012**, 22, 21841.
- (89) Li, L.; Huang, Y.; Peng, J.; Cao, Y.; Peng, X. J. *Mater. Chem. A* **2012**, 1, 2144.

(90) Sharma, G. D.; Daphnomili, D.; Biswas, S.; Coutsolelos, A. G. *Organic Electronics* **2013**, 14, 1811.

(91) Shi, S.; Wang, X.; Sun, Y.; Chen, S.; Li, X.; Li, Y.; Wang, H. *Journal of Materials Chemistry* **2012**, 22, 11006.

(92) Qin, H.; Li, L.; Guo, F.; Su, S.; Peng, J.; Cao, Y.; Peng, X. *Energy & Environmental Science* **2014**, 7, 1397.

Chapter 2
Materials and Methods

Table of contents

2.1 Synthetic Methods	43
2.1.1 General reagents and solvents	43
2.1.2 General Instrumentation	43
2.2 Dye Sensitized solar cells	44
2.2.1 Films used	44
2.2.2 Device Fabrication	45
2.3 Organic Solar Cells	46
2.3.1 Device Fabrication	46
2.4 Device Characterization	47
2.4.1 Charge Extraction (CE)	47
2.4.2 Incident Photon to Current Efficiency (IPCE)	49
2.4.3 Solar Cell Power Conversion Efficiency (η)	49
2.4.4 Transient Photovoltage (TPV)	50
2.4.5 Laser Transient Absorption Spectroscopy (L-TAS)	50
2.5 References	52

2.1 SYNTHETIC METHODS

The reagents, solvents and the main equipment used in this Ph. D. Thesis are described in this section.

2.1.1 General reagents and solvents

All of the chemical reagents were purchased from Sigma-Aldrich®, Frontier Scientific Ltd., Lumtec Ltd or Alfa Aesar® and they were used without further purification. The dry solvents used for solvent-sensitive reactions were purchased from Sigma-Aldrich® and Flucka® and common solvents from SdS.

2.1.2 General Instrumentation

The ^1H and ^{13}C NMR samples were measured on a Bruker Advance 400 (400MHz for ^1H and 100MHz for ^{13}C). The deuterated solvents are indicated when used in the respective chapters and the chemical shifts (δ) are given in ppm, referenced to the solvent residual peak. Coupling constants (J) are given in Hz.

High resolution Mass Spectra (HR-MS) were carried out on a Waters LCT Premier liquid chromatograph coupled time-of-flight mass spectrometer (HPLC/MS-TOF), using electrospray ionization (ESI) as ionization mode. Matrix assisted laser desorption (MALDI) were recorded on a BRUKER Autoflex time-of-flight mass spectrometer.

Uv-Vis absorption spectra were measured in a 1 cm path-length quartz cell using a Shimadzu® model 1700 spectrophotometer. The steady state fluorescence spectra were recorded Spectrofluorimeter Fluorolog from Horiba Jobin Yvon Ltd. The system is composed by a continuum 450W Xenon lamp, double monochromator for excitation, a solid sample holder, and detection in Right Angle or Front Face mode and absorbance measurements. Two

detectors PMT(UV-vis) and InGaAs (NIR) allow fluorescence measurements in the wavelengths range of the UV-Visible and NIR from 250 to 1600 nm.

The electrochemical measurements were carried out employing a conventional three-electrode cell connected to a CH instrument 660c potentiostat-galvanostat. The working electrode consisted of a platinum wire or a carbon electrode and the counter electrode was a platinum mesh. The reference electrode was a Ag/AgCl electrode (saturated KCl). All solutions were degassed with Argon prior the use. All the measurements were recorded in presence of 0.1M TBAPF₆ supporting electrolyte, using ferrocene as an internal reference.

2.2 DYE SENSITIZED SOLAR CELLS (DSSC)

2.2.1 Films used

In this Ph.D. Thesis we used 2 different cells depending on the measurement carried out. For Laser Transient Absorption Spectroscopy (L-TAS) experiments we need highly transparent thin film devices with an active area of 1cm². These films were made screen-printing 4-6mm thick TiO₂ paste (Solaronix Ltd) and sensitized with the appropriated organic dye used in the studies. The other films we need are to optimize the device efficiency. For these films the active area is smaller (0.16cm²) to decrease the losses by series resistance that affects the device fill factor. As the same way like other films these are also done by screen printing technique depositing a layer of 9 to 16mm of TiO₂ of 20nm TiO₂ nanoparticles (Dyesol, and Solaronix paste) and an additional layer of 4mm thick made of 400nm diameter particles of TiO₂ (so called the scatter layer) and sensitized with the appropriated dye See Figure 2.1.

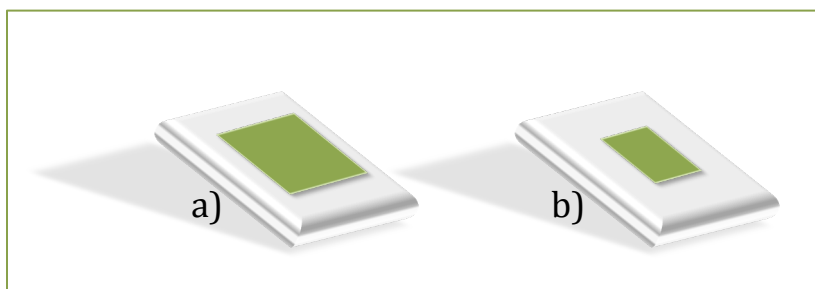


Figure 2.1: Scheme of different films used, a) Film for photophysical measurements and b) Film for device preparation

2.2.2 Device fabrication

The FTO (Fluorine doped tin oxide) glass (Hartford Glass inc. with $15 \Omega/\text{cm}^2$ resistance) was first cleaned three times; the first one in a detergent solution using an ultrasonic bath for 15 min, and then cleaned with ethanol two times. After, a treatment in a UV- O_3 system (PSD series UV-ozone cleaning, Novascan Technologies, Inc.) for 15 min is carried out. Then, the FTO glass plates were immersed into a 40 mM aqueous TiCl_4 solution at 70°C for 30 min and washed with water and ethanol.

A screen-printed double layer film of interconnected TiO_2 particles of 20nm (dyesol paste) and an additional layer of 400nm TiO_2 particles was used as the mesoporous negative electrode.

First a 8-14 μm thick transparent layer of 20 nm sized TiO_2 particles were deposited on the FTO conducting glass electrode and further coated by a 4 μm thick scattering layer of 400 nm sized TiO_2 particles with an active area of 0.16cm^2 . The resulting electrodes were gradually heated under airflow at 325°C for 5 min., 375°C for 5 min., 450°C for 15 min., and 500°C for 15 min. Then, The electrodes are treated again with an aqueous solution of TiCl_4 40mM at 70°C for 30min and then washed with ethanol. The electrodes were heated at 500°C for 30 min and cooled at room temperature.

Chapter 2

When the electrodes were cooled, they have been dipped in the dye solution in the optimal conditions in order to achieve the maximum efficiency possible (using a certain concentration, a good solvent a certain dipping time and if it is necessary a small quantity of Chenodeoxycholic acid to avoid aggregates).

The platinized counter electrode was made by adding a drop of $5 \cdot 10^{-3}$ M H_2PtCl_6 in ethanol dry solution onto a conducting glass substrate (FTO) and heated under airflow at $390^\circ C$ for 15 min.

After the time required for the immersion of the electrodes into the dye solution, the electrodes were washed with the solvent used and dried under air. At the end the working and counter electrodes were assembled in a sandwich form using a thermoplastic (Surlyn) frame that melts at $100^\circ C$.

The counter electrode has an internal space, which was filled with a liquid electrolyte using a vacuum backfilling system. After that this hole is sealed with a Bynel sheet and a thin glass cover by heating. The liquid electrolyte used consists in 2 pair redox coupling using iodine-iodide (I/I_3^-) or Co(II)/Co(III) with the presence of different additives in order to increase the performance of the devices and the characterization of them.

The composition of the different electrolyte solutions will be explained in more details in the respective chapters.

2.3 ORGANIC SOLAR CELLS (OSC)

2.3.1 Device fabrication

We used for OSC Indium Tin Oxide (ITO) 5 Ohm/square (PSiOTec, Ltd., UK) sodalime glass substrates. However, prior to use them we must remove the residual photoresist layer cleaned with acetone. The substrates were then placed in a holder and were sonicated first 10 min in acetone and two times

more in isopropanol. After that, the substrates were dried under Nitrogen flow. Moreover the ITO substrates are ozone-treated in a UV-Ozone cleaner for 30 min in ambient atmosphere, and subsequently coated in air with a layer of filtered (0.45 μm , cellulose acetate) solution of Poly(3,4-ethylenedioxythiophene) : poly(styrenesulfonate) (PEDOT:PSS, HC Starck Baytron P) (4500 rpm 30 seconds followed by 3500 rpm 30 seconds). The PEDOT:PSS film was dried at 120 °C under inert atmosphere for 15 min. The blend or Active Layer consists in a solution of donor derivative and PC₇₀BM as acceptor. The concentration used normally is 20mg/ml and the ratio between the donor and the acceptor is optimized for each device. Active layers were spin-coated in different conditions depending on the blend used.

The cathode layer was deposited by thermal evaporation in an ultra high vacuum chamber ($1 \cdot 10^{-6}$ mbar). Metals were evaporated through a shadow mask leading to devices with an area of 9 mm². LiF (0.6 nm) and Al (80 nm) were deposited at a rate of 0.1 Å/s and 0.5-1 Å/s respectively. Following fabrication, the films were maintained under a nitrogen atmosphere and stored in the dark until used. In the case of hole only and electron only devices the solar cells were prepared as explained above but for hole only devices the structure was ITO/PEDOT:PSS/donor:PC₇₀BM/Au and for electron only devices the structure was ITO/ZnOnp/donor:PC₇₀BM/Al.

2.4 DEVICE CHARACTERIZATION

2.4.1 Charge Extraction (CE)

As the name indicates with this technique we extract and measure the charge accumulate in the system under determinate conditions. First of all, the cell is simultaneously putted in open circuit and illuminated with a series of LEDs and these conditions are applied until the cell reaches the steady state. Then, The cell is also simultaneously short-circuited and the light is switched off. In that situation all the charges accumulated in the open circuit conditions can be

Chapter 2

extracted, allowing the measurement of the charge density¹.

The Charge extraction system consists in 6 white light LEDS. These pulses are generated and controlled by the Trigger (TGP, from Thrurlby Thandar Instruments). The decay in voltage is measured using an oscilloscope TDS 2022 from Tektronix©. All the measurements are done in the dark to eliminate stray light that can increase the error.

The accumulate charge Q (C) can be calculated following equation (1).

$$Q = \frac{1}{R} \int_{t=0}^{t=t} V(t) dt \quad (1)$$

Where R is the resistance in ohms (Ω) and V(t) is the voltage in volts (V) measured at each time.

To define the amount of charge accumulated in the semiconductor we use the charge density and it can be calculated from equation (2)

$$e_{density}^- = Q \cdot \frac{1}{C_e} \cdot \frac{1000}{d \cdot A \cdot (1-p)} \quad (2)$$

Where Q is the accumulate charge (that it has been calculate before); C_e is the charge of the electron ($1.609 \cdot 10^{19} \text{C/e}^-$), d is the film thickness in centimeters (cm), A is the area of the surface (cm^2) and p is the porosity of the film.

We can represent the different $e_{density}^-$ obtained at different voltages. The plot of these data can be fitted to an exponential curve defined by equation 3.

$$e_{density}^-(V) = A_0 + A_1 \cdot e^{V/m_c} \quad (3)$$

2.4.2 Incident Photon to Current Efficiency (IPCE)

In this technique we irradiate the cell using a range of different wavelengths, at each wavelength the solar cells convert the incoming photons into electrical current.

The IPCE values can be calculated using equation 4.

$$IPCE = \frac{1240 \cdot J_{sc}}{\lambda \cdot P_{lamp}} \cdot 100 \quad (4)$$

Where: J_{sc} is the short circuit photocurrent (mA/cm^2), λ is the wavelength for the incident light in nanometres (nm), P_{lamp} is the power of the incident light in Watts (W/m^2) and 1240 is the conversion factor of the energy of photons.

The instrument to measure the IPCE consists in a xenon lamp (Oriel 150 W) as the light source, a monochromator (PTIM-101) that automatically change the wavelength to promote homogeneous monochromatic light in all the exposed area of the cell, a 4 inch integrating sphere and a Keithley 2400 to measure the current generate.

2.4.3 Solar cell power conversion efficiency (η)

The overall efficiency of a solar cell is calculated using equation 5.

$$\eta_{eff} = \frac{J_{sc} \cdot V_{oc} \cdot ff}{P_{lamp}} \cdot 100 \quad (5)$$

Where J_{sc} is the photocurrent at short circuit; V_{oc} is the open circuit photovoltage; ff, the fill factor of the cell and P_{lamp} the light intensity. The devices are measured under sun-simulated solar spectrum AM 1.5G (at 48.2° zenith angle)² conditions with an Abet solar simulator and a Keithley 2400 source

meter to measure the current. A homemade software interface (Labview©) is used to register and record the I-V curves. To calibrate the light source intensity at 100mW/cm^2 (1 Sun) a calibrated silicone diode is used prior to each device measurement. When needed, a series of neutral filters are used to measure the efficiency of the cells at different intensities of light.

2.4.4 Transient Photovoltage (TPV)

The measurements of transient photovoltage provide us information about recombination dynamics in the devices between the charges accumulated at the semiconductor and the oxidized electrolyte³. The solar cell is illuminated with a set of white LEDs (in a similar way that the one used for charge extraction measurements) until the solar cell reaches steady state conditions. When the solar cell achieves the steady state condition a ultra short laser pulse with low intensity is applied to the device and a small perturbation in the equilibrium is created allowing an excess of charge to be generated producing a transient decay. The same laser pulse is used under different light intensities that lead to different device steady-state voltage and, thus, providing different transient decays.

The data obtained is fitted as an exponential equation (6)

$$V(t) = V_{oc} + V_1 \cdot e^{-(t/\tau)} \quad (6)$$

Where V (V) is plotted as a function of time. V_{oc} (V) is the voltage at open circuit, V_1 (V) is the voltage generated by the pulse and τ (s) is the recombination lifetime.

2.4.5 Laser Transient Absorption Spectroscopy (L-TAS)

The measurements of Laser Transient Absorption Spectroscopy provide us with information about excited short living species^{4,5}. Basically, a sample is irradiate

constantly (probe light) at a determinate wavelength that corresponds to the maximum absorption of the sample excited state. At the same time, we excite the sample with a short light pulse producing a change in the sample optical density. The change in optical density is monitored during a short period of time to monitor the variations.

The data collected is treated in order to obtain units of optical density; the data can be fitted to an exponential function equation (7)

$$\Delta O.D.(t) = A_0 + A_1 e^{-(t/\tau)^\beta} \quad (7)$$

Where A_0 (a.u.) is the baseline, A_1 (a.u.) is the signal amplitude, τ (s) is the lifetime of the transient and β (a.u) is the emprirical stretched factor whose value is between 0 and 1.

2.5 REFERENCES

(1) Duffy, N. W.; Peter, L. M.; Rajapakse, R. M. G.; Wijayantha, K. G. U. *The Journal of Physical Chemistry B* **2000**, *104*, 8916.

(2) Mishra, A.; Bäuerle, P. *Angewandte Chemie International Edition* **2012**, *51*, 2020.

(3) O'Regan, B. C.; Scully, S.; Mayer, A. C.; Palomares, E.; Durrant, J. *The Journal of Physical Chemistry B* **2005**, *109*, 4616.

(4) Haque, S. A.; Tachibana, Y.; Willis, R. L.; Moser, J. E.; Grätzel, M.; Klug, D. R.; Durrant, J. R. *The Journal of Physical Chemistry B* **1999**, *104*, 538.

(5) Tachibana, Y.; Moser, J. E.; Grätzel, M.; Klug, D. R.; Durrant, J. R. *The Journal of Physical Chemistry* **1996**, *100*, 20056.

Chapter 3

Light soaking effects on Charge Recombination and Device Performance in DSSC based on indoline-Cyclopentadithiophene Chromophores

Table of contents

3.1 Abstract	57
3.2 Introduction	57
3.3 Experimental Section	58
3.3.1 Synthesis and Characterization	58
3.3.2 Device preparation and Characterization	64
3.4 Results and Discussion	64
3.5 Conclusions	76
3.6 References	77

3.1 ABSTRACT

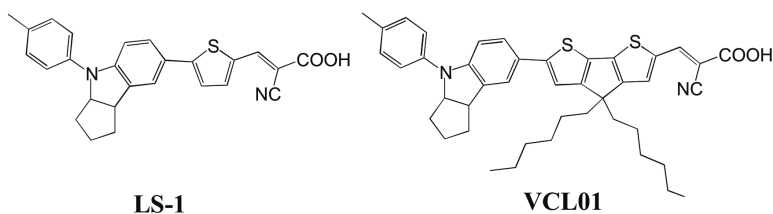
The synthesis, characterization, electrochemical and photophysical properties of a novel D- π -A indoline organic dye, **VCL01**, are described. Its performance characteristics in Dye Sensitized Solar Cell (DSC) devices under standard AM 1.5G illumination are also investigated. **VCL01** incorporates a cyclopentadithiophene unit as the π -bridge between the indoline donor and cyanoacetic acceptor units. In comparison to the reference dye **LS-1** containing only one thiophene unit in the π -bridge, **VCL01** shows a 40nm red shift in adsorption, an increase in molar absorptivity and a 0.13 V lower oxidation potential, all consistent with the more conjugated nature of this sensitizer. The efficiency of **VCL01** and **LS-1** DSC devices were 4.81% and 6.23% respectively, which upon >100 mins continuous light soaking under AM 1.5G illumination rose to 7.21% and 6.95%, representing an unprecedented 42% increase in efficiency for the **VCL01** device. This increase is overwhelmingly due to an increase in photocurrent but, remarkably, V_{oc} also increases by 50 mV upon illumination reflected in transient photovoltage data which indicate that electron lifetime increases considerably also. Time-Correlated Single Photon Counting data indicate that partly the light soaking effect can be attributed to improved TiO₂/dye interaction leading to enhanced electron injection.

3.2 INTRODUCTION

Development of dye Sensitized Solar Cells (DSCs) based on organic D- π -A sensitizers¹⁻³ is an active area of research as the properties of these sensitizers can be easily tailored by judicious selection of each individual unit and can be exploited commercially as efficient solar cells for indoor applications⁴ and building integrated photovoltaics (BIPV).⁵ Compared to those containing triphenylamine donor groups,⁶⁻¹⁴ D- π -A sensitizers containing indolines¹⁵⁻²² have been much less investigated despite the superior donating ability of these groups and the well-known stability they impart, which is a pre-requisite for long term device stability.

Chapter 3

In this present work we perform a comprehensive study of the novel sensitizer **VCL01** (Scheme 1) using the dye **LS-1** reported by Li *et al.*²³ as a reference. **VCL01** consists of an indoline and cyanoacetic acid and, in addition, a cyclopentadithiophene unit is used in the π -bridge to increase conjugation and the light-harvesting dye properties. Moreover, the long alkyl chains are expected to block recombination loss reactions between TiO_2 electrons and the oxidised electrolyte. Cyclopentadithiophene is used in many efficient D- π -A dyes and for this reason it was coupled with an indoline donor group here for the first time. A dramatic 42% increase in efficiency is observed for **VCL01** devices upon continuous light soaking of over 100mins. We ascribe this increase to improved interaction between dyes and TiO_2 leading to an enhancement in electron injection



Scheme 3.1: Molecular structures of dyes **LS-1** and **VCL01**.

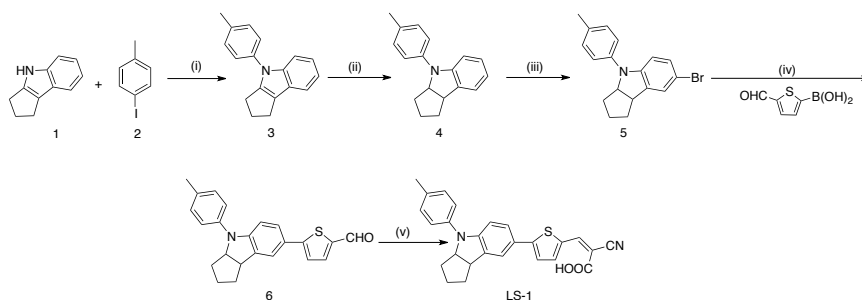
3.3 EXPERIMENTAL SECTION

3.3.1 Synthesis and characterization

LS-1 was synthesized according to the literature.²³

3, 4 and **5** were synthesized according to the literature²⁴

Synthesis of LS-1



Scheme 3.2: Synthetic route of **LS-1**. (Reaction conditions: (i) K_2CO_3 , Cu, 1,2-dichlorobenzene, 48 h, $150^\circ C$; (ii) $NaBH_4$, CH_3COOH , 4 h, $50^\circ C$; (iii) NBS, CH_3COCH_3 , 2 h, $0^\circ C$; (iv) $Pd^{II}(dppf)Cl_2$, 2M K_2CO_3 aqueous solution, dimethoxyethane, 2 h, $90^\circ C$; (v) cyanoacetic acid, piperidine, Chloroform, 12 h, reflux.)

Synthesis of 4-(p-tolyl)-1,2,3,4-tetrahydrocyclopenta[b]indole (3). In a round flask 3,4-dihydrocyclopenta[b]indole (9.4g, 0.06mol), 1-iodo-4-methylbenzene (16.8g, 0.07mol), Potassium carbonate (16g, 0.125g) and Cu (0.72g, 0.01mol) were added in 100mL of 1,2-dichlorobenzene. The solution was heated up at $150^\circ C$ for 48 hours. After that, the 1,2-dichlorobenzene was distilled. Then the mixture was extracted in CH_2Cl_2 and the organic layer was cleaned with brine. Then the organic layer was dried over Na_2SO_4 anhydrous. Then the crude is purified by column chromatographic using Hexane/Ethyl Acetate (9.5:0.5) as a solvent to obtain a yellow oil (4g, 27% of Yield). 1H -NMR (400 MHz, $CDCl_3$) δ_H : 7.46 (m, 1H); 7.38 (m, 1H); 7.29 (m, 4H); 7.09 (m, 2H); 2.87 (m, 4H); 2.53 (m, 2H); 2.41(s, 3H).

Synthesis of 4-(p-tolyl)-1,2,3,3a,4,8b-hexahydrocyclopenta[b]indole (4): In a schlenk flask $NaBH_4$ (8.4g), 0.22mol) was added slowly to a solution of **3** (4g, 0.016mol) in acetic acid (120mL). Then the mixture was heated up to reflux overnight. After that the mixture was stirred for 4 hours at $50^\circ C$. Then, Na_2CO_3 was slowly added until pH 7. Then we extracted with CH_2Cl_2 , and the organic layer was dried over $MgSO_4$. Then the crude is purified by column chromatographic using Hexane as a solvent to obtain a yellow oil (2.8g, 71% of

Yield). $^1\text{H-NMR}$ (400 MHz, CDCl_3) δ_{H} : 7.18(m, 5H); 7.05(t, $J=8.2\text{Hz}$, 1H); 6.94 (d, $J=8.2\text{Hz}$, 1H); 6.73 (t, $J=8.2\text{Hz}$, 1H); 4.76 (m, 1H); 3.85 (m, 1H); 2.36 (m, 3H) 2.06 (m, 1H); 1.92 (m, 2H); 1.82 (m, 1H); 1.66 (m, 1H); 1.56 (m, 1H).

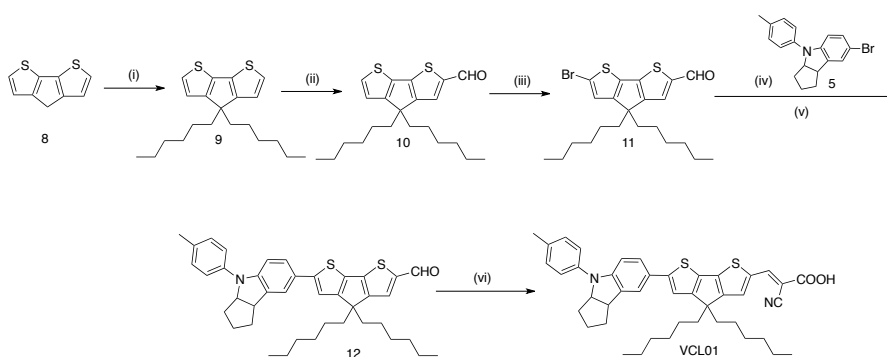
Synthesis of 1,2,3,3a,4,8b-hexahydrocyclopenta[b]indol-6-ylium (5): in a schlenk flask a solution of **4** (2.14g, 8.62mmol) and Acetone (90mL) was cold at 0°C . After that, N-bromosuccinimide (1.53g, 8.62mmol) was added and the mixture was stirred at 0°C in the dark for 2h. Then water was added. The crude product was extracted into CHCl_3 , and the organic layer was dried over Na_2SO_4 . Finally the sample was recrystallized in Hexane to obtain a white solid. (2.4g, 96% of Yield) $^1\text{H-NMR}$ (400 MHz, CDCl_3) δ_{H} : 7.14 (dd, $J=2.2\text{Hz}$, 1.2Hz, 1H); 7.11 (m, 4H); 7.06 (dd, $J=8.6\text{Hz}$, 1.2Hz, 1H); 6.70 (d, $J=8.8\text{Hz}$, 1H); 4.72 (m, 1H); 3.77 (m, 1H); 2.30 (s, 3H); 1.81 (m, 6H).

Synthesis of 5-(4-(*p*-tolyl)-1,2,3,3a,4,8b-hexahydrocyclopenta[b]indol-7-yl)thiophene-2-carbaldehyde (6): in a schlenk flask **5** (200mg, 0.61mmol), thiophen-2-ylboronic acid (135mg, 0.85mmol), $\text{Pd}^{\text{II}}(\text{dppf})\text{Cl}_2$ (20.1mg, 0.027mmol) and 20ml of dimethoxyethane was added and the mixture was degassed. Then the solution was stirred at room temperature for 30 minutes. After this time 3mL of K_2CO_3 2M was added and the mixture was degassed again. Then the mixture was heated up to 90°C for 2 hours. After cooling at room temperature water was added and the solution was extracted with Et_2O and washed with Brine. Then the crude is purified by column chromatographic using Hexane/Ethyl Acetate (8:2) as a solvent. (80mg, 36% of Yield). $^1\text{H-NMR}$ (400 MHz, CDCl_3) δ_{H} : 9.88 (s, 1H); 7.65 (d, $J=4.0\text{Hz}$, 1H); 7.39 (s, 1H); 7.35 (dd, $J=8.2\text{Hz}$, 2.0 Hz, 1H); 7.21 (d, $J=4.0\text{Hz}$, 1H); 7.16 (m, 4H); 6.81 (d, $J=8.2\text{Hz}$, 1H); 4.83 (m, 1H); 3.83 (m, 1H); 2.33 (s, 3H); 2.06 (m, 1H); 1.88 (m, 2H); 1.76 (m, 1H); 1.66 (m, 1H); 1.53 (m, 1H).

Synthesis of LS-1: In a schlenk flask **6** (0.08g, 0.22mmol), cyanoacetic acid (0.057g, 0.66mmol), piperidine (0.095g, 1.11mmol) and 15mL of dry chloroform was added and was refluxed overnight. Then the solution was acidified with

20% aqueous HCl and extracted with CHCl_3 . The organic layer was dried over anhydrous Na_2SO_4 and concentrated. The crude was purified by column chromatography (CHCl_3 /Methanol 9:1) on silica gel and the product was obtained as a violet solid (0.085g, 91% yield). $^1\text{H-NMR}$ (400 MHz, DMSO-d_6) δ_{H} : 8.34 (s, 1H); 7.91 (d, $J=4.0\text{Hz}$, 1H); 7.54 (m, 2H); 7.45 (dd, 8.2Hz, 2.0Hz, 1H); 7.21 (m, 4H); 6.82 (d, $J=8.2\text{Hz}$, 1H); 4.92 (m, 1H); 3.85 (m, 1H); 2.27 (s, 3H); 2.05 (m, 1H); 1.77 (m, 3H); 1.62 (m, 1H); 1.37 (m, 1H).

Synthesis of VCL01



Scheme 3.3: Synthetic route of **VCL01**. (Reaction conditions: (i) KI, $\text{BrC}_6\text{H}_{13}$, KOH, RT overnight; (ii) POCl_3 , DMF, 1,2-dichloroethane, 4h 0°C ; (iii) NBS, THF, 5h 0°C ; (iv) $n\text{-BuLi}$, THF, $\text{B}(\text{OCH}_3)_3$, -78°C ; (v) $\text{Pd}(\text{PPh}_3)_4$, 2 M K_2CO_3 aqueous solution, THF, 6 h, 80°C ; (vi) cyanoacetic acid, piperidine, chloroform, 12 h, reflux.)

9, **10** and **11** were synthesized according to the literature²⁵

Synthesis of 4,4-dihexyl-4H-cyclopenta[2,1-b:3,4-b']dithiophene (9):

A solution of 4H-cyclopenta[2,1-b:3,4-b']dithiophene (**8**) (0.7g, 3.92mmol), 1-bromohexane (1.27g, 7.84mmol), and KI(1.62mg, 0.013mmol) in DMSO (20mL) was cold at 0° . Then, KOH (0.44g, 7.84mmol) was added. The reaction was stirred overnight at room temperature under argon. Then water was added. The crude product was extracted into diethyl ether, and the organic layer was washed with saturated ammonium chloride and water, and dried over Na_2SO_4 . After removing the solvent under reduced pressure, the residue was purified by column chromatography using petroleum ether as a solvent to yield a colorless

oil (0.9g, 66% yield) $^1\text{H-NMR}$ (400 MHz, CDCl_3) d_{H} : 7.12 (d, $J=4.9\text{Hz}$, 2H); 6.91 (d, $J=4.9\text{Hz}$, 2H); 1.82 (m, 4H); 1.13 (m, 12H); 0.79 (t, $J= 6.8\text{Hz}$, 6H).

Synthesis of 4,4-dihexyl-4H-cyclopenta[2,1-b:3,4-b']dithiophene-2-carbaldehyde (10): A cold solution of **9** (0.90g, 2.6mmol) and DMF (0.22g, 3.12mmol) in 1,2-dichloroethane (20mL) at 0°C was added phosphorus chloride oxide (0.48g, 3.12mmol) under argon. The reaction was stirred at same temperature for 4 hours and then saturated sodium acetate aqueous solution (10mL) was added. The mixture was stirred at room temperature for 2 hours. The crude was extracted into dichloromethane, and the organic layer was washed with brine and water, and dried over sodium sulphate. After removing the solvent the residue was purified by column chromatography with petroleum ether and ethyl acetate (8:2) as a solvents to obtain a colourless oil (0.73g, 75% yield) $^1\text{H-NMR}$ (400 MHz, CDCl_3) d_{H} : 9.80 (s, 1H); 7.54 (s, 1H); 7.37 (d, $J=4.9\text{Hz}$, 2H); 6.95 (d, $J=4.9\text{Hz}$, 2H); 1.84 (m, 4H); 1.13 (m, 12H); 0.78 (t, $J= 6.8\text{Hz}$, 6H).

Synthesis of 6-bromo-4,4-dihexyl-4H-cyclopenta[2,1-b:3,4-b']dithiophene-2-carbaldehyde²⁵ (11): A cold solution of **10** (0.70g, 1.86mmol) in tetrahydrofuran (20mL) was added N-bromosuccinimide (0.4g, 2.23mmol) at 0°C under argon. The reaction mixture was warmed to room temperature and stirred for 5 hours and then water was added. The crude product was extracted into dichloromethane, and the organic layer was dried over sodium sulphate. The residue was purified by column chromatography (dichloromethane) to obtain yellow oil. (0.75g, 90% yield) $^1\text{H-NMR}$ (400 MHz, CDCl_3) d_{H} : 9.81 (s, 1H); 7.53 (s, 1H); 6.99 (s, 1H); 1.84 (m, 4H); 1.13 (m, 12H); 0.78 (t, $J= 6.8\text{Hz}$, 6H).

Syntheses of 4,4-dihexyl-6-(4-(p-tolyl)-1,2,3,3a,4,8b-hexahydrocyclopenta[b]indol-7-yl)-4H-cyclopenta[1,2-b:5,4-b']dithiophene-2-carbaldehyde (12): **5** (0.240g, 0.735mmol) was added to a round flask with 30mL of THF and was stirred under nitrogen atmosphere at -78°C . $^n\text{BuLi}$ 2M in hexane (0.33mL, 0.867mmol) was added and the mixture was stirred for 15 minutes at -78°C . After that, $\text{B}(\text{OMe})_3$ (0.12mL, 1.10mmol)

was added and the reaction was stirred overnight at -78°C . The crude was warmed at room temperature. In another Schlenk, $\text{Pd}(\text{PPh}_3)_4$ (0.075g, 0.02mmol), **11** (0.3g, 0.66mmol), K_2CO_3 2M (3mL), the crude, and THF (20mL) was added and the reaction was stirred at 70°C for 4 hours. Then water was added. The crude product was extracted into CHCl_3 , and the organic layer was dried over NaSO_4 . The residue was purified by column chromatography (Hexane/Dichloromethane 6:4) to obtain a red solid (0.270g, 60% yield). $^1\text{H-NMR}$ (400 MHz, CDCl_3) δ_{H} : 9.78 (s, 1H); 7.56 (s, 1H); 7.35 (s, 1H); 7.30 (dd, $J=8.4\text{Hz}$, 2Hz, 1H); 7.20 (m, 4H); 7.02 (s, 1H); 6.85 (d, $J=8.4\text{Hz}$, 1H); 4.80 (m, 1H); 3.78 (m, 1H); 2.32 (s, 3H); 2.06 (m, 1H); 1.87 (m, 8H); 1.66 (m, 1H); 1.13 (m, 16H); 0.80 (t, $J=6.8\text{Hz}$, 6H). $^{13}\text{CNMR}$ (100MHz, CDCl_3 , ppm): δ 182.46; 164.05; 157.13; 151.43; 149.02; 148.54; 142.44; 140.17; 136.00; 132.60; 132.12; 130.07; 125.50; 124.90; 122.33; 120.55; 115.64; 107.77; 69.55; 54.20; 45.50; 38.04; 35.34; 33.90; 31.80; 29.67; 24.75; 24.62; 22.83; 21.03; 14.23. MS-ESI (m/z): $[\text{M}+\text{Na}]^+$ calculated for $\text{C}_{40}\text{H}_{47}\text{NOS}_2\text{Na}$: 644.2991; found: 644.2991.

Synthesis of VCL01

In a schlenk flask **12** (0.21g, 0.34mmol), cyanoacetic acid (0.086g, 1.02mmol), piperidine (0.144g, 1.7mmol) and 10mL of dry chloroform was added and was refluxed overnight. Then the solution was acidified with 20% aqueous HCl and extracted with CHCl_3 . The organic layer was dried over anhydrous Na_2SO_4 and concentrated. The crude was purified by column chromatography (CHCl_3 /Methanol 9:1) on silica gel and the product was obtained as a violet solid (0.140g, 67% yield). $^1\text{H-NMR}$ (400 MHz, CDCl_3) δ_{H} : 8.27 (s, 1H); 7.80 (s, 1H); 7.49 (s, 1H); 7.45 (s, 1H); 7.34 (dd, $J=8.4\text{Hz}$, 2Hz, 1H); 7.20 (m, 4H); 6.85 (d, $J=8.4\text{Hz}$, 1H); 4.88 (m, 1H); 3.84 (m, 1H); 2.28 (s, 3H); 2.05 (m, 1H); 1.89 (m, 4H); 1.76 (m, 3H); 1.63 (m, 1H); 1.39 (m, 1H); 1.11 (m, 12H); 0.90 (m, 4H); 0.77 (t, $J=6.8\text{Hz}$, 6H). $^{13}\text{C NMR}$ (100MHz, DMSO-d_6 , ppm) δ 157.04; 150.80; 147.70; 139.50; 136.14; 135.96; 135.76; 131.82; 131.26; 130.48; 129.99; 125.27; 125.19; 124.41; 124.30; 121.93; 120.23; 119.94; 116.21; 107.26; 68.53; 53.57; 44.62; 37.11; 37.01; 34.97; 33.10; 31.09; 29.05; 24.15; 24.10; 22.13;

20.54; 13.97. MS-ESI (m/z): $[M-H]^-$ calculated for $C_{43}H_{47}N_2O_2S_2$: 687.3084; found: 687.3069.

3.3.2 Device preparation and characterization

As we have said in chapter 2 two different types of TiO_2 films were utilized depending on the measurements being conducted. Highly transparent thin films (8 μm) were utilized for L-TAS measurements. On the other hand, for efficient DSC devices were made using 9 μm thick films consisting of 20 nm TiO_2 nanoparticles (Dyesol[®] paste) and a scatter layer of 4 μm of 400 nm TiO_2 particles (CCIC, HPW-400).

All films were sensitized in dye solutions at concentrations of 0.125 mM in 1:1 acetonitrile:*tert*-butanol containing 1 mM chenoxylidic acid were prepared and the film immersed overnight at room temperature. The sensitized electrodes were washed with 1:1 acetonitrile:*tert*-butanol and dried under air. The electrolyte used consisted of 0.5 M 1-butyl-3-methylimidazolium iodide (BMII), 0.1 M lithium iodide, 0.05 M iodine and 0.5 M *tert*-butylpyridine in acetonitrile.

3.4 RESULTS AND DISCUSSION

The absorption and emission spectra in solution and the photophysical and electrochemical properties of **LS-1** and **VCL01** are collected in Table 3.1.

Table 3.1. Absorption, emission and electrochemical properties of **LS-1** and **VCL01**.

Dye	λ_{abs} (nm) ^a	λ_{em} (nm) ^a	E_{ox} (V v's Fc/Fc ⁺)	E_{0-0} (eV) ^c	E_{HOMO} (eV) ^d	E_{LUMO} (eV) ^e
LS-1	527 (20200)	704	0.31	1.99	-5.19	-3.20
VCL01	567 (34500)	765	0.14	1.82	-5.02	-3.20

^aMeasured in dichloromethane. In parenthesis molar extinction coefficient at λ_{abs} (in $M^{-1} cm^{-1}$). ^c E_{0-0} was determined from the intersection of absorption and emission spectra in dilute solutions. ^d E_{HOMO} was calculated using $E_{HOMO}(vs\ vacuum) = -4.88 - E_{ox}(vs\ Fc/Fc^+)$. ^e E_{LUMO} was calculated using $E_{LUMO} = E_{HOMO} + E_{0-0}$.

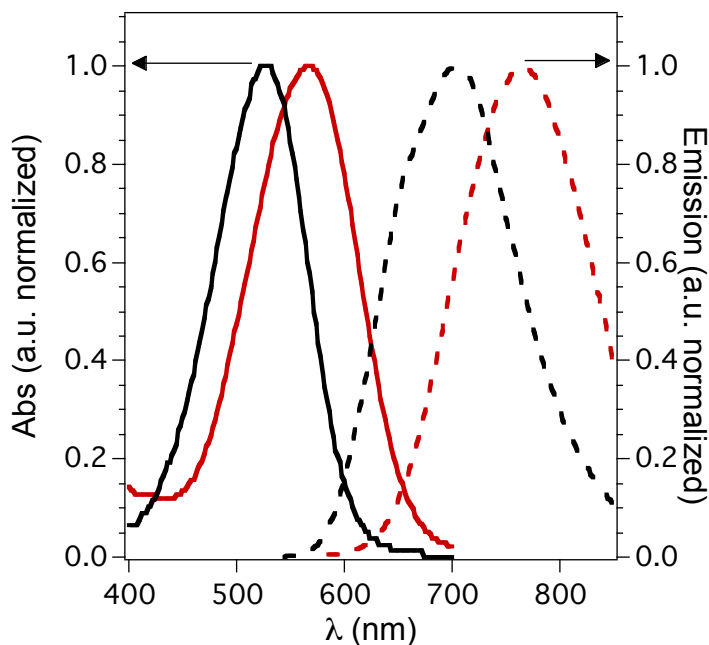


Figure 3.1: Absorption and emission spectra of **LS-1** and **VCL01** in dichloromethane.

LS-1 and **VCL01** both show absorption bands in the UV-Vis region of the solar spectrum which are assigned to π - π^* transitions. The increase in molar extinction coefficient and 40 nm red-shift in absorption maximum of **VCL01** with respect to **LS-1** is attributed to the increase in conjugation in this sensitizer afforded by the insertion of the cyclopentadithiophene unit. We note that the absorption maximum of **LS-1** at 527nm is different to that as reported as 483nm by Li *et al.*²³ This can be explained due to the dependence of the absorption spectra of D- π -A organic dyes on their degree of protonation in different acid/base media, as we have observed previously.⁷ This can be demonstrated by adding triethylamine (TEA) and trifluoroacetic acid (TFA) to a solution of **LS-1** which shows a blue shift and red shift respectively (Figure 3.2). A blue shifted

spectrum corresponds to the deprotonated state and a red-shifted spectrum to the protonated state, therefore, **LS-1** as reported in the study by Li *et al.*²³ would appear to be in the deprotonated state. In any case, both studies show similar absorption maxima for **LS-1** immobilized onto TiO₂ film (≈ 450 nm). It is noted that the absorption spectrum of **VCL01** also changes when in its protonated or deprotonated state.

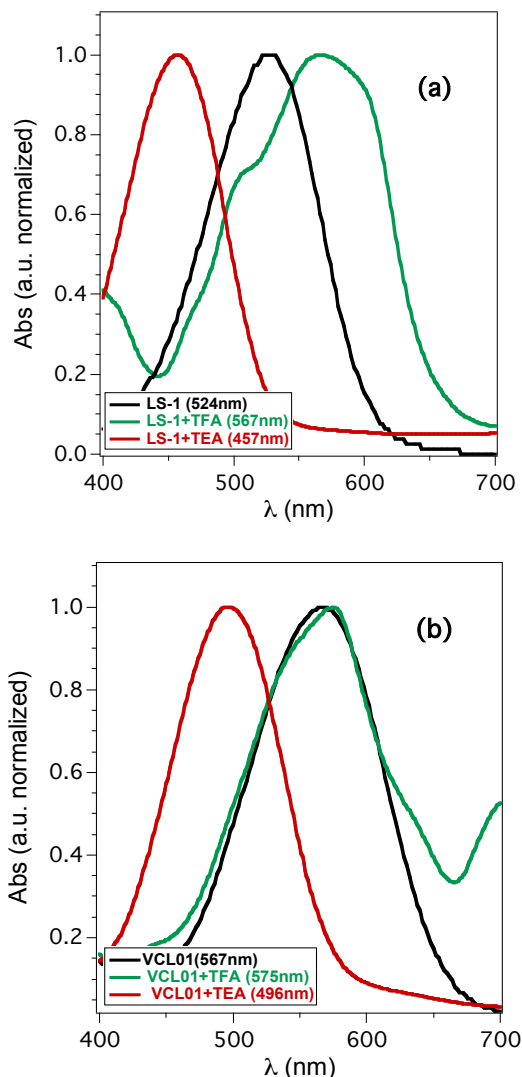


Figure 3.2: Absorption spectra of dichloromethane solutions of **LS-1** (a) and **VCL01** (b) in the presence of organic base (TEA, triethylamine) and organic acid (TFA, trifluoroacetic acid).

Cyclic voltammetry studies (Figure 3.3) indicate there is a significant difference of 0.13 V in ground state oxidation potential (E_{ox}) between **LS-1** and **VCL01** and again the effect of the cyclopentadithiophene unit is apparent reducing the E_{ox} of **VCL01**. The E_{HOMO} and E_{LUMO} in eV were calculated using the data in Table 1. E_{HOMO} and E_{LUMO} values indicate efficient dye regeneration by the iodide/triiodide redox electrolyte ($E_{redox} = 4.75$ eV) and also efficient electron injection into the TiO_2 conduction band ($E_{TiO_2} = 4.0$ eV) is energetically possible for these sensitizers.

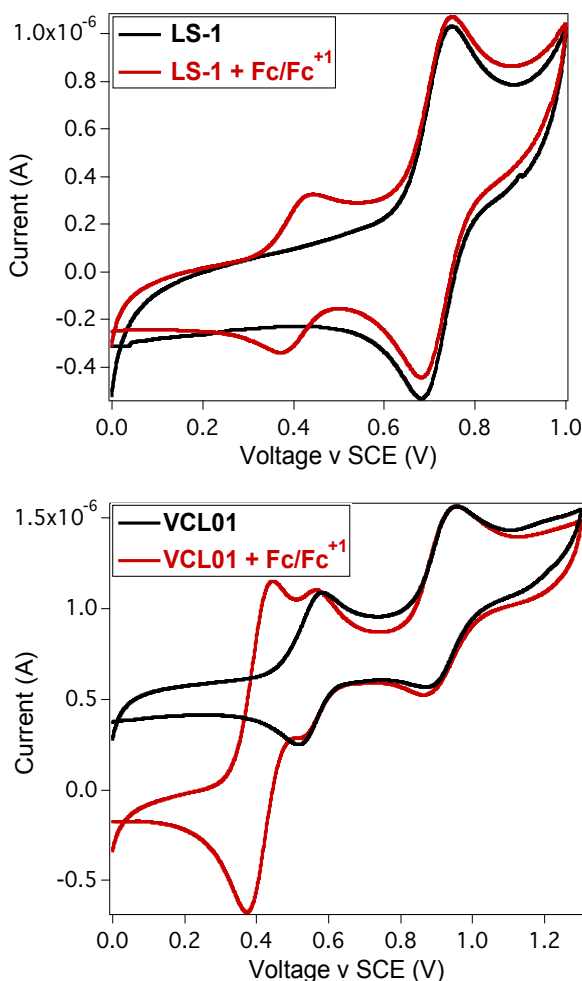


Figure 3.3: Cyclic voltammetry of **LS-1** (top) and **VCL01** (bottom) recorded in 0.1M

tetrabutylammonium hexafluorophosphate in 1:1 acetonitrile:*tert*-butanol at a scan rate of 10 mV s⁻¹. The working electrode consisted of a platinum wire and the counter electrode a platinum mesh. The reference electrode was the silver calomel electrode (saturated KCl). All solutions were degassed with argon for 5 mins prior to measurement. The red and black scans were recorded in the presence and absence of Ferrocene/Ferrocene⁺.

LS-1 and **VCL01** were used to fabricate DSC solar cells and the device properties are listed in Table 3.3. Devices were measured after periods of 0 and 120 mins of continuous illumination. The best efficiencies were found using 1mM chenoxyldecholic acid as co-adsorbent. With higher concentrations of chenoxyldecholic acid (10 mM), though **LS-1** devices increased somewhat in efficiency (also observed by Li *et. al*)²³, that of **VCL01** dropped sharply (see Table 3.2). For this reason a compromise was sought with a lower concentration of 1 mM of chenoxyldecholic acid used (Table 3.3)

Table 3.2. Device optimization of **LS-1** and **VCL01** DSCs.

Dye	V_{oc} (V)	J_{sc} (mA/cm ²)	FF (%)	η (%)*
LS-1 (No chenoxyldecholic acid)	0.66	8.44	67.41	3.79
LS-1 (10 mM chenoxyldecholic acid)	0.73	14.06	66.20	6.83
VCL01 (No chenoxyldecholic acid)	0.67	12.75	67.44	5.81
VCL01 (10 mM chenoxyldecholic acid)	0.60	5.25	71.22	2.27

Light soaking effect in D- π -A dyes (DSSC)

Table 3.3. Device properties of **LS-1** and **VCL01** DSCs.

Dye	V_{oc} (V)	J_{sc} (mA/cm ²)	FF (%)	η (%) [*]
LS-1 (0 mins)^a	0.689	12.90	70	6.23 (7.84)
LS-1 (120 mins)^b	0.704	13.81	71	6.95 (8.48)
VCL01 (0 mins)^a	0.649	10.99	68	4.81 (6.52)
VCL01 (120 mins)^b	0.699	14.69	70	7.21 (8.98)

^aRecorded after 0 mins illumination. ^bRecorded after 120 mins continuous illumination. ^{*}Efficiencies recorded with mask. In parenthesis efficiencies without mask.

Following 0 mins illumination **LS-1** shows a superior power conversion efficiency of 6.23% compared to only 4.81% for **VCL01**. However, following a period of 120 mins continuous illumination the efficiency of the **VCL01** device manifests a dramatic increase in efficiency to 7.21% compared to **LS-1** which shows a smaller increase in efficiency to 6.95%. This phenomenon was always observed with, however, the time necessary for the efficiency maximum to be reached varying somewhat. This was probably due to small differences in the quantity of dye being adsorbed onto the TiO₂ films after sensitization and/or small differences in TiO₂ film thickness. The increase in efficiency is caused due to an increase in J_{sc} upon illumination. The nature of the increase in efficiency is discussed later. It should be noted that the efficiency of the **LS-1** device is higher than that reported by Li *et al.*,²³ however, the electrolyte used is different in both studies.

The I-V curves recorded under AM 1.5G radiation and IPCE spectra recorded for **LS-1** and **VCL01** devices are shown in Figure 3.4. IPCE spectra show broad absorption in the UV-vis and a notable spectral red-shift for **VCL01**. Following light soaking the increase in device IPCE is consistent with the J_{sc} data in Table 2. Moreover, integration of the IPCE data agrees with the J_{sc} data in Table 2 within an error of 5 %.

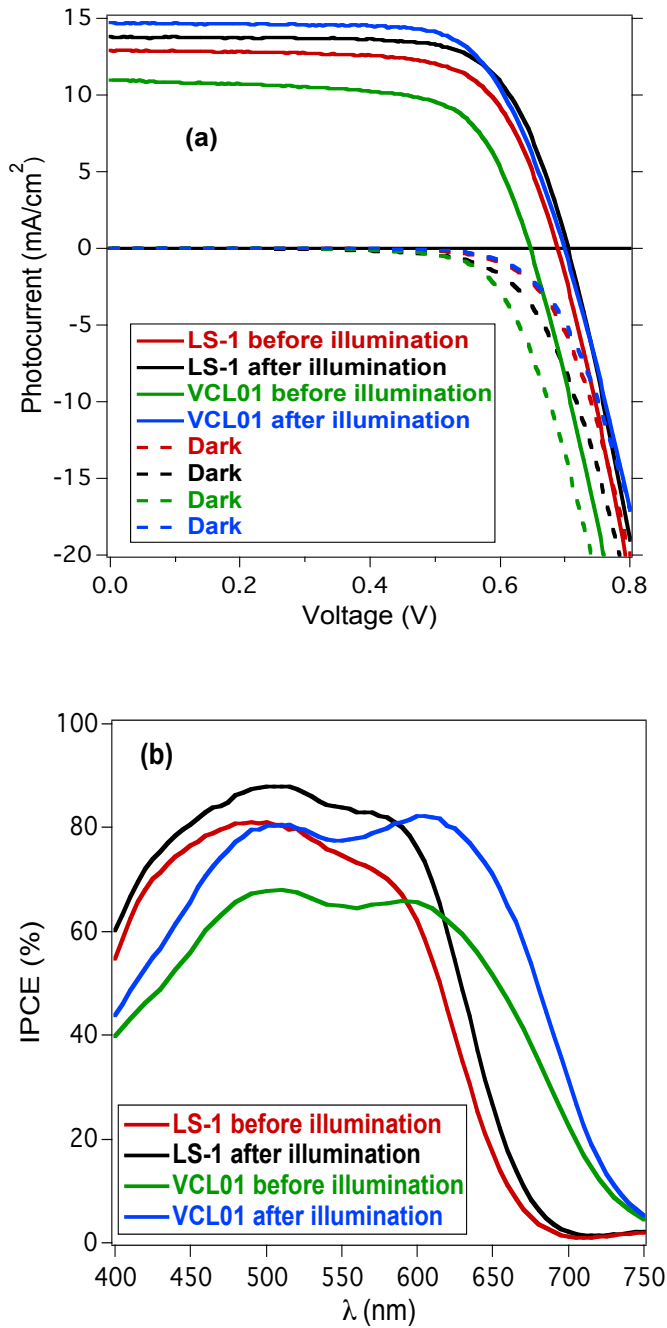


Figure 3.4: (a) I-V curves and (b) IPCE spectra for **LS-1** and **VCL01** DSC devices recorded under AM 1.5G radiation. Also shown are I-V dark curves.

Electron density and electron lifetime in these devices were probed using charge extraction and transient photovoltage measurements respectively (Figure 3.5). With 0 mins illumination the **LS-1** device shows a negligibly higher charge density than the **VCL01** device but almost an order of magnitude of difference longer electron lifetime under the same electron density. This explains the 40 mV higher V_{oc} for the **LS-1** device. Upon illumination for 120 mins, charge extraction data shows an increase in charge density for both devices suggesting a downward shift in the conduction band. Moreover charge density is now similar in both devices. Transient photovoltage data show that the effect of 120 mins light soaking on the devices is an increase in electron lifetime, with the increase notably more pronounced for the **VCL01** device (over 1 order of magnitude). The difference in lifetime between **LS-1** and **VCL01** is, however, narrowed significantly upon light soaking. This explains the very similar V_{oc} for the devices following illumination.

Transient absorption spectroscopy was then used to probe charge recombination and regeneration by the I_3^-/I^- redox couple in transparent DSC devices (Figure 3.6). The data recorded in the absence of red/ox active electrolyte (black) show long-lived decays assigned to the dye cation formed following photo-excitation and charge separation. These kinetics are similar to those which we have observed for D- π -A organic sensitizers previously.⁷ In the presence of redox couple the kinetics become bi-phasic with the loss of the cation signal due to regeneration by I^- and the appearance of a long-lived signal assigned to TiO_2 injected electrons and/or I_2^- (red decay). The $t_{50\%}$ (time taken for 50% of signal to disappear) for the regeneration reaction is estimated as 5 and 200 μ s for **LS-1** and **VCL01** respectively. This difference can be explained by the difference in ground state oxidation (E_{ox}) potential for these dyes, with the more positive potential of **LS-1**

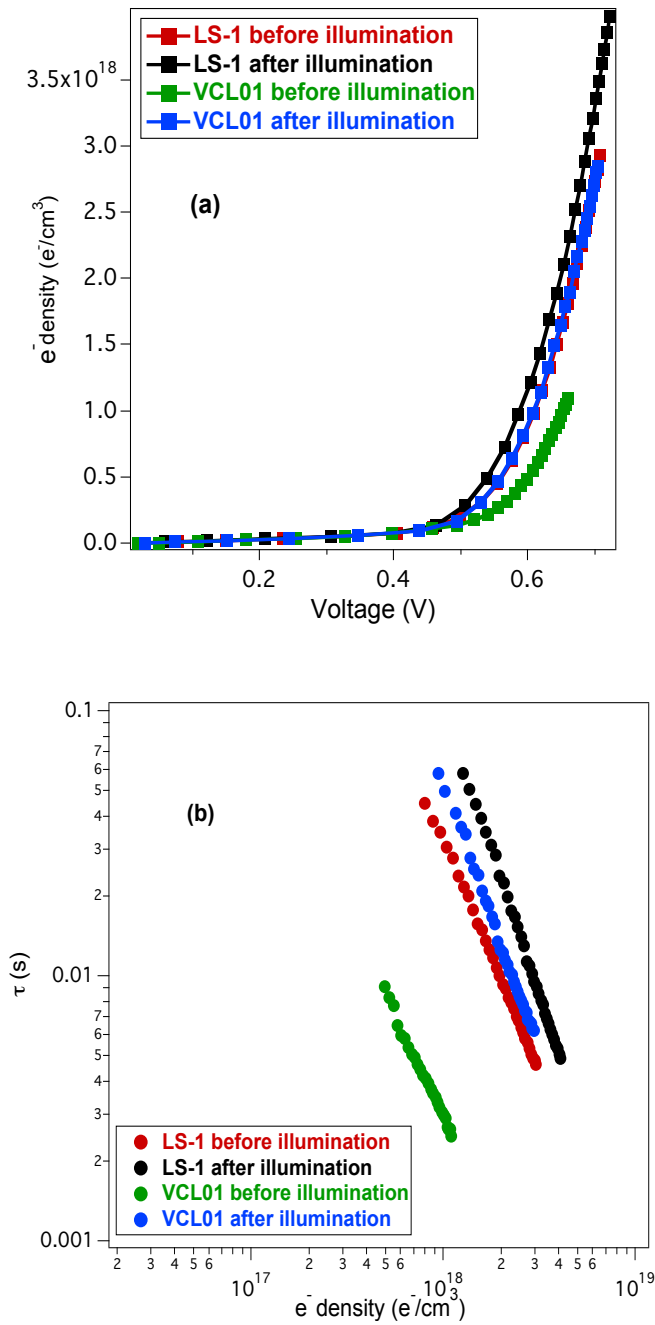


Figure 3.5: (a) Electron density as a function of cell voltage and (b) device electron lifetime τ as a function of charge density for LS-1 and VCL01 devices.

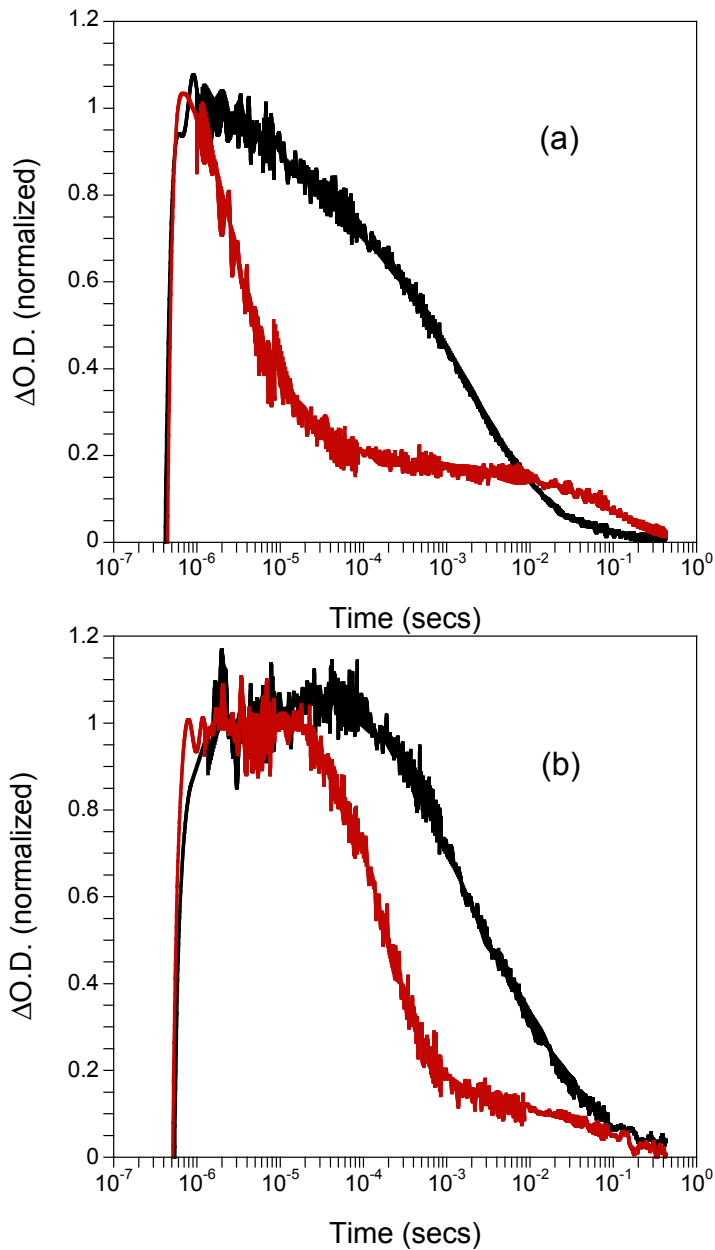


Figure 3.6: Transient absorption kinetics of (a) **LS-1** and (b) **VCL01** recorded for 1cm^2 area devices comprising $8\ \mu\text{m}$ TiO_2 films in the presence of a blank electrolyte (black) and an iodide/tri-iodide red/ox electrolyte (red). Kinetics were recorded at 800nm following excitation at 490 nm.

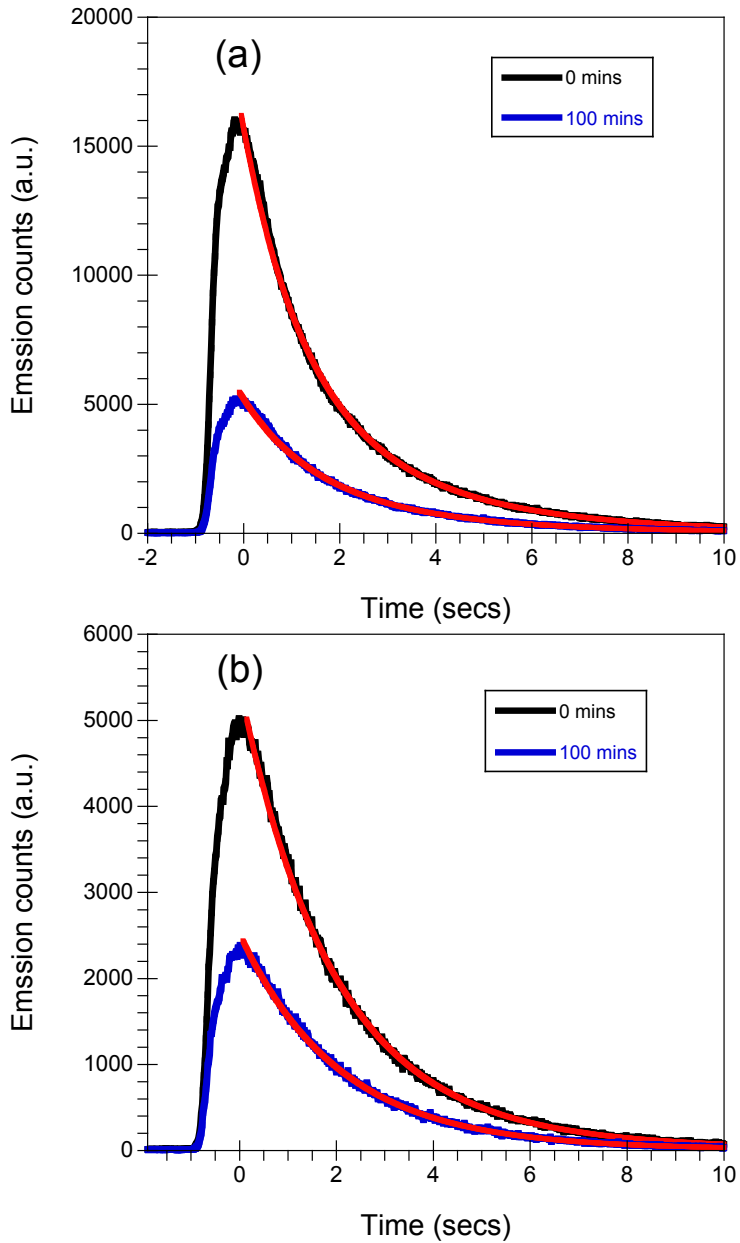


Figure 3.7 Emission lifetime decays for (a) **LS-1** and (b) **VCL01** devices after 0 and 100 mins AM 1.5G illumination light soaking measured at a 300 second acquisition time. Excitation wavelength was 470nm and emission wavelengths were 565 nm (**LS-1**) and 600 nm (**VCL01**).

Light soaking effect in D- π -A dyes (DSSC)

Returning to the effect of light soaking on device efficiency, generally, for most DSCs regardless of the sensitizer employed, from our experience^{26,27} and that of other groups²⁸⁻³⁰ an increase in efficiency is observed. In an exhaustive study by Listorti *et al.*³¹ involving DSC devices prepared with different materials (dyes, pastes, electrolytes etc.) in different laboratories the effect of light soaking on device parameters was investigated. In all cases an increase in both efficiency and J_{sc} was observed and explained as a downward shift in the TiO₂ conduction band resulting in lower V_{oc} . Luminescence lifetime studies indicated that this shift resulted in both faster electron injection and improved injection efficiency leading to higher J_{sc} and cell efficiency despite the lower V_{oc} .

Table 3.4. Emission lifetimes extracted from TC-SPC data of **LS-1** and **VCL01** DSC devices.

Dye	Lifetime (ns)*
LS-1 (0 mins)	1.20 (42%); 2.96 (58%)
LS-1 (100 mins)	1.39 (41%); 2.99 (59%)
VCL01 (0 mins)	1.83 (75%); 3.37 (25%)
VCL01 (100 mins)	2.02 (92%); 4.79 (8%)

*Emission decays were fitted with 2 exponential parameters. The percentage in parenthesis is the contribution of each parameter.

LS-1 and **VCL01** devices also show an increase in efficiency and J_{sc} following light soaking coupled with a small downward shift in the TiO₂ conduction band and increase in device electron lifetime. Emission lifetime studies of **LS-1** and **VCL01** devices measured using Time-Correlated Single Photon Counting (Figure 3.7) before and after light soaking show negligible differences in lifetime (Table 3.4), however, a notable quenching of emission intensity is observed after light soaking. This indicates that light soaking improves TiO₂/dye interaction resulting in improved quenching of dye excited states by TiO₂ electron injection. This also helps to explain the increase in device electron lifetime following light soaking, as the improvement in TiO₂/dye interaction

would improve the blocking of recombination of TiO₂ electrons with the electrolyte, with the much larger increase in electron lifetime for the **VCL01** device compared to the **LS-1** device due to the more bulky cyclopentadithiophene units. It is worth noting that no such affect was observed by leaving the cells in the dark indicating the positive effect of light soaking over device efficiency in these devices.

We therefore conclude that the improvement in device efficiency upon light soaking is less due to a change in the TiO₂ energetics and more to do with improved TiO₂/dye interaction resulting in a higher injection yield and larger J_{sc} on the one hand and improved blocking effect and larger V_{oc} on the other.

3.5 CONCLUSIONS

The synthesis and characterization of a novel indoline D- π -A sensitizer, **VCL01**, with a cyclopentadithiophene unit in the π -bridge was described and its performance determined in DSC devices. Though initially it showed an efficiency of 4.81%, this rose to 7.21% upon 120 mins light soaking under AM 1.5G illumination, representing an increase of 50%. This increase is mainly due to an increase in J_{sc} which is reflected in the improved IPCE spectra of devices following light soaking. Charge extraction data indicate a downward shift in the TiO₂ conduction band upon light soaking and transient photovoltage data show that device electron lifetime increases by over one order of magnitude. Time-correlated Single Photon Counting data explain partly the light soaking effect by an improvement in TiO₂/dye interaction leading to enhanced electron injection.

3.6 REFERENCES

- (1) Ooyama, Y.; Harima, Y. *ChemPhysChem* **2012**, *13*, 4032.
- (2) Yen, Y.-S.; Chou, H.-H.; Chen, Y.-C.; Hsu, C.-Y.; Lin, J. T. *J. Mater. Chem.* **2012**, *22*, 8734.
- (3) Wu, Y.; Zhu, W. *Chem. Soc. Rev.* **2013**, *42*, 2039.
- (4) <http://www.irishtimes.com/business/light-relief-solarprint-gets-funds-to-take-innovative-product-to-market-1.1248>.
- (5) <http://www.laserfocusworld.com/articles/2012/09/dyesol-bipv-solar-748-efficiency.html>.
- (6) Zeng, W.; Cao, Y.; Bai, Y.; Wang, Y.; Shi, Y.; Zhang, M.; Wang, F.; Pan, C.; Wang, P. *Chem. Mater.* **2010**, *22*, 1915.
- (7) Planells, M.; Pelleja, L.; Clifford, J. N.; Pastore, M.; De Angelis, F.; Lopez, N.; Marder, S. R.; Palomares, E. *Energy & Environmental Science* **2011**, *4*, 1820.
- (8) Zhang, G.; Bala, H.; Cheng, Y.; Shi, D.; Lv, X.; Yu, Q.; Wang, P. *Chem. Commun.* **2009**, 2198.
- (9) Choi, H.; Baik, C.; Kang, S. O.; Ko, J.; Kang, M.-S.; Nazeeruddin, M. K.; Grätzel, M. *Angew. Chem. Int. Ed.* **2008**, *47*, 327.
- (10) Chen, H.; Huang, H.; Huang, X.; Clifford, J. N.; Forneli, A.; Palomares, E.; Zheng, X.; Zheng, L.; Wang, X.; Shen, P.; Zhao, B.; Tan, S. *J. Phys. Chem. C* **2010**, *114*, 3280.
- (11) Teng, C.; Yang, X.; Yang, C.; Li, S.; Cheng, M.; Hagfeldt, A.; Sun, L. *J. Phys. Chem. C* **2010**, *114*, 9101.
- (12) Chen, B.-S.; Chen, D.-Y.; Chen, C.-L.; Hsu, C.-W.; Hsu, H.-C.; Wu, K.-L.; Liu, S.-H.; Chou, P.-T.; Chi, Y. *J. Mater. Chem.* **2011**, *21*, 1937.
- (13) Aljarilla, A.; Lopez-Arroyo, L.; de la Cruz, P.; Oswald, F.; Meyer, T. B.; Langa, F. *Org. Lett.* **2012**, *14*, 5732.
- (14) Ning, Z.; Zhang, Q.; Wu, W.; Pei, H.; Liu, B.; Tian, H. *J. Org. Chem.* **2008**, *73*, 3791.
- (15) Horiuchi, T.; Miura, H.; Sumioka, K.; Uchida, S. *Journal of the American Chemical Society* **2004**, *126*, 12218.
- (16) Ito, S.; Miura, H.; Uchida, S.; Takata, M.; Sumioka, K.; Liska, P.; Comte, P.; Pechy, P.; Grätzel, M. *Chem. Commun.* **2008**, 5194.
- (17) Zhu, W.; Wu, Y.; Wang, S.; Li, W.; Li, X.; Chen, J.; Wang, Z.-s.; Tian, H. *Adv. Funct. Mater.* **2011**, *21*, 756.
- (18) Cui, Y.; Wu, Y.; Lu, X.; Zhang, X.; Zhou, G.; Miapéh, F. B.; Zhu, W.; Wang, Z.-S. *Chem. Mater.* **2011**, *23*, 4394.
- (19) Wu, Y.; Zhang, X.; Li, W.; Wang, Z.-S.; Tian, H.; Zhu, W. *Adv. Energy Mat.* **2012**, *2*, 149.
- (20) Liu, B.; Zhu, W.; Zhang, Q.; Wu, W.; Xu, M.; Ning, Z.; Xie, Y.; Tian, H. *Chem. Commun.* **2009**, 1766.

- (21) Wu, Y.; Marszalek, M.; Zakeeruddin, S. M.; Zhang, Q.; Tian, H.; Gratzel, M.; Zhu, W. *Energy Environ. Sci.* **2012**, *5*, 8261.
- (22) Liu, B.; Li, W.; Wang, B.; Li, X.; Liu, Q.; Naruta, Y.; Zhu, W. *J. Power Sources* **2013**, *234*, 139.
- (23) Li, W.; Wu, Y.; Zhang, Q.; Tian, H.; Zhu, W. *ACS Appl. Mater. Interfaces* **2012**, *4*, 1822.
- (24) O. Miyata, N. Takeda, Y. Kimura, Y. Takemoto, N. Tohnai, M. Miyata and T. Naito, *Tetrahedron*, 2006, **62**, 3629-3647.
- (25) R. Li, J. Liu, N. Cai, M. Zhang and P. Wang, *J. Phys. Chem. B*, 2010, **114**, 4461-4464.
- (26) K.-L. Wu, C.-H. Li, Y. Chi, J. N. Clifford, L. Cabau, E. Palomares, Y.-M. Cheng, H.-A. Pan and P.-T. Chou, *J. Am. Chem. Soc.*, 2012, **134**, 7488-7496.
- (27) K.-L. Wu, W.-P. Ku, J. N. Clifford, E. Palomares, S.-T. Ho, Y. Chi, S.-H. Liu, P.-T. Chou, M. K. Nazeeruddin and M. Gratzel, *Energy Environ. Sci.*, 2013, **6**, 859-870.
- (28) B. O'Regan and D. T. Schwartz, *Chem. Mater.*, 1998, **10**, 1501-1509.
- (29) S. Ferrere and B. A. Gregg, *J. Phys. Chem. B*, 2001, **105**, 7602-7605.
- (30) A. Hagfeldt, U. Björkstén and M. Gratzel, *J. Phys. Chem.*, 1996, **100**, 8045-8048.
- (31) A. Listorti, C. Creager, P. Sommeling, J. Kroon, E. Palomares, A. Fornelli, B. Breen, P. R. F. Barnes, J. R. Durrant, C. Law and B. O'Regan, *Energy Environ. Sci.*, 2011, **4**, 3494-3501.

Chapter 4

High Efficient Push-Pull Porphyrin dyes for Dye Sensitized Solar cells.
The importance of molecular design

Table of contents

4.1 Abstract	83
4.2 Introduction	83
4.3 Experimental Section	85
3.3.1 Synthesis and Characterization	85
3.3.2 Device preparation	94
4.4 Results and Discussion	94
4.5 Conclusions	103
4.6 References	104

4.1 ABSTRACT

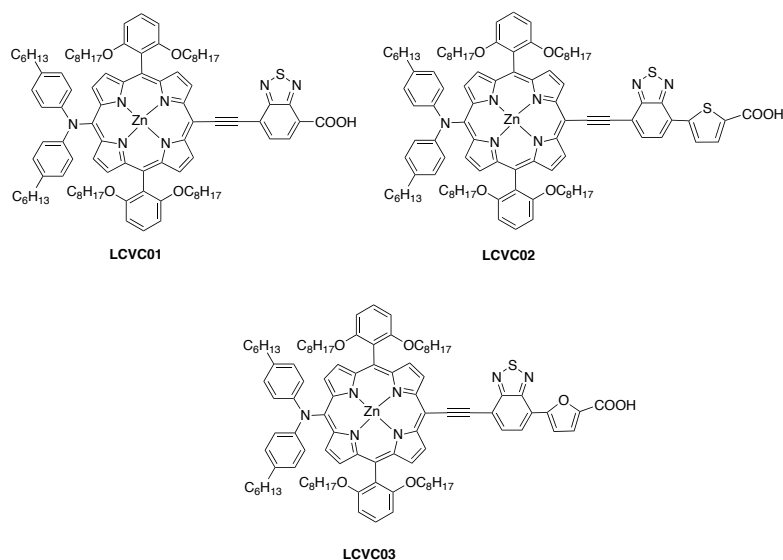
A new series of porphyrins have been synthesized in order to study their applicability in DSSC. The strategy followed to synthesize these porphyrins was the synthesis of a donor and acceptor zinc porphyrin introducing 2,1,3-benzothiadazole (BDT) group as a π -conjugated linker between the anchoring group and the porphyrin (**LCVC01**) and also the introduction of a thiophene (**LCVC02**) and a furan (**LCVC03**) between the BDT moiety and the anchoring group. These series of porphyrins were investigated for their application in DSSC devices. Devices of all of these dyes were characterized achieving a record cell of 10.4% for **LCVC02** but only a 3.84% and 2.55% were achieved for **LCVC01** and **LCVC03** respectively. The introduction of a thiophene shows us the importance to introduce a chemical group, such as thiophene, between of the BDT and the anchoring group. However the election of this group has to be accurate because, as we can see in this study, the change of one atom increases the recombination rate and decreases the device performance due to the interaction of oxygen atoms with iodine species.

4.2 INTRODUCTION

Dye Sensitized Solar Cells (DSSC) have attracted great much attention in recent years due to their potential low cost and the solar-energy conversion efficiency when compared to conventional photovoltaic devices^{1,2}. A great number of sensitizers have been synthesized looking for the highest conversion efficiency as, for example, Ruthenium complexes that show high efficiencies due to the broad absorbance range from the UV-Visible and some of the complexes even expand their absorption to the near infrared (NIR)³⁻⁷. However, the moderate molar extinction coefficients of the Ruthenium complexes, their synthesis and the hard purification process have lead to new efforts towards the synthesis of novel Ruthenium-free dyes. Most of these new organic dyes have, as general molecular structure, the Donor- π -Acceptor (D- π -A) combination⁸. This configuration allows easy tunability of the absorption properties, as well as, higher molar extinction coefficient.

Since the seminal paper by Sun and collaborations, many organic dyes have been reported with high efficiencies not only in iodine electrolyte^{9,10}, but even better efficiencies when using cobalt electrolyte¹¹⁻¹⁵. Moreover, recent studies on porphyrins have shown very promising results due to the high molar extinction coefficients of their Soret and Q band¹⁶. A landmark paper shows that the D- π -A structure consisting on the core of the porphyrin as π -moiety, leads to high efficiencies employing iodine as electrolyte¹⁷⁻²⁰. Furthermore, the best efficiencies have been achieved using a cobalt electrolyte reaching an efficiency of 11.9% and 12.3%, for iodine/iodide and cobalt electrolytes respectively. However, these efficiencies can only be achieved with the use of co-sensitized semiconductor mesoporous TiO₂ films with the Y123 dye²¹. Recently, Aswani Yella et al. reported an efficiency close to 13%, which is the highest reported efficiency ever for a DSSC^{22,23}

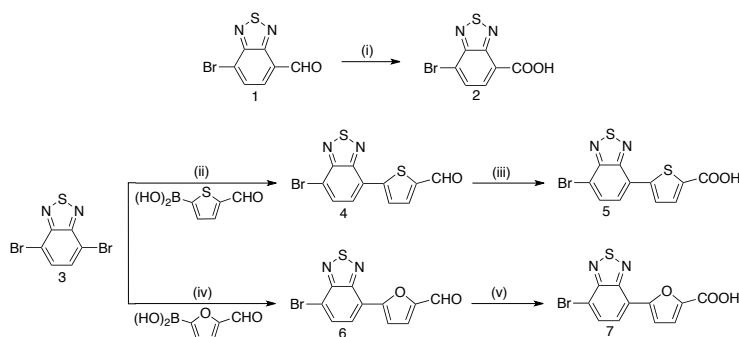
Based on the above mentioned results we synthesized a series of new porphyrins, namely **LCVC01** (GY21), **LCVC02** and **LCVC03**. We aim to study the effect of introducing a thiophene (LCVC02) and a furan group (LCVC03) between the benzothiadazole (BDT) and the anchoring group. The structures of these porphyrins are shown in Scheme 4.1.



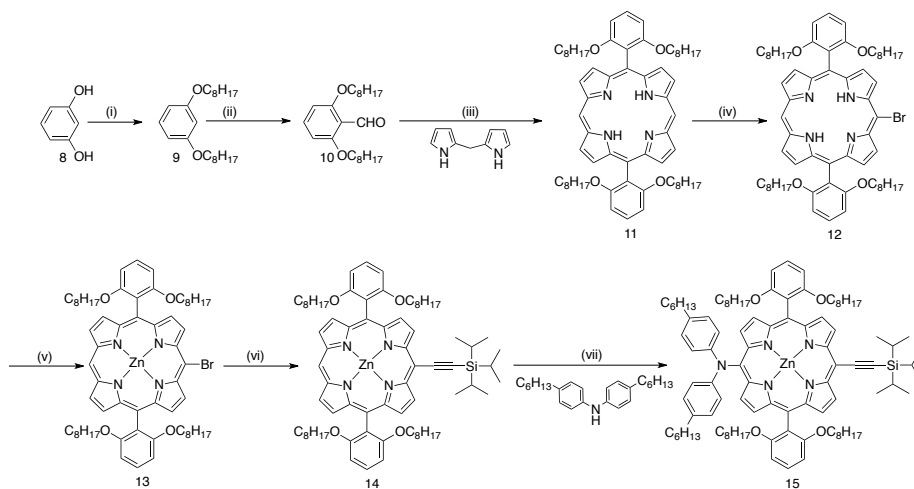
Scheme 4.1: Molecular structures of **LCVC01**, **LCVC02** and **LCVC03** dyes.

4.3 EXPERIMENTAL SECTION

4.3.1 Synthesis and characterization

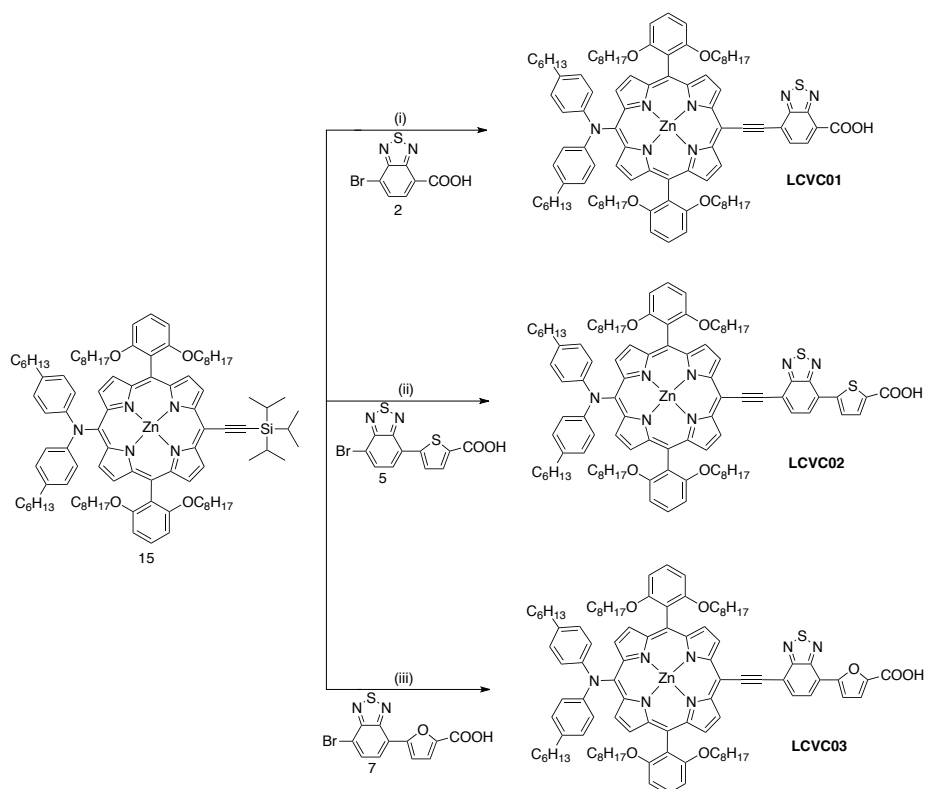


Scheme 4.2: Synthetic route for the **acceptor moieties**. (Reaction conditions: (i) NaClO₂, Sulfamic acid aqueous, Acetone, 4 h, RT; (ii) Pd^{II}(dppf)Cl₂, 2M K₂CO₃ aqueous solution, THF, 2 h, 76°C; (iii) NaClO₂, Sulfamic acid aqueous, Acetone, 4 h, RT; (iv) Pd^{II}(dppf)Cl₂, 2M K₂CO₃ aqueous solution, THF, 2 h, 76°C; (v) NaClO₂, Sulfamic acid aqueous, Acetone, 4 h, RT; Pd^{II}(dppf)Cl₂, 2M K₂CO₃ aqueous solution, dimethoxyethane, 2 h, 90°C;



Scheme 4.3: Synthetic route for the **common part of porphyrins**. (Reaction conditions: (i) 1-Bromooctane, K₂CO₃, Acetone, reflux, 4 days; (ii) TMEDA, THF, 0°C, ⁿBuLi, 3 h, 0°C, DMF, 2 h, RT; (iii) TFA, DCM, 4 h, 23°C, DDQ, 1h; (iv) NBS, DCM, 6 h, 0°C; (v) Zn(OAc)₂·2H₂O, DCM/Methanol, 3 h, 23°C; (vi) triisopropylsilylacetylene, Pd(PPh₃)₂Cl₂,

CuI, THF, NEt_3 , 4 h, reflux; (vii) Diphenylamine, iodobenzene diacetate, tetrachloroaurate dehydrate, DCM, 30 minutes, RT, $\text{Zn}(\text{OAc})_2 \cdot 2\text{H}_2\text{O}$, DCM/Methanol, 3 h, 23°C ;



Scheme 4.4: Synthetic route for the **LCVC01**, **LCVC02** and **LCVC03** dyes. (Reaction conditions: (i) TBAF 1M in THF, THF, 30 minutes, 23°C , **2**, NEt_3 , $\text{Pd}_2(\text{dba})_3$, ASPh_3 , THF, 4 h, reflux; (ii) TBAF 1M in THF, THF, 30 minutes, 23°C , **5**, NEt_3 , $\text{Pd}_2(\text{dba})_3$, ASPh_3 , THF, 4 h, reflux; (iii) TBAF 1M in THF, THF, 30 minutes, 23°C , **7**, NEt_3 , $\text{Pd}_2(\text{dba})_3$, ASPh_3 , THF, 4 h, reflux;

Synthesis of 7-bromobenzo[*c*][1,2,5]thiadiazole-4-carboxylic acid **2:** A solution at 0°C of 7-bromobenzo[*c*][1,2,5]thiadiazole-4-carbaldehyde (0.1g; 0.41mmol) in Acetone (70mL), NaClO_2 (0.109g, 1.21mmol), was added slowly. Then, a solution of sulfamic acid (0.117g; 1.21mmol) in Milli-Q-grade deionized water (8mL) was added and the solution was then stirred at room temperature for 4h. Then, the reaction was quenched with HCl (0.1M, 250mL) and the mixture was extracted with CHCl_3 . The combined extracts were washed with water and dried over anhydrous MgSO_4 . The solvent was removed under

reduced pressure to give as the desired product (white solid). (0.093g, 88% Yield). ^1H NMR (CDCl_3 , 400 MHz) δ_{H} : 8.45 (d, $J=7.7\text{Hz}$, 1H); 8.05 (d, $J=7.7\text{Hz}$, 1H).

Synthesis of 5-(7-bromobenzo[*c*][1,2,5]thiadiazol-4-yl)thiophene-2-carbaldehyde (4): In a Schlenk flask **3** (0.5 g, 1.70mmol), (5-formylthiophen-2-yl) boronic acid (0.268 g, 1.70mmol), $\text{Pd}^{\text{II}}(\text{dppf})\text{Cl}_2$ (0.056 g, 0.0765mmol) and 50ml of THF was added and the mixture was degassed. Then the solution was stirred at room temperature for 30 minutes. After this time 7 mL of K_2CO_3 2M was added and the mixture was degassed again. Then, the mixture was heated up to 76°C for 2 hours. After cooling, at room temperature, we added water and the solution was extracted with Et_2O and washed with brine. Then the crude is purified by column chromatography using Hexane/Ethyl Acetate (8:2) as a solvent to give us the desired product (yellow solid) (150mg, 27% Yield). ^1H NMR (THF_{d-8} , 400 MHz) δ_{H} : 9.95 (s, 1H); 8.25 (d, $J=4.0\text{Hz}$, 1H); 8.06 (d, $J=7.7\text{Hz}$, 1H); 8.00 (d, $J=7.7\text{Hz}$, 1H); 7.93 (d, $J=4.0\text{Hz}$, 1H). ^{13}C NMR (100MHz, THF_{d-8} , ppm) δ 183.18; 162.87; 160.35; 153.92; 145.65; 136.99; 134.36; 132.99; 129.00; 128.05; 115.27 MS-ESI (m/z): $[\text{M}-\text{H}]$ calculated for $\text{C}_{11}\text{H}_4\text{N}_2\text{BrN}_2\text{OS}_2$: 322.8954; found: 322.8958.

Synthesis of 5-(7-bromobenzo[*c*][1,2,5]thiadiazol-4-yl)thiophene-2-carboxylic acid (5): NaClO_2 (0.124g, 1,38mmol), was added slowly to at 0°C solution of 5-(7-bromobenzo[*c*][1,2,5]thiadiazol-4-yl)thiophene-2-carbaldehyde, **4** (150mg; 0.46mmol) in acetone (100mL). Then, a solution of sulfamic acid (0.134g; 1.38mmol) in Milli-Q-grade deionized water (10mL) was added to proceed at room temperature for 4h. Then the reaction was quenched with HCl (0.1M, 250mL) and the mixture was extracted with CHCl_3 . The combined extracts were washed with water and dried over anhydrous MgSO_4 . The solvent was removed under reduced pressure to give as the desired product (white solid). (0.131g, 84% Yield). ^1H NMR (CDCl_3 , 400 MHz) δ_{H} : 8.12 (m, 3H); 7.82 (d, $J=4.0\text{Hz}$, 1H). ^{13}C NMR (100MHz, $\text{DMSO}-d_6$, ppm) δ 162.85; 152.94; 150.82; 143.52; 135.81; 133.44; 132.49; 127.95; 127.18; 125.07; 113.22.

Synthesis of 5-(7-bromobenzo[c][1,2,5]thiadiazol-4-yl)furan-2-carbaldehyde (6): In a Schlenk flask **3** (0.5 g, 1.70 mmol), (5-formylfuran-2-yl)boronic acid (0.237 g, 1.70mmol), Pd^{II}(dppf)Cl₂ (0.056 g, 0.0765mmol) and 50ml of THF was added and the mixture was degassed. Then, the solution was stirred at room temperature for 30 minutes. Thereafter, 7mL of K₂CO₃ 2M were added and the mixture was degassed again. Then the mixture was heated up to 76°C for 2 hours. After cooling at room temperature water was added and the solution was extracted with Et₂O and washed with brine. Then the crude was purified by column chromatography using Hexane/DCM (8:2) as a solvent to give us the desired product (yellow solid) (0.160g, 29% Yield). ¹H NMR (CDCl₃, 400 MHz) δ_H: 9.72(s, 1H); 8.14 (d, J=7.7Hz, 1H); 7.94 (d, J=7.7Hz, 1H); 7.87 (d, J=3.6Hz, 1H); 7.41 (d, J=3.6Hz, 1H); ¹³C NMR (100MHz, CDCl₃, ppm) δ 177.71; 154.39; 154.017; 152.31; 150.92; 132.45; 126.50; 123.88; 121.50; 115.65; 114.89 MS-ESI (*m/z*): [M+Na]⁺ calculated for C₁₁H₅N₂BrN₂NaO₂S: 330.9147; found: 330.9137.

Synthesis of 5-(7-bromobenzo[c][1,2,5]thiadiazol-4-yl)furan-2-carboxylic acid (7): A solution at 0°C of 5-(7-bromobenzo[c][1,2,5]thiadiazol-4-yl)furan-2-carbaldehyde **6** (0.160 g; 0.51mmol) in acetone (110mL), NaClO₂ (0.140 g, 1.55mmol), was added slowly. Then, a solution of sulfamic acid (0.151 g; 1.55mmol) in Milli-Q-grade deionized water (10mL) was added and the solution was then stirred at room temperature for 4h. Then, the reaction was quenched with HCl (0.1M, 250mL) and the mixture was extracted with CHCl₃. The combined extracts were washed with water and dried over anhydrous MgSO₄. The solvent was removed under reduced pressure to give as the desired product (yellow solid). (0.133 g, 80% Yield). ¹H NMR (DMSO-d₆ 400 MHz) δ_H: 8.12 (d, J=7.7Hz, 1H); 7.99 (d, J=7.7Hz, 1H); 7.69 (d, J=3.6Hz, 1H); 7.42 (d, J=3.6Hz, 1H); ¹³C NMR (100MHz, DMSO-d₆, ppm) δ 159.13; 153.00; 151.44; 149.83; 144.88; 132.54; 125.28; 120.91; 119.82; 113.90; 113.45.

Synthesis of 1,3-Dioctoxybenzene (9): A mixture of resorcinol **8** (11g, 0.1mol), 1-bromooctane (69.6mL, 0.4mol) and K₂CO₃ (69g, 0.5mol) was refluxed for 4 days in dry acetone (500mL). The solvent was removed under reduced pressure and the mixture is extracted with EtOAc (3x100mL). The

organic layer was washed with water and dried over anhydrous MgSO_4 . After removal of solvent under reduced pressure, the product was purified by column chromatography using hexane as a solvent to give the desirable product. (18g, 54% yield). ^1H NMR (CDCl_3 , 400 MHz) δ_{H} : 7.13 (t, $J=8.2\text{Hz}$, 1H); 6.45 (m, 3H); 3.91 (t, $J=6.6\text{ Hz}$, 4H); 1.75 (m, 4H); 1.43 (m, 4H); 1.33-1.23 (m, 16H); 0.88 (t, $J=6.7\text{Hz}$, 6H).

Synthesis of 2,6-Dioctoxybenzaldehyde (10): A three-neck flask was equipped with an addition funnel and charged with 1,3-Dioctoxybenzene **9** (5g, 0.15mol) and tetramethylethylenediamine (TMEDA) (0.57mL) in 42 mL of THF. The solution was degassed and cooled to 0°C . Then n-butyllithium (11.2mL, 0.03mol) was added dropwise, (during 20min) and allowed to stir for 3 hours. After warming to room temperature DMF (2.19mL, 0.03mol) was added dropwise and the solution was stirred for 2 hours. The reaction was quenched with water, and the mixture was extracted with ether (3x40mL), dried over MgSO_4 , and the solvent was removed under vacuum. The product was recrystallized from hexanes to yield a white solid. (3.5g, 65% Yield). ^1H NMR (CDCl_3 , 400 MHz) δ_{H} : 10.11 (s, 2H); 9.23 (d, $J=4.6\text{Hz}$, 4H); 8.50 (d, $J=4.6\text{Hz}$, 4H); 7.69 (t, $J=8.2\text{Hz}$, 2H); 7.00 (d, $J=8.2\text{Hz}$, 4H); 3.82 (t, $J=6.4\text{ Hz}$, 8H); 0.92-0.78 (m, 16H); 0.67-0.60 (m, 8H); 0.56-0.40 (m, 36H); -3.03(s, 2H).

Synthesis of 5,15-Bis(2,6-dioctoxyphenyl)porphyrin (11): Dipyrrromethane (1.51g, 10.35mmol) and 2,6-Dioctoxybenzaldehyde **10** (3.75g, 10.35mmol) were solved in DCM (1.35L) and degassed. Then, Trifluoroacetic acid (0.69mL, 9.32mmol) was added and the mixture was stirred at 23°C for 4h under Nitrogen conditions. After that, DDQ (3.53g, 15.25mmol) was added and the mixture was stirred for an additional 1 h. Then, the mixture was basified with Et_3N (1.75mL) and filtered through silica. The solvent was removed under vacuum and the residue was purified by column chromatography using a mixture of Hexane/DCM (2/1) as eluent to give us the desired product (purple powder), (1.6g, 31.50% Yield). ^1H NMR (CDCl_3 , 400 MHz) δ_{H} : 10.11 (s, 2H); 9.23 (d, $J=4.5\text{Hz}$, 4H); 8.95 (d, $J=4.5\text{Hz}$, 4H); 7.69 (t, $J=8.5\text{Hz}$, 2H); 7.00 (d, $J=8.5\text{Hz}$, 4H); 3.81 (t, $J=6.5\text{ Hz}$, 8H); 0.92-0.87 (m, 8H); 0.85-0.78 (m, 8H); 0.64-0.59 (m, 8H); 0.55-0.48(m, 28H); 0.45-0.39 (m, 8H); -3.03(s, 2H).

Synthesis of 5-Bromo-10,20-bis(2,6-dioctoxyphenyl)porphyrin (12): A stirred solution of 5,15-Bis(2,6-dioctoxyphenyl)porphyrin **11** (1.6g, 1.64mmol) in DCM (600mL) was slowly added a solution of NBS (0.31g, 1.72mmol) in DCM (100mL). The reaction was stirred at 0°C for 6h. The reaction was quenched with acetone (20mL), the solvent was removed under vacuum. The residue was purified by column using Hexane/DCM (2:1) as eluent to give us the desired product. (Purple powder) (1.4g, 70% Yield). ¹H NMR (CDCl₃, 400 MHz) δ_H: 10.02 (s, 1H); 9.63 (d, J=4.8Hz, 2H); 9.18 (d, J=4.8Hz, 2H); 8.90 (m, 4H); 7.70(t, J= 8.1Hz, 2H); 7.01 (d, J=8.4Hz, 4H); 3.85 (t, J=6.6 Hz, 8H); 0.98-0.90 (m, 8H); 0.88-0.80 (m, 8H); 0.69-0.61 (m, 8H); 0.58-0.49 (m, 36H); -2.85 (s, 2H).

Synthesis of [5-Bromo-10,20-bis(2,6-di-octoxyphenyl)porphinato]zinc (II) (13): A mixture of 5-Bromo-10,20-bis(2,6-dioctoxyphenyl)porphyrin (1.44g, 1.36mmol) **12** and Zn(OAc)₂·2H₂O (3g, 13.66mmol) in a mixture of DCM (280mL) and MeOH (150mL) was stirred at 23°C for 3 h. The reaction was quenched with water (60mL), and the mixture was extracted with DCM. The combined extracts were washed with water and dried over anhydrous MgSO₄. The solvent was removed under reduced pressure to give as the desired product. (1.34g, 88% Yield). ¹H NMR (CDCl₃, 400 MHz) δ_H: 10.05 (s, 1H); 9.68 (d, J=4.8Hz, 2H); 9.22 (d, J=4.8Hz, 2H); 8.95 (t, J=4.8Hz, 4H); 7.68(t, J= 8.5Hz, 2H); 6.99 (d, J=8.5Hz, 4H); 3.81 (t, J=6.7 Hz, 8H); 0.91-0.84 (m, 8H); 0.78-0.71 (m, 8H); 0.57-0.40 (m, 44H).

Synthesis of [5,15-Bis(2,6-di-octoxyphenyl)-10-(triisopropylsilyl)ethynylporphinato] zinc (II) (14). A mixture of zinc complex **13** (1.34g, 1.19mmol), triisopropylsilylacetylene (0.47mL, 2.99mmol), Pd(PPh₃)₂Cl₂ (0.16g, 0.23mmol), CuI (0.066g, 0.35mmol), THF (45mL) and Net₃ (7.3mL) was refluxed for 4 h under dinitrogen. The solvent was removed under vacuum. The residue was purified by column chromatography using Hexane/DCM (3:2) to give as the desired product (purple solid) (1.3g 89.6% Yield). ¹H NMR (CDCl₃, 400 MHz) δ_H: 10.02 (s, 1H); 9.72 (d, J=4.6Hz, 2H); 9.20 (d, J=4.6Hz, 2H); 8.93 (d, J=4.4Hz, 2H); 8.91 (d, J=4.4Hz, 2H); 7.66 (t, J=8.4Hz, 2H); 6.99 (d, J=8.4Hz,

4H); 3.80 (t, J=6.8Hz, 8H); 1.61-1.57 (m, 21H); 1.09-1.00 (m, 8H); 0.91-0.81 (m, 8H); 0.69-0.44 (m, 44H).

Synthesis of [5-Bis(4-hexylphenyl)amino-15-(Triisopropylsily)ethynyl-10,20-bis(2,6-di-octooxyphenyl)porphyrinato] Zinc(II) (15). To a stirred solution of [5,15-Bis(2,6-di-octooxyphenyl)-10-(triisopropylsilyl)ethynylporphyrinato] zinc (II) **14** (370.0 mg, 0.30 mmol) and Diphenylamine (0.310 g, 0.91mmol) in CH₂Cl₂ (150 mL) was added iodobenzene diacetate (99 mg, 0.310 mmol) and sodium tetrachloroaurate dihydrate (184 mg, 0.465 mmol) at 0 °C and stirred for 30 minutes at room temperature under open air. After completion of the reaction (monitored by TLC) the reaction mixture were quenched with a saturated solution of sodium thiosulfate and separated the organic layer. Extracted the aqueous layer with CH₂Cl₂; combined organic phase was washed with brine, and dried over Na₂SO₄. The solvent was removed in vacuum obtaining the mixture. This mixture was reacted with Zn(OAc)₂·2H₂O in a mixture of DCM (280mL) and MeOH (150mL) and was stirred at 23°C for 3 h. The reaction was quenched with water (60mL), and the mixture was extracted with DCM. The combined extracts were washed with water and dried over anhydrous MgSO₄. The solvent was removed under reduced pressure to give as the desired product (0.382g 82% Yield). ¹H NMR (CDCl₃, 400 MHz) δ_H: 9.63 (d, J=4.6Hz, 2H); 9.16 (d, J=4.6Hz, 2H); 8.83 (d, J=4.4Hz, 2H); 8.67 (d, J=4.4Hz, 2H); 7.61 (t, J=8.4Hz, 2H); 7.20 (d, J=8.4Hz, 4H); 6.91 (t, J=8.5Hz, 8H); 3.79 (t, J=6.2Hz, 8H); 2.43 (t, J=7.5Hz, 4H); 1.53-1.49 (m, 4H); 1.44-1.41 (m, 21H); 1.32-1.27 (m, 12H); 0.95 (m, 8H); 0.88-0.76 (m, 22H); 0.61-0.44 (m, 44H).

Synthesis of LCVC01: To a solution of [5-Bis(4-hexylphenyl)amino-15-(Triisopropylsily)ethynyl-10,20-bis(2,6-di-octooxyphenyl)porphyrinato] Zinc(II) **15** (240mg, 0.154mmol) in dry THF (20mL) was added TBAF (0.78mL) 1M in THF. The solution was stirred at 23°C for 30min under dinitrogen. The mixture was quenched with H₂O and then extracted with CH₂Cl₂. The organic layer was dried anhydrous MGSO₄ and the solvent was removed under reduced pressure. The residue and 7-bromobenzo[c][1,2,5]thiadiazole-4-carboxylic acid **2** (190mg, 0.76) were dissolved in a mixture of dry THF (36mL) and NEt₃ (7mL) and the

solution was degassed with dinitrogen for 10min. Then, Pd₂(dba)₃ (42mg, 0.046mmol) and ASPH₃ (100mg, 0.30mmol) were added to the mixture. The solution was refluxed for 4 hours under dinitrogen. The solvent was removed under reduced pressure. After that, the residue was purified by column chromatography (silica gel) using DCM/CH₃OH =20/1 as eluent. Recrystallization from CH₃OH/Ether to give **LCVC01** (180mg, 74%) ¹H NMR (THFd-8, 400 MHz) δ_H: 9.97 (d, J=4.6Hz, 2H); 9.04 (d, J=4.6Hz, 2H); 8.81 (d, J=4.6Hz, 2H); 8.55 (d, J=4.6Hz, 2H); 8.54 (s, 1H); 8.30 (d, J=7.6Hz, 1H); 7.67 (t, J=8.4Hz, 2H); 7.20 (d, J=8.4Hz, 4H); 7.04 (d, J=8.4Hz, 4H); 6.92 (d, J=8.4Hz, 4H); 3.87 (t, J=6.3Hz, 8H); 2.47 (t, J=7.4Hz, 4H); 1.58-1.51 (m, 4H); 1.36-1.27 (m, 12H); 1.00-0.57 (m, 66H).

Synthesis of LCVC02: To a solution of [5-Bis(4-hexylphenyl)amino-15-(Triisopropylsilyl)ethynyl-10,20-bis(2,6-di-octoxyphenyl)porphyrinato] Zinc(II) **15** (165mg, 0.106mmol) in dry THF (15mL) was added TBAF (0.54mL) 1M in THF. The solution was stirred at 23°C for 30min under dinitrogen. The mixture was quenched with H₂O and then extracted with CH₂Cl₂. The organic layer was dried anhydrous MgSO₄ and the solvent was removed under reduced pressure. The residue and 5-(7-bromobenzo[c][1,2,5]thiadiazol-4-yl)thiophene-2-carboxylic acid **5** (180mg, 0.53mmol) were dissolved in a mixture of dry THF (30mL) and NEt₃ (4.8mL) and the solution was degassed with dinitrogen for 10min. Then, Pd₂(dba)₃ (29mg, 0.031mmol) and ASPH₃ (71mg, 0.212mmol) were added to the mixture. The solution was refluxed for 4 hours under dinitrogen. The solvent was removed under reduced pressure. Then, the residue was purified by column chromatography (silica gel) using DCM/CH₃OH =20/1 as eluent. Recrystallization from CH₃OH/Ether to give **LCVC02** (115mg, 66%) ¹H NMR (THFd-8, 400 MHz) δ_H: 9.96 (d, J=4.6Hz, 2H); 9.03 (d, J=4.6Hz, 2H); 8.80 (d, J=4.6Hz, 2H); 8.55 (d, J=4.6Hz, 2H); 8.27 (s, 2H); 8.24 (d, J=4.0Hz, 1H); 7.84 (d, J=4.0Hz, 1H); 7.65 (t, J=8.4Hz, 2H); 7.19 (d, J=8.4Hz, 4H); 7.02 (d, J=8.4Hz, 4H); 6.91 (d, J=8.0Hz, 4H); 3.85 (t, J=6.4Hz, 8H); 2.46 (t, J=7.3Hz, 4H); 1.59-1.51 (m, 4H); 1.28 (m, 12H); 0.97-0.55 (m, 66H). ¹³C NMR (100MHz, THF-d₈, ppm) δ 160.78; 156.76; 153.02; 152.11; 151.53; 151.28; 151.02; 134.90; 132.57; 132.06; 131.27; 130.81; 130.42; 130.34; 129.16;

128.21; 127.29; 122.39; 121.49; 121.46; 115.27; 105.71; 68.73; 35.98; 32.54; 32.36; 30.45; 29.58; 29.50; 29.40; 25.98; 23.32; 23.10; 14.23; 14.10 MS-ESI (*m/z*): [M+Na]⁺ calculated for C₁₀₁H₁₂₁N₇NaO₆S₂Zn: 1678.8003; found: 1678.7963.

Synthesis of LCVC03: To a solution of [5-Bis(4-hexylphenyl)amino-15-(Triisopropylsilyl)ethynyl-10,20-bis(2,6-di-octoxyphenyl)porphyrinato] Zinc(II) **15** (150mg, 0.09mmol) in dry THF (15mL) was added TBAF (0.50mL) 1M in THF. The solution was stirred at 23°C for 30min under dinitrogen. The mixture was quenched with H₂O and then extracted with CH₂Cl₂. The organic layer was dried anhydrous MgSO₄ and the solvent was removed under reduced pressure. The residue and 5-(7-bromobenzo[c][1,2,5]thiadiazol-4-yl)furan-2-carboxylic acid **7** (146mg, 0.45) were dissolved in a mixture of dry THF (24mL) and NEt₃ (4mL) and the solution was degassed with dinitrogen for 10min. Then, Pd₂(dba)₃ (24mg, 0.026mmol) and ASPH₃ (60mg, 0.18mmol) were added to the mixture. The solution was refluxed for 4 hours under dinitrogen. The solvent was removed under reduced pressure. The residue was purified by column chromatography (silica gel) using DCM/CH₃OH =20/1 as eluent. Recrystallization from CH₃OH/Ether to give **LCVC03** (112mg, 76%). ¹H NMR (THFd-8, 400 MHz) δ_H: 9.80 (d, J=4.6Hz, 2H); 9.04 (d, J=4.6Hz, 2H); 8.81 (d, J=4.6Hz, 2H); 8.56 (d, J=4.6Hz, 2H); 8.41 (d, J=7.7Hz, 1H); 8.34 (d, J=7.7Hz, 1H); 7.93 (d, J=3.6Hz, 1H); 7.67 (t, J=8.3Hz, 2H); 7.41 (d, J=3.6Hz, 1H); 7.21 (d, J=8.7Hz, 4H); 7.04 (d, J=8.7Hz, 4H); 6.93 (d, J=6.7Hz, 4H); 3.87 (t, J=6.5Hz, 8H); 2.47 (t, J=7.4Hz, 4H); 1.60-1.51 (m, 4H); 1.30 (m, 12H); 1.01-0.57 (m, 66H). ¹³C NMR (100MHz, THF-d8, ppm) δ 160.78; 156.75; 153.03; 152.10; 151.88; 151.53; 151.28; 151.02; 134.90; 132.57; 132.05; 131.31; 130.82; 130.34; 129.16; 125.75; 123.93; 122.40; 121.49; 115.27; 114.40 105.17; 68.72; 35.98; 32.54; 32.36; 29.91; 29.60; 29.50; 29.40; 25.98; 23.32; 23.10; 14.23; 14.10 MS-ESI (*m/z*): [M]⁺ calculated for C₁₀₁H₁₂₁N₇O₇SZn: 1639.8334; found: 1639.8365.

4.3.2 Device preparation

All the devices for this work have been made as described in Chapter 2.

Two types of TiO₂ films were utilized depending on the measurements being conducted. Highly transparent thin films (8 μm) were utilized for L-TAS measurements. On the other hand, efficient DSC devices were made using 14 μm thick films consisting of 20 nm TiO₂ nanoparticles (Dyesol® paste) and a scatter layer of 4 μm of 400 nm TiO₂ particles (CCIC, HPW-400). All films were sensitized in dye solutions at concentrations of 0.125 mM in Ethanol containing 20mM chenoxyldecholic acid were prepared and the film immersed overnight at room temperature. The sensitized electrodes were washed with Ethanol and dried under air. For this work we have used iodine electrolyte consisted of 0.5 M 1-butyl-3-methylimidazolium iodide (BMII), 0.1 M lithium iodide, 0.05 M iodine and 0.5 M *tert*-butylpyridine in acetonitrile;

4.4 RESULTS AND DISCUSSIONS

In Figure 4.1 we can see the absorption spectra of **LCVC01**, **LCV02** and **LCV03 dyes**. Their photophysical and electrochemical characteristics are listed in Table 4.1

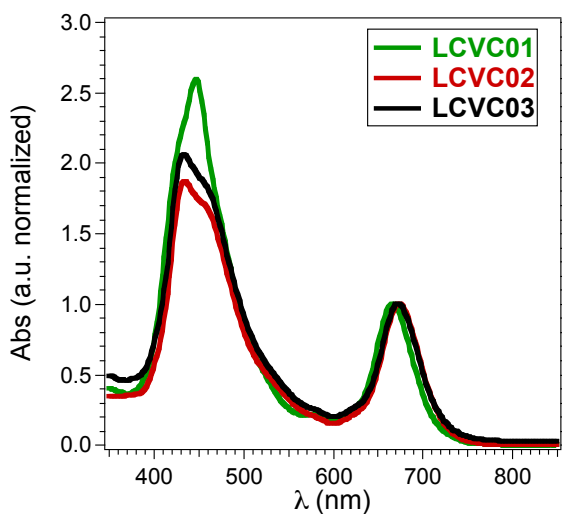


Figure 4.1: Absorption spectra of **LCVC01**, **LCV02** and **LCV03**

As shown in Figure 4.1 all the dyes exhibit typical porphyrin spectra with the bands associated to them. At around 450nm we observed an intense Soret band and between 600-700nm a lower intense Q-band. The absorption and emission values of three porphyrins are similar. The oxidation potentials of **LCVC02** and **LCVC03** are the same. However is 20mV lower comparing with the **LCVC01**. This is due to the presence of thiophene and furan between the BDT moiety and the carboxylic acid in **LCVC02** and **LCVC03** respectively. We do not observe a great difference in the HOMO and LUMO levels of the molecules and the values of them are in the case of the LUMO high enough to inject in the TiO₂, and the HOMO level low enough to regenerate from the electrolyte.

Table 4.1. Absorption, emission and electrochemical properties of **LCVC01**, **LCVC02** and **LCVC03**

Dye	λ_{abs} (nm) ^a	λ_{em} (nm) ^a	E_{ox} (V v's Fc/Fc+) ^b	E_{0-0} (eV) ^c	E_{HOM} (eV) ^d	E_{LUM} (eV) ^e
LCVC01	448(212); 579(18); 668(87)	705	0.19	1.82	-5.07	-3.25
LCVC02	434(92); 674(47)	715	0.17	1.81	-5.05	-3.24
LCVC03	434(145); 674(70)	690	0.17	1.82	-5.05	-3.23

^aMeasured in Tetrahydrofuran. In parenthesis molar extinction efficient at λ_{abs} (in M⁻¹ cm⁻¹). ^c E_{0-0} was determined from the intersection of absorption and emission spectra in dilute solutions. ^d E_{HOMO} was calculated using $E_{HOMO}(vs\ vacuum) = -4.88 - E_{ox}(vs\ Fc/Fc+)$. ^e E_{LUMO} was calculated using $E_{LUMO} = E_{HOMO} + E_{0-0}$.

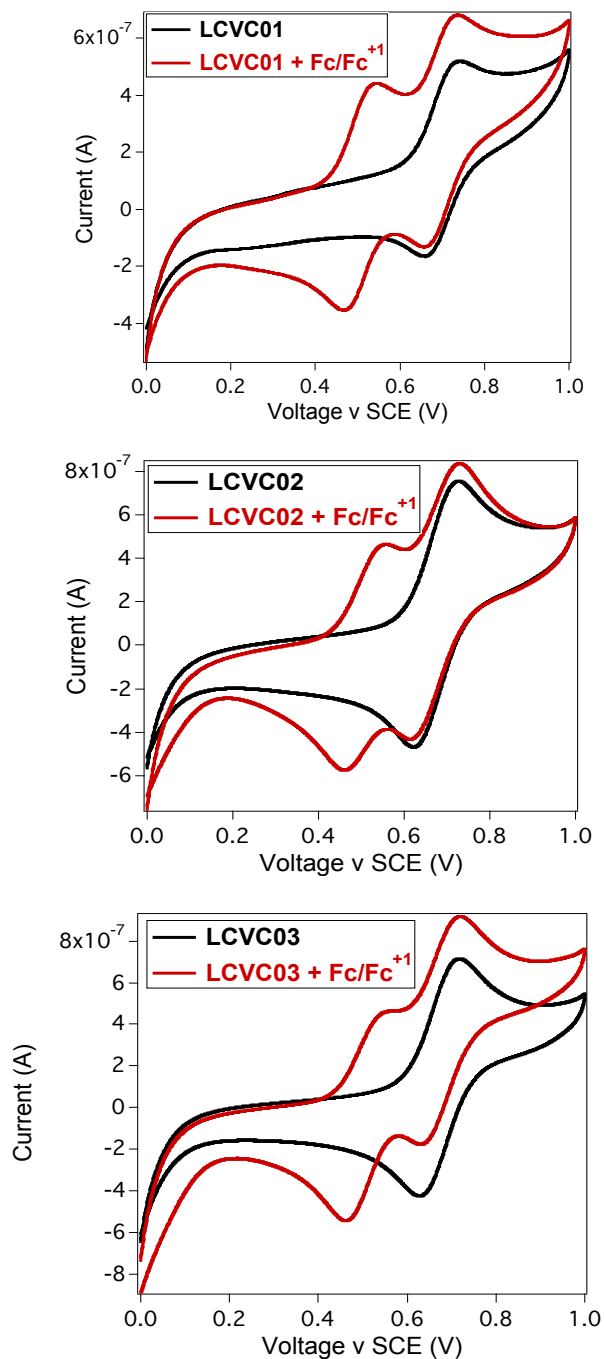


Figure 4.2: Cyclic voltammetry of **LCVC01** (top), **LCVC02** (middle) and **LCVC03** (bottom) recorded in 0.1M tetrabutylammonium hexafluorophosphate in 1:1 acetonitrile:tert-butanol at a scan rate of 10 mV s^{-1} . The working electrode consisted of a

platinum wire and the counter electrode a platinum mesh. The reference electrode was the silver calomel electrode (saturated KCl). All solutions were degassed with argon for 5 mins prior to measurement. The red and black scans were recorded in the presence and absence of Ferrocene/Ferrocene+.

Comparing the frontier orbitals of three molecules we observed that probability to find the highest occupied molecular orbital (HOMO) of three dyes is located predominantly on the donor moiety of the molecule. The probability to localize the lowest unoccupied molecular orbital (LUMO) is similar for LCVC02 and LCVC03 showing a significant shift through the acceptor due to the presence of the BDT acting as an electron drawing moiety that we don't observe for LCVC01 dye. With this observation we can say that in the case of LCVC02 and LCVC03 an increase of Charge Transfer.

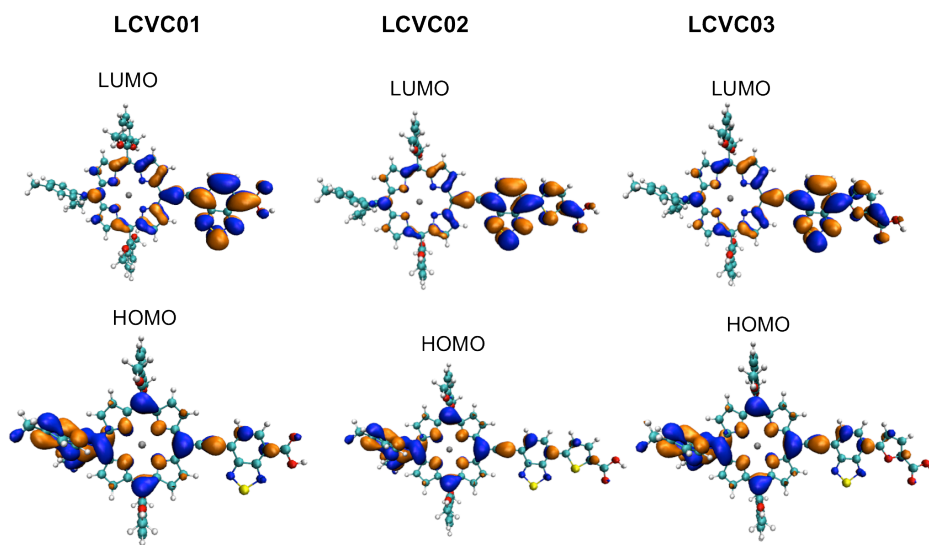


Figure 4.3: Frontier molecular orbitals of **LCVC01**, **LCVC02** and **LCVC03** at the B3LYP/6-31G (d) level

LCVC01, **LCVC02** and **LCVC03** were used to fabricate DSSC solar cells and measured under illumination conditions (AM 1.5G 100 mW/m²). Device properties are listed in Table 4.2.

Table 4.2: Photovoltaic parameters obtained with **LCVC01**, **LCVC02** and **LCVC03**

Dye	V_{oc} (V)	J_{sc} (mA/cm ²)	FF (%)	η (%)*
LCVC01	0.65	7.69	75.40	3.84 (4.52)
LCVC02	0.70	20.00	74.41	10.41 (12.51)
LCVC03	0.58	5.81	74.42	2.55 (2.82)

The photocurrent density observed for **LCVC01** and **LCVC03** is lower when compared to **LCVC02**. The best J_{sc} corresponds to **LCVC02** that displays an impressive 20.00 mA/cm², such current is actually as high as the best perovskite solar cells, in contrast with the 7.7 and 5.8 achieved for **LCVC01** and **LCVC03** respectively. The open circuit voltage (V_{oc}) for **LCVC01** is 650mV. As reported before²² the introduction of a group between the BDT and the anchoring group as in the case of **LCVC02** made that the V_{oc} increase in 50mV. Despite this effect is not observed for **LCVC03** with a low V_{oc} of 580mV. All dyes present similar values of fill-factor (FF). In Figure 4.3(a) is showed the I-V curves of **LCVC01**, **LCVC02** and **LCVC03**. In figure 4.3(b) is showed the incident-photon-to-current conversion (IPCE) of the champion cell of **LCVC02** exhibiting an IPCE up to 800nm. IPCE spectrum shows two maxima due to the Soret and Q bands of the porphyrin at 480nm of 76% and 670nm almost 90%.

Electron density and electron lifetime (Figure 4.4 and 4.5) in these devices were probed using charge extraction and transient photovoltage measurements respectively²⁴⁻²⁶. We observed higher charge density for **LCVC02** when compared to **LCVC01**. However the greater difference is comparing **LCVC03** that presents a lower charge density. From the TPV measurements (Figure 4.5) a slower recombination dynamics can be seen for **LCVC02** and a similar electron lifetime is also observed for **LCVC01**, which explains the similar voltage achieved for these devices. Also in agreement with the shortest electron lifetime for **LCVC03**. The difference obtained can be explained due to the differences in the $e^-_{TiO_2}/electrolyte^+$ recombination rate. Some studies reported before^{10,27,28} show that the introduction of heteroatoms could bind to I_3^- and I_2

forming complexes. Due to this, more species are present in the TiO₂ surface accelerating the recombination rate. In our study we have seen how this hypothesis effects a change in the device performance by just the change of only one atom in the molecular structure.

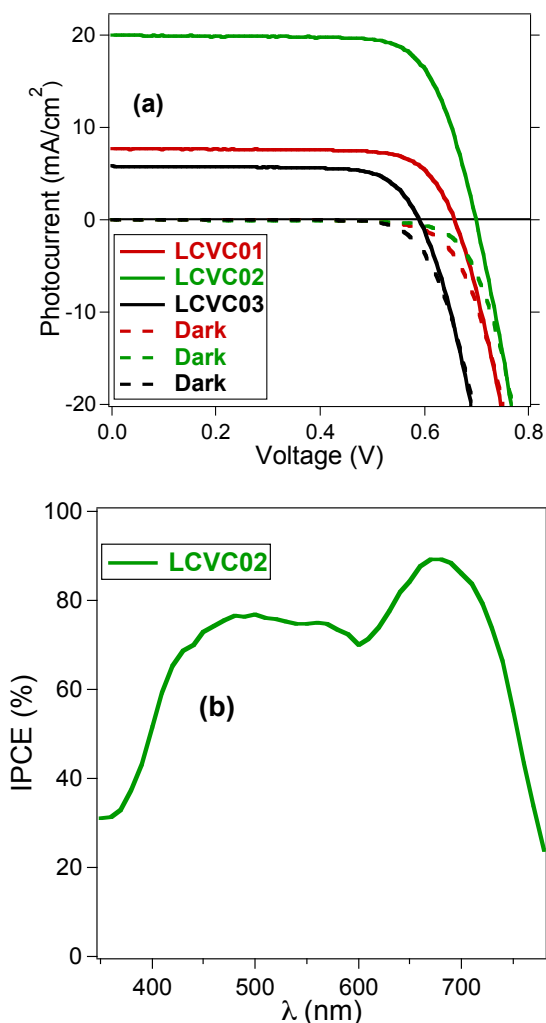


Figure 4.3 (a) I-V curves for LCVC01, LCVC02 and LCVC03 (b) IPCE spectra of LCVC02. DSC devices recorded under AM 1.5G radiation. Also shown are I-V dark curves.

In order to probe charge recombination and regeneration by the I_3^-/I^- redox couple in transparent DSC devices Laser transient absorption spectroscopy has been used. In figure 4.6 a, b, c we can see the charge recombination decays between the photo-injected electrons at the TiO_2 and the oxidized dye for **LCVC01**, **LCVC02** and **LCVC03** respectively. The data was recorded in absence of electrolyte (black) and corresponds to the long-lived decays assigned to the dye cation formed following photo-excitation. In red color we monitored the same process but in presence of electrolyte (red) with loss of cation signal due to the regeneration by I^- .

In order to estimate the regeneration efficiency we quantified the lifetime at the FWHM (full width at half maximum) of the signal which is 20, 60 and 60 μ s for **LCVC01**, **LCVC02** and **LCVC03** showing a small difference comparing **LCVC01** with **LCVC02** and **LCVC03** due to the small difference in oxidation potentials having **LCVC01** more positive oxidation potential and presenting more driving force.

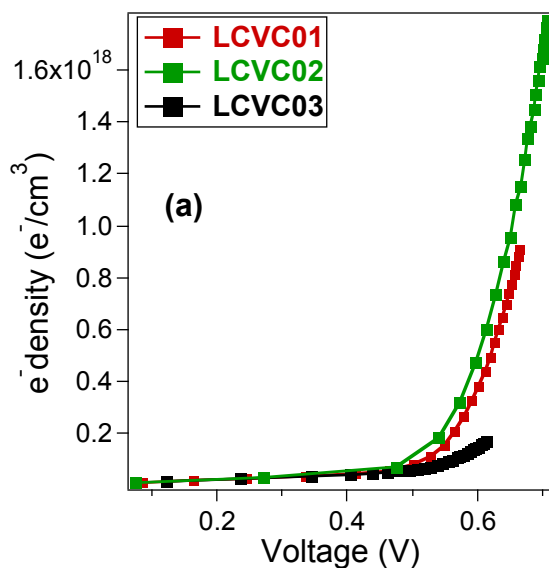


Figure 4.4: Electron density as a function of cell voltage for **LCVC01**, **LCVC02** and **LCVC03** devices.

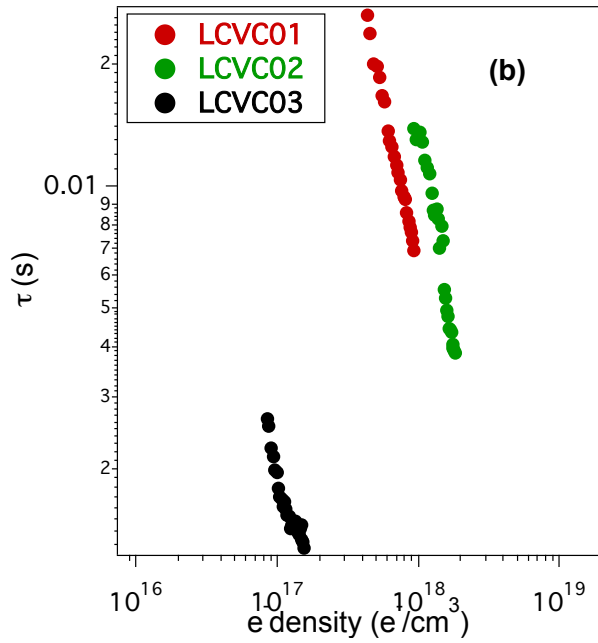
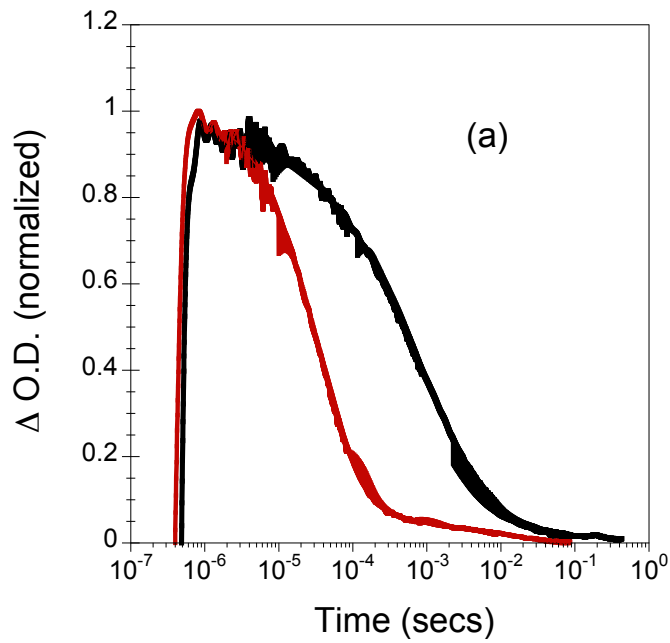


Figure 4.5: Device electron lifetime τ as a function of charge density for LCVC01, LCVC02 and LCVC03 devices.



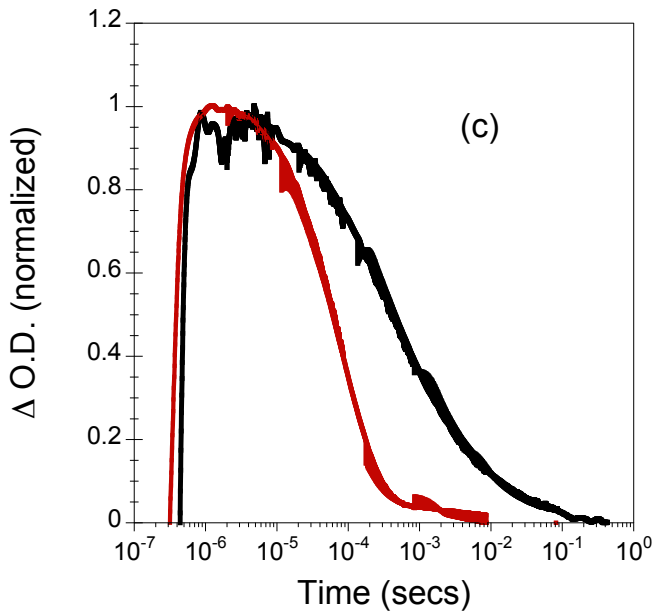
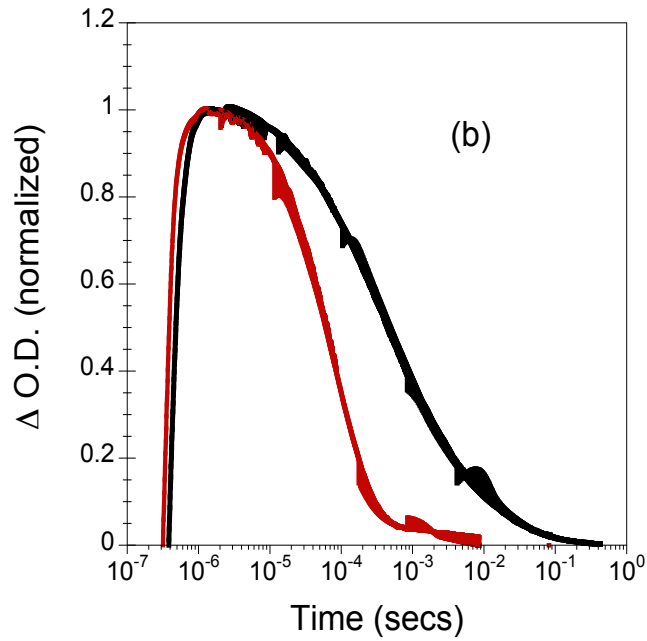


Figure: 4.6 Transient absorption kinetics of (a) **LCVC01**, (b) **LCVC02** and (c) **LCVC03** recorded for 1cm^2 area devices comprising $8\ \mu\text{m}$ TiO_2 films in the presence of a blank

electrolyte (black) and an iodide/tri-iodide red/ox electrolyte (red). Kinetics were recorded at 825nm for LCVC01, 775nm for LCVC02 and 825nm for LCVC03 following excitation at 600nm.

4.5 CONCLUSIONS

We have been synthesized a new series of push pull porphyrins using a diphenylamine as a donor moiety and an acid group as anchoring group with the introduction of a BDT group between the porphyrin core and the anchoring group for **LCVC01** and the introduction of a thiophene and a furan between the BDT and the anchoring group for **LCVC02** and **LCVC03** dyes. The DSSC performance gave us a record cell of 10.4% for **LCVC02**, however only a 3.84% and 2.55% were achieved for **LCVC01** and **LCVC03** respectively. As we have studied in the past the thiophene introduced in **LCVC02** reduce recombination reaction. Moreover, the introduction of a furan moiety doesn't make the same effect. In that case, the electronegativity of the oxygen atom interacts with the electrolyte oxidized species placing them closely to the TiO₂ surface and accelerating the recombination rate.

4.6 REFERENCES

- (1) O'Regan, B.; Gratzel, M. *Nature* **1991**, *353*, 737.
- (2) Gratzel, M. *Nature* **2001**, *414*, 338.
- (3) Nazeeruddin, M. K.; De Angelis, F.; Fantacci, S.; Selloni, A.; Viscardi, G.; Liska, P.; Ito, S.; Takeru, B.; Grätzel, M. *Journal of the American Chemical Society* **2005**, *127*, 16835.
- (4) Nazeeruddin, M. K.; Kay, A.; Rodicio, I.; Humphry-Baker, R.; Mueller, E.; Liska, P.; Vlachopoulos, N.; Graetzel, M. *Journal of the American Chemical Society* **1993**, *115*, 6382.
- (5) Han, L.; Islam, A.; Chen, H.; Malapaka, C.; Chiranjeevi, B.; Zhang, S.; Yang, X.; Yanagida, M. *Energy & Environmental Science* **2012**, *5*, 6057.
- (6) Wang, Q.; Ito, S.; Grätzel, M.; Fabregat-Santiago, F.; Mora-Seró, I.; Bisquert, J.; Bessho, T.; Imai, H. *The Journal of Physical Chemistry B* **2006**, *110*, 25210.
- (7) Chen, C.-Y.; Wu, S.-J.; Wu, C.-G.; Chen, J.-G.; Ho, K.-C. *Angewandte Chemie International Edition* **2006**, *45*, 5822.
- (8) Mishra, A.; Fischer, M. K. R.; Bäuerle, P. *Angewandte Chemie International Edition* **2009**, *48*, 2474.
- (9) Li, R.; Lv, X.; Shi, D.; Zhou, D.; Cheng, Y.; Zhang, G.; Wang, P. *The Journal of Physical Chemistry C* **2009**, *113*, 7469.
- (10) Planells, M.; Pelleja, L.; Clifford, J. N.; Pastore, M.; De Angelis, F.; Lopez, N.; Marder, S. R.; Palomares, E. *Energy & Environmental Science* **2011**, *4*, 1820.
- (11) Bai, Y.; Zhang, J.; Zhou, D.; Wang, Y.; Zhang, M.; Wang, P. *Journal of the American Chemical Society* **2011**, *133*, 11442.
- (12) Feldt, S. M.; Gibson, E. A.; Gabrielsson, E.; Sun, L.; Boschloo, G.; Hagfeldt, A. *Journal of the American Chemical Society* **2010**, *132*, 16714.
- (13) Yum, J.-H.; Baranoff, E.; Kessler, F.; Moehl, T.; Ahmad, S.; Bessho, T.; Marchioro, A.; Ghadiri, E.; Moser, J.-E.; Yi, C.; Nazeeruddin, M. K.; Grätzel, M. *Nat Commun* **2012**, *3*, 631.

- (14) Zeng, W.; Cao, Y.; Bai, Y.; Wang, Y.; Shi, Y.; Zhang, M.; Wang, F.; Pan, C.; Wang, P. *Chemistry of Materials* **2010**, *22*, 1915.
- (15) Zhou, D.; Yu, Q.; Cai, N.; Bai, Y.; Wang, Y.; Wang, P. *Energy & Environmental Science* **2011**, *4*, 2030.
- (16) Li, L.-L.; Diau, E. W.-G. *Chemical Society Reviews* **2013**, *42*, 291.
- (17) Chang, Y.-C.; Wang, C.-L.; Pan, T.-Y.; Hong, S.-H.; Lan, C.-M.; Kuo, H.-H.; Lo, C.-F.; Hsu, H.-Y.; Lin, C.-Y.; Diau, E. W.-G. *Chemical Communications* **2011**, *47*, 8910.
- (18) Hsieh, C.-P.; Lu, H.-P.; Chiu, C.-L.; Lee, C.-W.; Chuang, S.-H.; Mai, C.-L.; Yen, W.-N.; Hsu, S.-J.; Diau, E. W.-G.; Yeh, C.-Y. *Journal of Materials Chemistry* **2010**, *20*, 1127.
- (19) Lu, H.-P.; Tsai, C.-Y.; Yen, W.-N.; Hsieh, C.-P.; Lee, C.-W.; Yeh, C.-Y.; Diau, E. W.-G. *The Journal of Physical Chemistry C* **2009**, *113*, 20990.
- (20) Wagner, K.; Griffith, M. J.; James, M.; Mozer, A. J.; Wagner, P.; Triani, G.; Officer, D. L.; Wallace, G. G. *The Journal of Physical Chemistry C* **2010**, *115*, 317.
- (21) Yella, A.; Lee, H.-W.; Tsao, H. N.; Yi, C.; Chandiran, A. K.; Nazeeruddin, M. K.; Diau, E. W.-G.; Yeh, C.-Y.; Zakeeruddin, S. M.; Grätzel, M. *Science* **2011**, *334*, 629.
- (22) Yella, A.; Mai, C.-L.; Zakeeruddin, S. M.; Chang, S.-N.; Hsieh, C.-H.; Yeh, C.-Y.; Grätzel, M. *Angewandte Chemie International Edition* **2014**, *53*, 2973.
- (23) Mathew, S.; Yella, A.; Gao, P.; Humphry-Baker, R.; CurchodBasile, F. E.; Ashari-Astani, N.; Tavernelli, I.; Rothlisberger, U.; NazeeruddinMd, K.; Grätzel, M. *Nat Chem* **2014**, *6*, 242.
- (24) O'Regan, B. C.; Lpez-Duarte, I.; Martnez-Díaz, M. V.; Forneli, A.; Albero, J.; Morandeira, A.; Palomares, E.; Torres, T. s.; Durrant, J. R. *Journal of the American Chemical Society* **2008**, *130*, 2906.

(25) Reynal, A.; Forneli, A.; Martinez-Ferrero, E.; Sánchez-Díaz, A.; Vidal-Ferran, A. n.; O'Regan, B. C.; Palomares, E. *Journal of the American Chemical Society* **2008**, *130*, 13558.

(26) Zewdu, T.; Clifford, J. N.; Hernandez, J. P.; Palomares, E. *Energy & Environmental Science* **2011**, *4*, 4633.

(27) Miyashita, M.; Sunahara, K.; Nishikawa, T.; Uemura, Y.; Koumura, N.; Hara, K.; Mori, A.; Abe, T.; Suzuki, E.; Mori, S. *Journal of the American Chemical Society* **2008**, *130*, 17874.

(28) O'Regan, B. C.; Walley, K.; Juozapavicius, M.; Anderson, A.; Matar, F.; Ghaddar, T.; Zakeeruddin, S. M.; Klein, C. d.; Durrant, J. R. *Journal of the American Chemical Society* **2009**, *131*, 3541.

Chapter 5

Novel Porphyrin-based small molecule using indoline as secondary donor for solution processed bulk-heterojunction organic solar cells.

Table of contents

4.1 Abstract	111
4.2 Introduction	111
4.3 Experimental Section	113
3.3.1 Synthesis and Characterization	113
3.3.2 Device preparation	117
4.4 Results and Discussion	118
4.5 Conclusions	124
4.6 References	125

5.1 ABSTRACT

We have synthesized and characterized a new symmetric molecule based on our “push-pull” strategy (**VC53**) using a core of porphyrin as a main donor moiety and the indoline group as secondary electron donor for solution processed bulk-heterojunction organic solar cells obtaining an efficiency of 1.2% with a photocurrent of 5 mA cm^{-2} ensuring efficient electron transfer to PC70BM.

5.2 INTRODUCTION

Bulk-heterojunction organic solar cells (BHJ-OSC) based on both; polymers¹⁻⁴ and small molecules⁵ have been intensively developed in recent years and are still in continuous progress due to the great promising alternatives that these organic materials present for solar cells (such us implementation in buildings). These materials can be prepared in multi-scale and, additionally, the use of solution-processed techniques for device fabrication promise to lower the cost of the solar cell^{6,7}. In spite of these clear advantages, these kind of devices are always accompanied with some other unsolved scientific matters that defines the entire field development such as studies related on charge generation or the determination of all losses mechanisms and the long-standing question about device stability.⁸⁻¹³

Recent published results for solution-processed small molecule bulk-heterojunction organic solar cells (smOSC) have demonstrated efficiencies reaching 8% under standard measurement conditions¹⁴⁻¹⁶ by using different molecular designs; On the other hand, the approach of using conjugated donor-acceptor (D-A) frameworks facilitate the internal charge transfer because their “push-pull” properties and, in addition, the energetic levels can be easily tuned by introducing different electron donors or acceptor moieties.^{17,18}

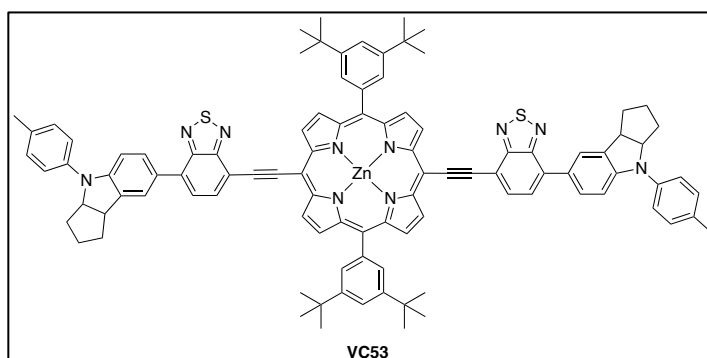
In addition, the porphyrins (POR) have been also widely studied and used in many BHJ-OSC¹⁷⁻²¹ and DSSC²²⁻²⁵; PORs are based and inspired on photosynthetic systems, they provide extensive π -conjugated systems, with a fast electron transfer, and an extremely high absorption coefficients. Furthermore, their electrochemical properties can be tuned by both; the

insertion of the metal in the cavity or/and the addition of moieties to the periphery using well-established synthetic procedures.¹⁸

In contrast, the use of porphyrins as small molecule in solution processed BHJ smOSC provides, in general, lower device efficiencies¹⁷⁻²⁰ than polymeric electron donor materials.

The main reasons are: in first place, the poor solubility of these materials in most common-in-use organic solvents for processing, and, secondly, the weak intermolecular interactions with the acceptor moieties. For both reasons the addition of an additive is usually required.²¹ Despite of that, the use of porphyrin in smOSC has recently reach values of efficiencies as high as 7%²⁶, competing very close with other small molecule moieties.

In the present work, a porphyrin based on symmetric “push-pull” framework has been designed and synthesized. The architecture, described as D-A-D-A-D, is based on a porphyrin core at the centre of the molecular backbone and the indoline^{27,28} moieties, as secondary donors placed at the periphery. The benzothiadazole moiety²⁹ is used as intramolecular acceptor moiety. This design allows a relative low HOMO energy values favouring higher open circuit voltages, V_{oc} , and proper LUMO energy levels that leads to efficient charge dissociation to the main fullerene acceptor.



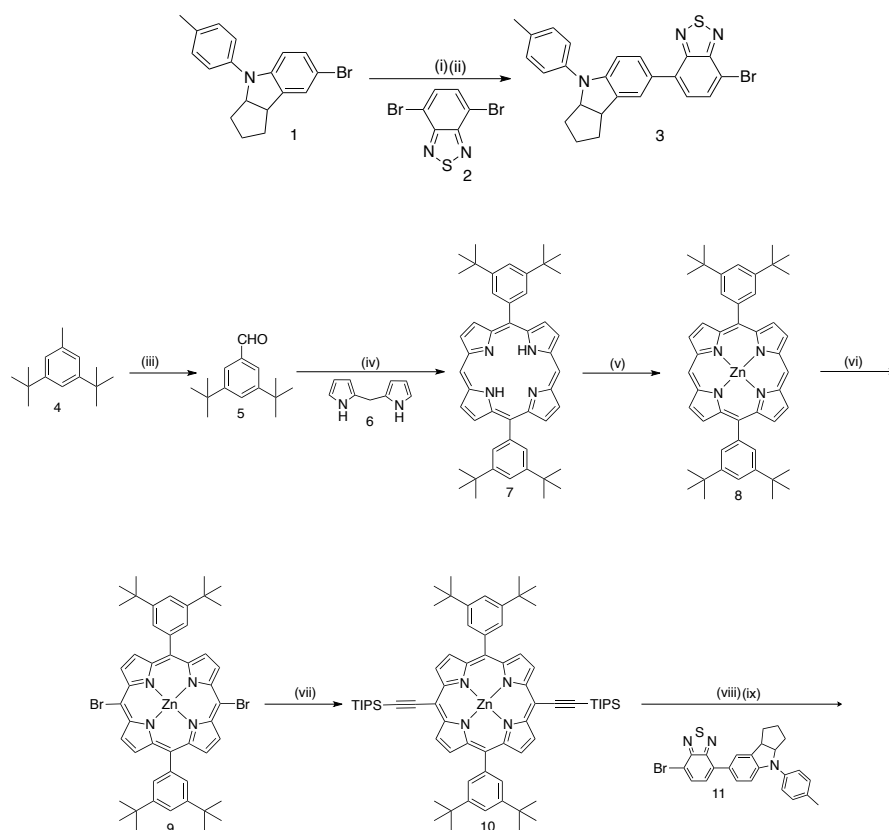
Scheme 5.1: Molecular structure of VC53

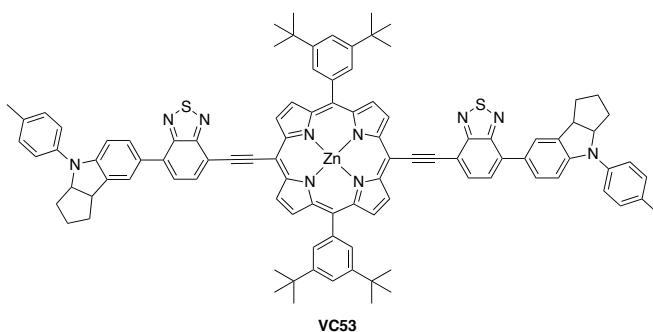
The complete devices were fabricated and analysed in this work. The most relevant parameters are presented below, as well as, the charge recombination measurements that will help to explain what limits the final device performance.

5.3 EXPERIMENTAL SECTION

5.3.1 Synthesis and characterization

The Synthesis of VC53 is shown in Scheme 2. The intermediate **3** was synthesized via in-situ Suzuki coupling. The synthesis of the dye **VC53** was carried out by attaching the intermediate **3** to the *meso* positions via Sonagashira coupling. The intermediates and **VC53** were characterized by $^1\text{H-NMR}$, $^{13}\text{CNMR}$ and MALDI mass spectroscopy.





Scheme 5.2: Synthetic route of **VC53**. (*Reaction conditions*): (i) n-BuLi, THF, B(OCH₃)₃, -78°C; (ii) Pd(PPh₃)₄, 2M K₂CO₃ aqueous solution, THF, 6 h, 80°C; (iii) NBS, AIBN, benzene, 4h, reflux, hexamethylenetetramine, EtOH/H₂O, 4h, reflux, HCl, 30 minutes, reflux; (iv) TFA, DCM, 4 h, 23°C, DDQ, 1h; (v) Zn(OAc)₂·2H₂O, DCM/Methanol, 3 h, 23°C; (vi) NBS, DCM, 6 h, 0°C; (vii) triisopropylsilylacetylene, Pd(PPh₃)₂Cl₂, CuI, THF, NEt₃, 4 h, reflux; (viii) TBAF, THF, 30min, RT; (ix) Pd(PPh₃)₄, NEt₃, CuI, Toluene, 4 h, reflux;

Synthesis of 4-bromo-7-(4-(p-tolyl)-1,2,3,3a,4,8b-hexahydrocyclopenta[b]indol-7-yl)benzo[c][1,2,5]thiadiazole (3): 7-bromo-4-(p-tolyl)-1,2,3,3a,4,8b-hexahydrocyclopenta[b]indole **1** (0.300g, 0.914mmol) was added to a round flask with 30mL of THF and was stirred under nitrogen atmosphere at -78°C. A solution of ⁿBuLi 2M in hexane (0.41mL, 1.09mmol) was added and the mixture was stirred for 15 minutes at -78°C. After that, B(OMe)₃ (0.15mL, 1.37mmol) was added and the reaction was stirred overnight at -78°C. The crude was warmed at room temperature. In another Schlenk vessel, Pd(PPh₃)₄ (0.094g, 0.025mmol), **2** (0.24g, 0.82mmol), K₂CO₃ 2M (4mL), the reaction mixture, and THF (25mL) were mixed and the reaction was stirred at 70°C for 6 hours. After the reaction, distilled water was added. The crude product was extracted using CHCl₃, and the organic layer was dried over NaSO₄. The residue was purified by column chromatography (Hexane/Dichloromethane 6:4) to obtain the desired product (0.230g, 54.4% yield). ¹H-NMR (400 MHz, CDCl₃) δ_H: 7.84 (d, J=7.7Hz, 1H); 7.68 (s, 1H); 7.63 (dd, J=8.4Hz, 2Hz, 1H); 7.48 (d, J=7.7Hz, 1H); 7.20 (m, 4H); 6.97 (d, J=8.4Hz,

1H); 4.84 (m, 1H); 3.91 (m, 1H); 2.33 (s, 3H); 2.06 (m, 1H); 1.92 (m, 2H); 1.79 (m, 1H); 1.64 (m, 2H).

Synthesis of 3,5-di-*tert*-butylbenzaldehyde (5): A solution of 3,5-di-*tert*-butyltoluene (25g, 0.122mol), N-bromosuccinimide (33.0g, 0.185mol) and azobisisobutyronitrile (AIBN) (0.9g, 0.0055mol) in benzene was heated with reflux under magnetic stirring for 4 hours. The reaction mixture was cooled, filtered through paper and the solvent was evaporated under vacuum. The residue was dissolved in 70mL of a solvent mixture composed by EtOH/H₂O (1:1) and hexamethylenetetramine (50.0g, 0.357mol) was added. The solution was heated under reflux for 4 hours. Concentrate HCl was added (21mL) and the heating under reflux was continued for 30min. The ethanol solution was removed under reduced pressure, and the remaining aqueous layer was extracted with ether. The organic layer was dried over Na₂SO₄ and the solvent removed. Recrystallization from EtOH afforded the desired product as white crystals. (20.0g, 75% yield). ¹H-NMR (400 MHz, CDCl₃) δ_H: 10.0 (s, 1H); 7.70 (m, 3H); 1.35 (s, 18H).

Synthesis of 5,15-Bis-(3,5-bis-*tert*-butylphenyl)porphyrin (7): dipyrromethane (2.00g, 13.70mmol) and 3,5-di-*tert*-butylbenzaldehyde (2.98g, 13.70mmol) were dissolved in DCM (1.78L) and degassed. Then, trifluoroacetic acid (0.91mL, 12.33mmol) was added and the mixture was stirred at 23°C for 4h under nitrogen. After that, DDQ (4.70g, 20.55mmol) was added and the mixture was stirred 1 h more. After, the mixture was basified with Et₃N (2.31mL) and filtered through silica. The solvent was removed under vacuum and the residue was purified by column chromatography using a mixture of Hexane/DCM (2/1) as eluent to give us the desired product (purple powder), (2.5g, 26.56% Yield)¹H NMR (CDCl₃, 400 MHz) δ_H: 10.32 (s, 2H) 9.43 (d, J=4.6Hz, 4H); 9.18 (d, J=4.6Hz, 4H); 8.15 (d, J=1.6Hz, 4H); 7.81 (t, J=1.6H, 2H); 1.58 (s, 36H); 3.01 (s, 2H).

Synthesis of [5,15-Bis-(3,5-bis-*tert*-butylphenyl)porphinato]-zinc(II) (8): A mixture of 5,15-Bis-(3,5-bis-*tert*-butylphenyl)porphyrin **7** (2.50g, 3.63mmol) and Zn(OAc)₂·2H₂O (5.20g, 36.39mmol) were mixed in DMF (150mL) and the solution was refluxed during 3 h. The reaction was quenched with water

(160mL), and the mixture was extracted using DCM (2x100mL). The combined extracts were washed with water and dried over anhydrous MgSO_4 . The solvent was removed under reduced pressure to give as the desired product. (2.34g, 86% Yield). ^1H NMR (CDCl_3 , 400 MHz) δ_{H} : 10.32 (s, 2H) 9.44 (d, $J=4.6\text{Hz}$, 4H); 9.20 (d, $J=4.6\text{Hz}$, 4H); 8.14 (d, $J=1.6\text{Hz}$, 4H); 7.83 (t, $J=1.6\text{Hz}$, 2H); 1.57 (s, 36H).

Synthesis of [5,15-Bis-bromo-10,20-bis-(3,5-bis-*tert*-butylphenyl)porphinato]-zinc(II) (9): To a stirred solution of 5,15-Bis-(3,5-bis-*tert*-butylphenyl)porphinato]-zinc(II) **8** (2.34g, 3.11mmol) in DCM (120mL) NBS was added (1.10g, 6.22mmol) and the solution was stirred for 30 minutes. After, the reaction was quenched with acetone (20mL) and the solvent was removed under vacuum. The solution was filtered and the residue was washed with MeOH to give us the desired product. (Purple powder) (2.57g, 91% Yield). ^1H NMR (CDCl_3 , 400 MHz) δ_{H} : 9.66 (d, $J=4.6\text{Hz}$, 4H); 8.89 (d, $J=4.6\text{Hz}$, 4H); 8.01 (d, $J=1.6\text{Hz}$, 4H); 7.92 (t, $J=1.6\text{Hz}$, 2H); 1.57 (s, 36H).

Synthesis of [5,15-Bis-(3,5-bis-*tert*-butylphenyl)-10,20-bis-triisopropylsilylethynylporphinato]zinc(II) (10): A mixture of [5,15-Bis-bromo-10,20-bis-(3,5-bis-*tert*-butylphenyl)porphinato]-zinc(II) **9** (0.20g, 0.22mmol), triisopropylsilylacetylene (0.08mL, 0.35mmol), $\text{Pd}(\text{PPh}_3)_2\text{Cl}_2$ (0.03g, 0.04mmol), CuI (4.18mg, 0.02mmol), THF (20mL) and Net_3 (2mL) was stirred for 16h. Then, the solvent was removed under reduced pressure. The residue was purified by column chromatography using Hexane/DCM (3:2) to give as the desired product (purple solid) (0.19g, 77.2% Yield). ^1H NMR (CDCl_3 , 400 MHz) δ_{H} : 7.74 (d, $J=4.6\text{Hz}$, 4H); 8.95 (d, $J=4.6\text{Hz}$, 4H); 8.00 (d, $J=1.6\text{Hz}$, 4H); 7.79 (t, $J=1.6\text{Hz}$, 2H); 1.53 (s, 36H); 1.42 (m, 42H).

Synthesis of VC53: To a solution of **10** (185mg, 0.165mmol) in dry THF (10mL) was added TBAF (2mL) 1M in THF. The solution was stirred at 23°C for 30min under nitrogen. The mixture was quenched with H_2O and then extracted with CH_2Cl_2 . The organic layer was dried anhydrous MgSO_4 and the solvent was removed under reduced pressure. The residue and **3** (230mg, 0.498mmol) were dissolved in a mixture of dry toluene (10mL) and NEt_3 (5mL) and the solution was degassed with nitrogen during 10min. After, $\text{Pd}(\text{PPh}_3)_4$ (38mg,

0.030mmol) and CuI (6.30mg, 0.030mmol) were added to the mixture. The solution was refluxed for 4 hours under nitrogen. The solvent was removed under reduced pressure. The residue was purified by column chromatography (silica gel) using DCM/CH₃OH =20/1 as eluent to afford pure product (92 mg, yield 36%) ¹H-NMR (400 MHz, THF-d₈) δ_H: 9.90 (d, J=4.5Hz, 4H); 8.87 (d, J=4.5Hz, 4H); 8.19 (m, 5H); 8.05 (s, 1H); 8.03 (s, 2H); 7.97 (t, J=2.0Hz, 2H); 7.93 (dd J=8.5Hz, 2.0Hz, 2H) 7.86 (d, J=7.5Hz, 2H); 7.27 (d, J=8.5Hz, 4H); 7.18 (d, J=8.5Hz, 4H); 7.00 (d, J=8.5Hz, 2H); 4.92 (m, 2H); 3.92 (m, 2H); 2.33 (s, 3H); 2.09 (m, 4H); 1.94 (m, 1H); 1.86 (m, 1H); 1.63 (s, 36H). MALDI: m/z calcd for C₁₀₀H₉₀N₁₀S₂Zn 1558.6083, found 1560.6116

5.3.2 Device fabrication

Indium Tin Oxide (ITO) 5 Ohm/square (PSiOTec, Ltd., UK) sodalime glass substrates were first cleaned with acetone to remove the residual photoresist layer. The substrates were then placed in a teflon holder and cleaned by ultrasonic treatment in acetone (1 × 10 min) and in isopropanol (2 × 10 min), and dried under a nitrogen flow. The ITO substrates were ozone-treated in a UV-ozone cleaner for 20 min, and subsequently coated in air with a layer of filtered (0.45 mm, cellulose acetate) solution of Poly(3,4-ethylenedioxythiophene) : poly(styrenesulfonate) (PEDOT:PSS, HC StarckBaytron P) (4500 rpm 30 seconds followed by 3500 rpm 30 seconds). The PEDOT:PSS film was dried at 120 °C under inert atmosphere for 15 min. Active blend was prepared in a concentration of 20 mg/ml (total concentration), using porphyrin (VC53) as a donor derivative and PC70BM in a mixed solution of chlorobenzene and dichlorobenzene 3:1 v/v and 3% of pyridine to help porphyrin solubility; the blend was left under stirring 48 hour; the active layer was spin coated at 8000 rpm in air over the PEDOT:PSS layer obtaining a thin layer 85 nm thick. After the deposition the active layer was exposed to a thermal annealing post-treatment at 130°C for 2 min.

The cathode layer was deposited by thermal evaporation in an ultra high vacuum chamber (1×10^{-6} mbar). The metals were evaporated through a shadow mask leading to devices with a defined area of 9 mm^2 ; The LiF (0.6 nm) and the Al (100 nm) layers were deposited at the evaporation rate of 0.1 \AA/s and $0.5\text{-}1 \text{ \AA/s}$ respectively.

5.4 RESULTS AND DISCUSSION

The absorption and emission spectra of **VC53** in solution is shown below and their photophysical and electrochemical characteristics are listed in Table 5.1.

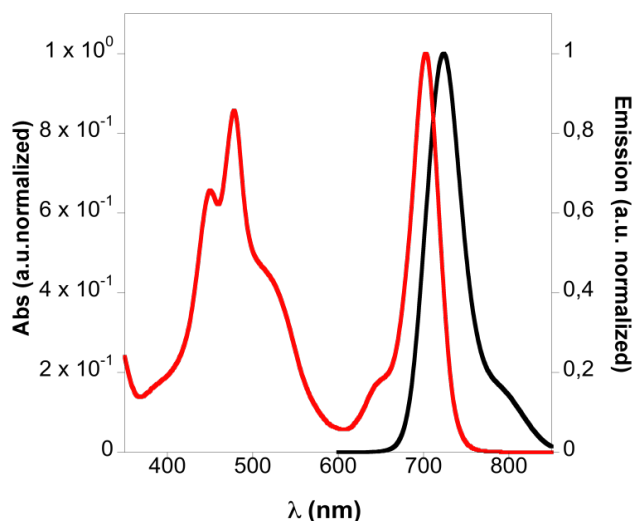


Figure 5.1. The normalized absorption (red) and emission (black) spectra of **VC53** in THF

As we can see, the absorption and emission spectra for **VC53** show the typical bands associated with porphyrins, An Intense Soret Band at 440 nm and 480 nm and also an intense Q band at 702nm. The cyclic voltammetry measurements give as a results a oxidation potential peak of $E_{ox} = 0.150\text{V}$ and the corresponding E_{LUMO} calculated was $E_{LUMO} = -3.28\text{eV}$ that is energetically high enough to achieve exciton dissociation at the bulk-heterojunction the interface⁸

Table 5.1. UV-Visible, steady-state fluorescence and electrochemical data for **VC53**

Dye	λ_{abs} (nm) ^a	λ_{em} (nm) ^a	E_{ox} (V v's Fc/Fc ⁺)	E_{0-0} (eV) ^c	E_{HOMO} (eV) ^d	E_{LUMO} (eV) ^e
VC53	527 (392)					
	480 (493)	723	0.150	1.75	-5.03	-3.28
	702 (574)					

^aMeasured in THF. In parenthesis the molar extinction coefficient (ϵ) at λ_{abs} ($10^{-3}M^{-1} cm^{-1}$). ^bMeasured in 0.1M tetrabutylammonium hexafluorophosphate in THF at scan of 30 mVs⁻¹. The working electrode consisted of a platinum wire and the counter electrode a platinum mesh. The reference electrode was the silver calomel electrode (saturated KCl). All solutions were degassed with argon for 5 min prior to measurement. ^c E_{0-0} was determined from the intersection of absorption and emission spectra in dilute solution. ^d E_{HOMO} was calculated using $E_{HOMO}(vs\ vacuum) = -4.48 - E_{ox}(vs\ Fc/Fc^+)$. ^e E_{LUMO} was calculated using $E_{LUMO} = E_{HOMO} + E_{0-0}$

The Light Harvesting Efficiency (LHE) obtained from the UV-visible absorption spectra of thin films is shown in figure 5.2. It is known that one of the main advantages is the great capability of porphyrins to absorb light in a broader light spectra taking into account the contribution of indoline groups; however, the limitation on thickness needed for efficient solar cells reduces the light harvesting efficiency of the film.

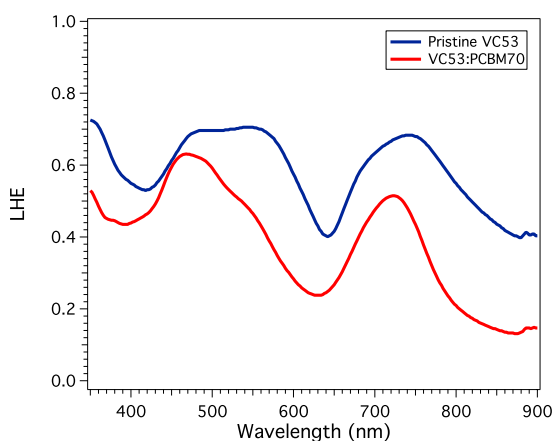


Figure 5.2. The Light Harvesting Efficiency (from the UV-Visible absorption spectra) of a

pristine VC53 film (blue) and VC53:PCBM₇₀ film (Red). The thickness of these films corresponds to same thickness obtained in complete devices which is 85-90 nm

Laser transient absorption spectroscopy (L-TAS) was employed with the aim to determine the charge transfer kinetics between the porphyrin and the fullerene as shown in figure 5.3. The thin BHJ film was excited at $\lambda_{ex}= 480\text{nm}$ corresponding to a maximum of the film absorption; The decay transient was measured from micro- to milliseconds time scale and the signal was fitted to a power-law exponential decay (Eq. 5.1), indicating an inhomogeneous distribution of localized states and, due to the slow time scale monitored, the reaction can be assigned to non-geminate recombination process between the porphyrin and the fullerene derivate with a half-lifetime of 3 microseconds and a α parameter of 0.5 at room temperature.^{30,31,32}

$$\tau = \tau_{n0} * n^{\alpha} \quad (\text{Eq. 5.1})$$

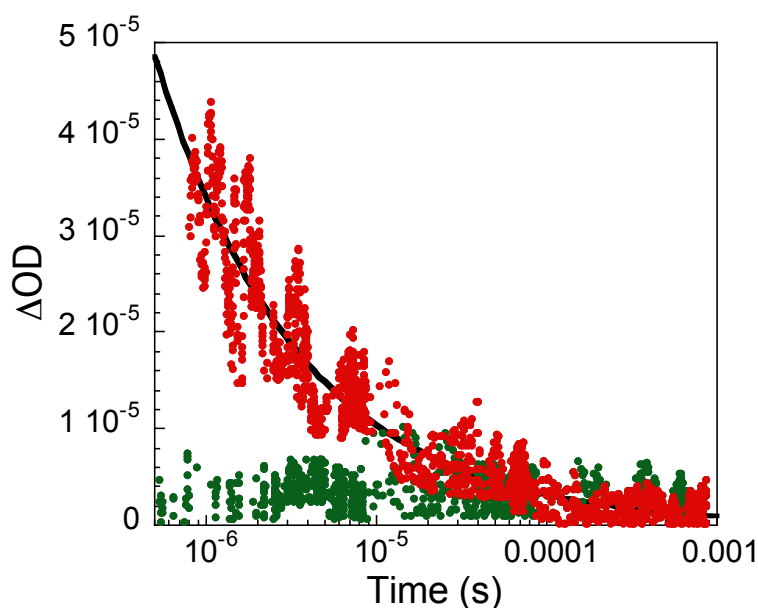


Figure 5.3. Transient absorption decays of VC53:PC₇₀BM film (Red) and pristine VC53 film (Green) recorded at $\lambda_{probe}=800\text{nm}$ for $\lambda_{ex}=480 \text{ nm}$. The black line corresponds to the power law fitting of the measured decay.

The design of this molecule allows favourable molecular aggregation (π - π stacking) due to the presence of the shorter alkyl chains linked over the core of the porphyrin; we expect this translate into an increase of the intra-molecular electron transport minimizing geminate recombination processes.

Once the L-TAS kinetics were measured, we fabricated complete devices as described above in the experimental section; we obtained an average device efficiency of 1.2% under AM 1.5G simulated conditions as shown in figure 5.4.

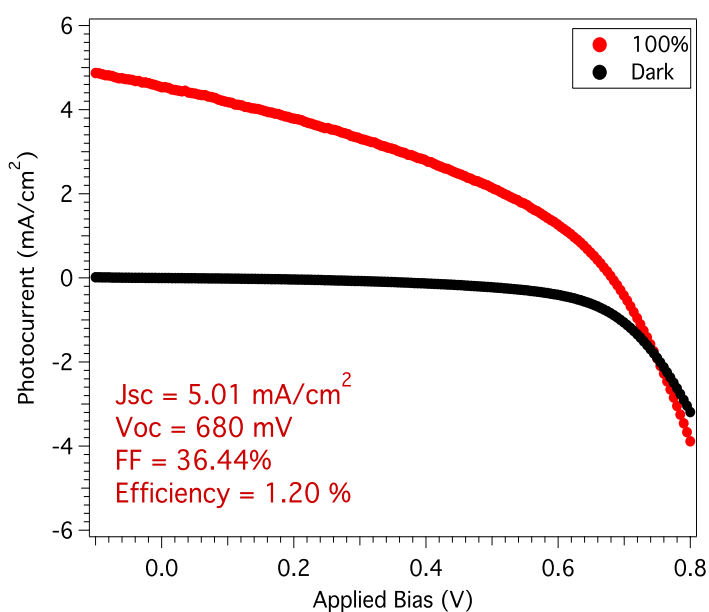


Figure 5.4. Measured current versus voltage (I-V) curves for VC53:PCBM₇₀ devices at 100 mW cm⁻² and in dark.

The photocurrent obtained ($J_{sc} = 5 \text{ mA cm}^{-2}$) is notable and correlates well with the LHE measurement shown above. Taking into account the LUMO energy difference between VC53 (-3.28 eV) and the fullerene derivate (-4.0 eV) it seems that exciton dissociation was efficient.⁴

The obtained V_{oc} of 680mV is not noticeably high; however represent a reasonable value taking into account the theoretical maximum value around 1V

obtained from energy level positioning difference of both VC53 ($\text{HOMO}_{\text{donor}}$: -5.03 eV) and fullerene derivate ($\text{LUMO}_{\text{acceptor}}$: -4.0 eV) using calculation procedures previously reported by other authors.³³

The FF of 36.5% is unambiguously the main limiting factor of the overall device performance and is known that strongly depends on carrier mobility and the balanced degree between hole and electron charges being generated at the blend and transported through the device active layer to the selective metal contacts. From the results obtained from LHE measurements and taking into account that electron mobility basically depends on the fullerene derivate, we can anticipate that this device present a poor hole mobility that limits the device performance.^{34,35}

The CE and TPV measurements were carried out as it have been previously reported by our group among others.^{12,13,36} In Figure 5.5, we can appreciate a clear linear region at earlier applied bias until values close to the experimental V_{oc} corresponding to 1 sun illumination, where an exponential trend appears. As we have reported and other authors have confirmed, the linear region is indicative that the device works as a capacitor and charges are likely to be stored at the electrodes^{11,37}; On the contrary, under 1 sun illumination the exponential trend can be assigned to the charge being accumulated at the film and producing the splitting of the quasi Fermi levels in both materials. The energy difference between those quasi Fermi levels is equal to the observed V_{oc} at 1 sun.

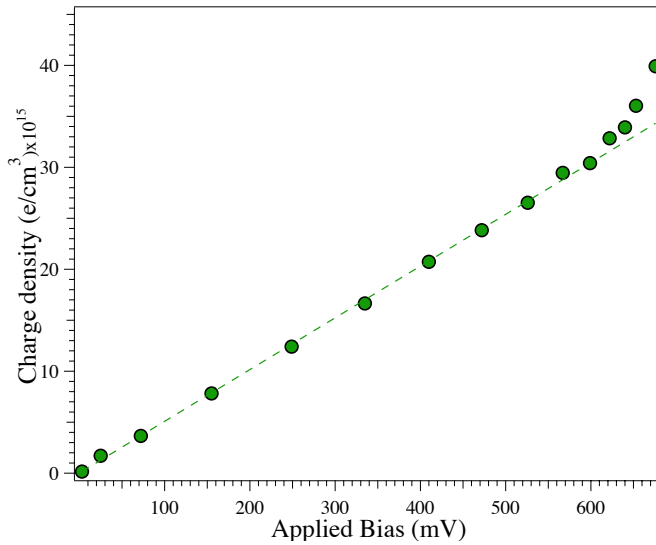


Figure 5.5. Measured charge density at different light bias, dashed line represents the linear trend related to the geometric capacitance of a VC53:PCBM₇₀ complete device.

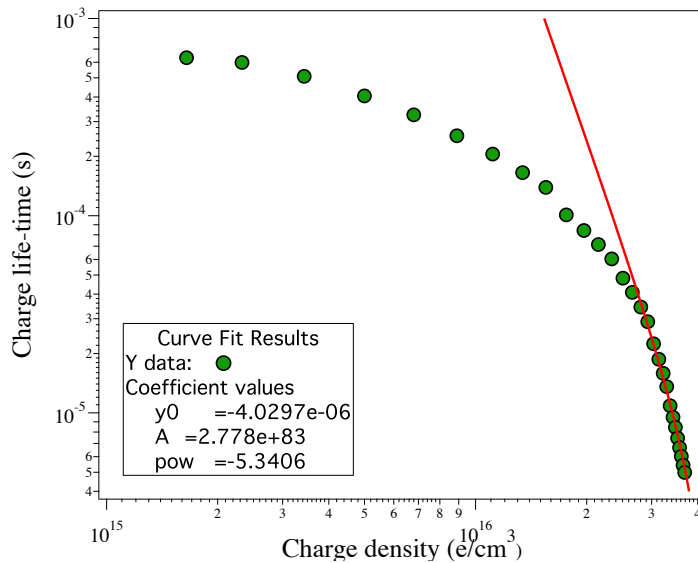


Figure 5.6. Measured charge lifetime at different charge density of a VC53:PC₇₀BM complete device.

In the charge lifetime vs accumulated charge measurements (Figure 5.6), extracted using TPV and CE, we clearly differentiate two regions, the first one corresponding to a smoother decay at times between $4 \cdot 10^{-4}$ s and $1.5 \cdot 10^{-5}$ s that

does not corresponds to the real carrier life-time as it measured from the geometric capacitance of the cell and it should be attributed to the discharge time of the capacitor; The second region, measured life-time values below 10^{-5} s, truly correspond to the charge carrier recombination dynamics of the VC53:PC₇₀BM solar cell. The latest data from the TPV were fitted to a power law (Equation 5.1) obtaining an $\alpha \sim 5$ indicating that the overall charge recombination is not only determined by non-geminate bimolecular recombination kinetics (with expected value of 2) but also by recombination processes at the electrodes interface due likely to the unbalanced mobility between holes and electrons.

5.5 CONCLUSIONS

A new porphyrin has been synthesized and characterized in order to study its applicability in smOPVs. The average efficiency achieved was 1.2% using as acceptor moiety PC70BM. The main limitation observed for this type of molecules is the low mobility of charges (holes) that impedes the use of thicker films that will lead to higher photocurrent. The recombination lifetime measured under working conditions is in the order of other OPV devices including both, small molecules and polymers. Thus, further work on this direction (improving mobility) should be the focus on the design and synthesis of porphyrins for applications in OPV using solution processed methods.

5.6 REFERENCES

- (1) Moliton, A.; Nunzi, J. M. *Poly. Int.* **2006**, *55*, 583.
- (2) Thompson, B. C.; Fréchet, J. M. J. *Angew. Chem. Int. Ed.* **2008**, *47*, 58.
- (3) Servaites, J. D.; Ratner, M. A.; Marks, T. J. *Energy Environ. Sci.* **2011**, *4*, 4410.
- (4) Li, G.; Zhu, R.; Yang, Y. *Nature Photonics* **2012**, *6*, 153.
- (5) Lin, Y.; Li, Y.; Zhan, X. *Chem. Soc. Rev.* **2012**, *41*, 4245.
- (6) Krebs, F. C. *Sol. Energy Mater. Sol. Cells* **2009**, *93*, 394.
- (7) Osedach, T. P.; Andrew, T. L.; Bulovic, V. *Energy Environ. Sci.* **2013**, *6*, 711.
- (8) Clarke, T. M.; Durrant, J. R. *Chem Rev* **2010**, *110*, 6736.
- (9) Clarke, T. M.; Ballantyne, A.; Shoaee, S.; Soon, Y. W.; Duffy, W.; Heeney, M.; McCulloch, I.; Nelson, J.; Durrant, J. R. *Adv. Mater.* **2010**, *22*, 5287.
- (10) Janssen, R. A. J.; Nelson, J. *Adv. Mater.* **2013**, *25*, 1847.
- (11) Guerrero, A.; Montcada, N. F.; Ajuria, J.; Etxebarria, I.; Pacios, R.; Garcia-Belmonte, G.; Palomares, E. *J. Mater. Chem. A* **2013**, *1*, 12345.
- (12) Sánchez-Díaz, A.; Burtone, L.; Riede, M.; Palomares, E. *J. Phys. Chem. C* **2012**, *116*, 16384.
- (13) Sánchez-Díaz, A.; Pacios, R.; Muñecas, U.; T., T.; Palomares, E. *Organic Electronics* **2011**, *12*, 329.
- (14) Kyaw, A. K. K.; Wang, D. H.; Gupta, V.; Zhang, J.; Chand, S.; Bazan, G. C.; Heeger, A. J. *Adv. Mater.* **2013**, *25*, 2397.
- (15) Zhou, J.; Zuo, Y.; Wan, X.; Long, G.; Zhang, Q.; Ni, W.; Liu, Y.; Li, Z.; He, G.; Li, C.; Kan, B.; Li, M.; Chen, Y. *J. Am. Chem. Soc.* **2013**, *135*, 8484.
- (16) Liu, Y.; Chen, C.-C.; Hong, Z.; Gao, J.; Yang, Y. M.; Zhou, H.; Dou, L.; Li, G.; Yang, Y. *Scientific Reports* **2013**, *3*, 3356.
- (17) Shi, S.; Wang, X.; Sun, Y.; Chen, S.; Li, X.; Li, Y.; Wang, H. *Journal of Materials Chemistry* **2012**, *22*, 11006.
- (18) Huang, Y.; Li, L.; Peng, X.; Peng, J.; Cao, Y. *Journal of Materials Chemistry* **2012**, *22*, 21841.
- (19) Sharma, G. D.; Daphnomili, D.; Biswas, S.; Coutsolelos, A. G. *Organic Electronics* **2013**, *14*, 1811.
- (20) Li, L.; Huang, Y.; Peng, J.; Cao, Y.; Peng, X. *J. Mater. Chem. A* **2012**, *1*, 2144.

(21) Hatano, J.; Obata, N.; Yamaguchi, S.; Yasuda, T.; Matsuo, Y. *J. Mater. Chem.* **2012**, *22*, 19258.

(22) Mathew, S.; Yella, A.; Gao, P.; Humphry-Baker, R.; Curchod, F. E.; Ashari-Astani, N.; Tavernelli, I.; Rothlisberger, U.; Nazeeruddin, M. K.; Grätzel, M. *Nat Chem* **2014**, *6*, 242.

(23) Wang, C.-L.; Hu, J.-Y.; Wu, C.-H.; Kuo, H.-H.; Chang, Y.-C.; Lan, Z.-J.; Wu, H.-P.; Wei-Guang Diao, E.; Lin, C.-Y. *Energy & Environmental Science* **2014**, *7*, 1392.

(24) Yella, A.; Lee, H.-W.; Tsao, H. N.; Yi, C.; Chandiran, A. K.; Nazeeruddin, M. K.; Diao, E. W.-G.; Yeh, C.-Y.; Zakeeruddin, S. M.; Grätzel, M. *Science* **2011**, *334*, 629.

(25) Yella, A.; Mai, C.-L.; Zakeeruddin, S. M.; Chang, S.-N.; Hsieh, C.-H.; Yeh, C.-Y.; Grätzel, M. *Angewandte Chemie International Edition* **2014**, *53*, 2973.

(26) Qin, H.; Li, L.; Guo, F.; Su, S.; Peng, J.; Cao, Y.; Peng, X. *Energy & Environmental Science* **2014**, *7*, 1397.

(27) Demeter, D.; Jeux, V.; Leriche, P.; Blanchard, P.; Olivier, Y.; Cornil, J.; Po, R.; Roncali, J. *Adv. Funct. Mater.* **2013**.

(28) Cabau, L.; Pallejà, L.; Clifford, J. N.; Kumar, C. V.; Palomares, E. *J. Mater. Chem. A* **2013**, *1*, 8994.

(29) Li, W.; Wu, Y.; Zhang, Q.; Tian, H.; Zhu, W. *Appl. Mater. Interfaces* **2012**, *4*, 1822.

(30) Nogueira, A. F.; Montanari, I.; Nelson, J.; Durrant, J. R. *J. Phys. Chem.* **2003**, *107*, 1567.

(31) Ohkita, H.; Cook, S.; Astuti, Y.; Duffy, W.; Tierney, S.; Zhang, W.; Heeney, M.; McCulloch, I.; Nelson, J.; Bradley, D. D. C.; Durrant, J. R. *J. AM. CHEM. SOC.* **2008**, *130*, 3030.

(32) Eng, M. P.; Barnes, P. R. F.; Durrant, J. R. *J. Phys. Chem. Lett.* **2010**, *1*, 3096.

(33) Montcada, N. F.; Pelado, B.; Viterisi, A.; Albero, J.; Coro, J.; de la Cruz, P.; Langa, F.; Palomares, E. *Org. Electron.* **2013**, *14*, 2826.

(34) Lee, O. P.; Yiu, A. T.; Beaujuge, P. M.; Woo, C. H.; Holcombe, T. W.; Millstone, J. E.; Douglas, J. D.; Chen, M. S.; Fréchet, J. M. J. *Adv Mater* **2011**, *23*, 5359.

(35) Dibb, G. F. A.; Jamieson, F. C.; Maurano, A.; Nelson, J.; Durrant, J. R. *J. Phys. Chem. Lett.* **2013**, *4*, 803.

(36) Shuttle, C. G.; O'Regan, B.; Ballantyne, A. M.; Nelson, J.; Bradley, D. D. C.; Mello, A. J.; Durrant, J. R. *Appl. Phys. Lett.* **2008**, *92*, 093311.

(37) Bolognesi, M.; Sánchez-Díaz, A.; Ajuria, J.; Pacios, R.; Palomares, E. *Phys. Chem. Chem. Phys.* **2011**, *13*, 6105.

Chapter 6
Final Conclusions

FINAL CONCLUSIONS

In this Thesis, the synthesis and characterization of novel sensitizers for their applications in DSSC and OPVs have been described. For all of the Sensitizers presented the device performance have been done in order to study their applicability for the photovoltaic devices studying how change the efficiency of the devices versus the structure of the molecule.

Basically we can summarize the conclusions as follows:

- **In Chapter 3** we have design a new sensitizer called **VCL01** using as reference the **LS-1** with the difference to include a cyclopentadithiophene unit in the π -bridge in the VCL01 and also the performance in DSC devices is described. We observed for the VCL01 dye a moderate efficiency of 4.81%. However under 120mins of irradiation this efficiency has been increase in almost 50% showing a 7.21%. The increase observed was due to the increase in J_{sc} reflected in the IPCE. And increase in the V_{oc} is also observed due an increase of the electron lifetime seen in the Transient photovoltage measurements. After 120min of irradiation there is an improvement in the interaction between the dye and the TiO_2 , promoting a fast electron injection in the semiconductor.
- **In Chapter 4** we have design and synthesized a family of porphyrins called **LCVC01**, **LCVC02** and **LCVC03** in order to study how affect the introduction or not of a group between the BDT and the anchoring group and the importance to choose the correct group. The results achieved indicate that the introduction of a group not always is a good issue. Here we have presented the example of one group (thiophene) with a record efficiency of 10.4% and in other case we have introduced a furan group achieving a modest efficiency of 2.55%. With the photophysical studies of these molecules we have seen that the

introduction of a thiophene group in LCVC02 reduce the recombination rate making it a good option. However the introduction of a furan group for LCVC03 not only is showed a worse efficiency if not it seems that the oxygen atom interacts with electrolyte oxidized placing them closely to the semiconductor surface accelerating the recombination reactions.

- **In chapter 5** a porphyrin for OPVs applications have been synthesized. The efficiency achieved was 1.2% with PC₇₁BM. Further optimizations and new design for small molecules is needed to achieve good porphyrins with better device performance.

ANNEX

Scientific Contribution

Journal Articles related with this Thesis

Light soaking effects on Charge Recombination and Device Performance in Dye Sensitized Solar Cells Based on Indoline-Cyclopentadithiophene Chromophores. Lydia Cabau, Laia Pellejà, John N. Clifford* Challuri Vijay Kumar* and Emilio Palomares (*J. Mater. Chem. A*, 2013,1, 8994-9000).

Synthesis of new high efficient Push-pull porphyrins for Dye Sensitized Solar Cells. Lydia Cabau, Antonio Moncho, Challuri Vijay Kumar, John N. Clifford, Núria López and Emilio Palomares. (Writed)

Journal Articles not related with this Thesis

Dye Molecular Structure Device Open-Circuit Voltage Correlation in Ru(II) Sensitizers with Heteroleptic Tridentate Chelates for Dye-Sensitized Solar Cells. Kuan-Lin Wu, Cheng-Hsuan Li, Yun Chi, John N. Clifford, Lydia Cabau, Emilio Palomares, Yi-Ming Cheng, Hsiao-An Pan and Pi-Tai Chou. (*J. Am. Chem. Soc.*, 2012,134 (17), pp 7488-7496).

Indoline as Electron Donor Unit in “Push-Pull” Organic Small Molecules for Solution Processed Organic Solar Cells: Effect of The Molecular π -Bridge on Device Efficiency. Fernández Montcada, Nuria; Cabau, Lydia; Kumar, Challuri; Cambaru, Werther; Palomares, Emilio. Submitted

Conferences

Frontiers in organic, dye-sensitized and Hybrid solar cells. VII International Summer School of Krutyn, Poland 2011.

Hybrid and Organic Photovoltaics (HOPV 2014) Lausanne- Switzerland 2014. Poster Presentation

Lydia Cabau; Vijay Kumar Challuri; John N. Clifford; Laia Pellejà; Emilio Palomares. Effect of light soaking on efficiency in Dye Sensitized Solar Cells

